

Classical theory of Pairing correlation in atomic nucleus

Yu-Min Zhao

Shanghai Jiao Tong University

In the Xinxiang Talent summer school, I gave a series of lectures on pairing correlation in atomic nucleus. At the beginning I do not know how to and what to teach in a school of students at different levels. It was a challenge, but I finally made it. My strategy is to choose the very original and fundamental theories, including the background of pairing phenomenon, seniority/quasispin theory, the BCS, and the concept quasiparticle. In this part all details of the theory was derived, step by step, in blackboard. I hope all participants appreciated this. Then I used the last hour to discuss very quickly some further developments of the pairing theory, including broken pair approximation, our nucleon-pair approximation, Fermion dynamical symmetry model and the interacting boson model.

One thing I hope that all participants should well receive is why and how pairing correlation comes into nuclear theory. The logic is as follows. The dominant part of the nuclear force is of short-range nature (and attractive). This leads to the rough shape of the single-particle potential, which is more or less similar to the density distribution of nucleons in atomic nucleus. The residual part in the basis of the mean field, still, is largely a short-range interaction. This interaction can be simplified, and simulated pretty well by the delta interaction. Many properties of effective interactions in the nuclear shell model calculations can be reasonably traced back to the delta interaction. Of course, the delta interaction can be improved, and some modifications such as surface delta interactions, isospin dependent delta interactions, are introduced and studied in many papers. In order to get insights of physics, and encouraged by the features of delta interactions, the pairing Hamiltonian was suggested. One can say, of course, the pairing interaction is a simplification of the delta interaction.

The pairing correlation of a single- j shell is a very nice model. This is one of the most beautiful formulation in nuclear theory, in particular the quasispin theory. For degenerate single-particle configuration, the generalization is straightforward.

When the single-particle splitting is too large, one can go to the BCS method. The BCS was first suggested in the study of superconductivity of metal conductors. This theory has a very similar feature as the Paring theory in nuclear physics. That is why Professor Arima said many times that nuclear physicists wasted one opportunity of Nobel Prize, and that is also why this approach was applied to nuclear physics promptly, i.e., right after the BCS paper was published. The BCS wave function is composed of S pairs, which we have shown by simple examples. The treatment of BCS ground state as a vacuum of annihilation operator of “quasiparticle” is an interesting idea. Quasiparticle theory is very useful in applications.

In these lectures I did not go to the generalized seniority scheme. One can refer to the fat book by Igal Talmi for this. Either, I did not go the Bogoliubov transformation, and one may refer to the book by Peter Ring.

Below I present my lecture notes (in Chinese). Most of these notes were actually written during my stay in the hotel. I did not check the formulas, there might be numerous typos and mistakes. For the discussion of further developments of pair models, I refer to Section 2.4 of my review paper (Physics Reports, Volume 545, page 1, published in 2014).

I also welcome any questions from all of you concerning the content of my lectures by email:
ymzhao@sjtu.edu.cn

第七章 配对关联

配对现象是自然界中很普遍的现象.

7.1 准自旋算符

当两个核子耦合为角动量为零时, 我们就说这两个核子是配对的. 对于单轨道情况, 根据式(5.139), 两个核子耦合为总自旋为零的归一化波函数为

$$\Psi_{J=0,M=0} = \frac{1}{\sqrt{2}} \left(a_j^\dagger \times a_j^\dagger \right)^{(0)} |0\rangle = \frac{1}{\sqrt{2(2j+1)}} \sum_m (-)^{j-m} a_{jm}^\dagger a_{j-m}^\dagger |0\rangle. \quad (7.1)$$

因为费米子产生算符的交换对称性以及 m 为半整数, 显然我们有

$$\begin{aligned} (-)^{j-1/2} a_{j-1/2}^\dagger a_{j+1/2}^\dagger &\equiv (-)^{j-(-1/2)} a_{j+1/2}^\dagger a_{j-1/2}^\dagger, \\ (-)^{j-3/2} a_{j-3/2}^\dagger a_{j+3/2}^\dagger &\equiv (-)^{j-(-3/2)} a_{j+3/2}^\dagger a_{j-3/2}^\dagger, \dots, \end{aligned}$$

即对于任意 m , 有

$$(-)^{j-m} a_{j+m}^\dagger a_{j-m}^\dagger \equiv (-)^{j-(-m)} a_{j-m}^\dagger a_{j+m}^\dagger,$$

因此我们可以定义

$$S_+ = \sum_{m>0} (-)^{j-m} a_{jm}^\dagger a_{j-m}^\dagger \equiv \sum_{m<0} (-)^{j-m} a_{jm}^\dagger a_{j-m}^\dagger = \frac{1}{2} \sum_m (-)^{j-m} a_{jm}^\dagger a_{j-m}^\dagger.$$

利用上式, 我们把式(7.1) 写为

$$\Psi_{J=0,M=0} = \sqrt{\frac{2}{2j+1}} S_+ |0\rangle. \quad (7.2)$$

对于 S_+ 取厄米共轭, 我们定义 S_- 为

$$S_- = (S_+)^\dagger = \sum_{m>0} (-)^{j-m} a_{j-m} a_{jm}.$$

下面我们计算 S_- 与 S_+ 的对易式

$$\begin{aligned} [S_-, S_+] &= S_- S_+ - S_+ S_- \\ &= \sum_{m>0, m'>0} (-)^{j-m} (-)^{j-m'} a_{j-m'} a_{jm'} a_{jm}^\dagger a_{j-m}^\dagger \\ &\quad - \sum_{m>0, m'>0} (-)^{j-m} (-)^{j-m'} a_{jm}^\dagger a_{j-m}^\dagger a_{j-m'} a_{jm'} . \end{aligned} \quad (7.3)$$

为此我们利用费米子对易式(2.253)、(2.254)、(2.255)、(2.257)，处理上式中第一项

$$\begin{aligned} &(-)^{j-m} (-)^{j-m'} a_{j-m'} a_{jm'} a_{jm}^\dagger a_{j-m}^\dagger \\ &= (-)^{j-m} (-)^{j-m'} a_{j-m'} (\delta_{mm'} - a_{jm}^\dagger a_{jm'}) a_{j-m}^\dagger \\ &= \delta_{mm'} a_{j-m'} a_{j-m}^\dagger - (-)^{j-m} (-)^{j-m'} a_{j-m'} a_{jm}^\dagger a_{jm'} a_{j-m}^\dagger \\ &= \delta_{mm'} - \delta_{mm'} a_{j-m}^\dagger a_{j-m'} - (-)^{j-m} (-)^{j-m'} (\delta_{-m'm} - a_{jm}^\dagger a_{j-m'}) a_{jm'} a_{j-m}^\dagger \\ &= \delta_{mm'} - \delta_{mm'} a_{j-m}^\dagger a_{j-m'} + \delta_{-m'm} a_{jm'} a_{j-m}^\dagger \\ &\quad + (-)^{j-m} (-)^{j-m'} a_{jm}^\dagger a_{j-m'} a_{jm'} a_{j-m}^\dagger \\ &= \delta_{mm'} + \delta_{-m'm} - \delta_{mm'} a_{j-m}^\dagger a_{j-m'} - \delta_{-m'm} a_{j-m}^\dagger a_{jm'} \\ &\quad + (-)^{j-m} (-)^{j-m'} a_{jm}^\dagger a_{j-m'} a_{jm'} a_{j-m}^\dagger . \end{aligned} \quad (7.4)$$

类似地处理上式中的最后一项

$$\begin{aligned} &(-)^{j-m} (-)^{j-m'} a_{jm}^\dagger a_{j-m'} a_{jm'} a_{j-m}^\dagger \\ &= (-)^{j-m} (-)^{j-m'} a_{jm}^\dagger a_{j-m'} (\delta_{-m'm} - a_{j-m}^\dagger a_{jm'}) \\ &= -\delta_{-m'm} a_{jm}^\dagger a_{j-m'} - (-)^{j-m} (-)^{j-m'} a_{jm}^\dagger a_{j-m'} a_{j-m}^\dagger a_{jm'} \\ &= -\delta_{-m'm} a_{jm}^\dagger a_{j-m'} - \delta_{mm'} a_{jm}^\dagger a_{jm'} + (-)^{j-m} (-)^{j-m'} a_{jm}^\dagger a_{j-m}^\dagger a_{j-m'} a_{jm'} \end{aligned} \quad (7.5)$$

整理以上两式，代入式(7.3)，注意到式(7.3)中 $m > 0, m' > 0$ ，此时 $\delta_{-mm'} = 0$ 。我们由此得到

$$\begin{aligned} [S_-, S_+] &= S_- S_+ - S_+ S_- \\ &= \sum_{m>0, m'>0} \left[\delta_{mm'} - \delta_{mm'} a_{j-m}^\dagger a_{j-m'} - \delta_{mm'} a_{jm}^\dagger a_{jm'} \right] \\ &= \frac{2j+1}{2} - \sum_m a_{jm}^\dagger a_{jm} = \Omega_j - N_j , \end{aligned} \quad (7.6)$$

式中

$$\Omega_j = \frac{2j+1}{2}, \quad N_j = \sum_m a_{jm}^\dagger a_{jm}. \quad (7.6)$$

我们定义算符

$$S_z = \frac{1}{2} [N_j - \Omega_j].$$

我们有

$$[S_-, S_+] = -2S_z, \quad [S_+, S_-] = 2S_z. \quad (7.7)$$

下面我们计算下面的对易式

$$\begin{aligned} [S_z, S_+] &= \left[\frac{1}{2} \left(-\Omega_j + \sum_{m'} a_{jm'}^\dagger a_{jm'} \right), \sum_{m>0} (-)^{j-m} a_{jm}^\dagger a_{j-m}^\dagger \right] \\ &= \frac{1}{2} \sum_{m'} \sum_{m>0} \left[a_{jm'}^\dagger a_{jm'}, (-)^{j-m} a_{jm}^\dagger a_{j-m}^\dagger \right] \\ &= \frac{1}{2} \sum_{m'} \sum_{m>0} \left((-)^{j-m} a_{jm'}^\dagger a_{jm'} a_{jm}^\dagger a_{j-m}^\dagger - (-)^{j-m} a_{jm}^\dagger a_{j-m}^\dagger a_{jm'}^\dagger a_{jm'} \right). \end{aligned} \quad (7.8)$$

我们处理上式括号中的第一项

$$\begin{aligned} &(-)^{j-m} a_{jm'}^\dagger a_{jm'} a_{jm}^\dagger a_{j-m}^\dagger = (-)^{j-m} a_{jm'}^\dagger (\delta_{mm'} - a_{jm}^\dagger a_{jm'}) a_{j-m}^\dagger \\ &= (-)^{j-m} \delta_{mm'} a_{jm'}^\dagger a_{j-m}^\dagger - (-)^{j-m} a_{jm'}^\dagger a_{jm}^\dagger (\delta_{-mm'} - a_{j-m}^\dagger a_{jm'}) \\ &= (-)^{j-m} \left[\delta_{mm'} a_{jm'}^\dagger a_{j-m}^\dagger - \delta_{-mm'} a_{jm'}^\dagger a_{jm}^\dagger + a_{jm'}^\dagger a_{jm}^\dagger a_{j-m}^\dagger a_{jm'} \right]. \end{aligned}$$

把上式代入式(7.8) 得到

$$\begin{aligned} [S_z, S_+] &= \frac{1}{2} \left[\sum_{m>0} (-)^{j-m} a_{jm}^\dagger a_{j-m}^\dagger - \sum_{m>0} (-)^{j-m} a_{j-m}^\dagger a_{jm}^\dagger \right] \\ &= \sum_{m>0} (-)^{j-m} a_{jm}^\dagger a_{j-m}^\dagger = S_+. \end{aligned} \quad (7.9)$$

类似地, 我们计算对易式

$$\begin{aligned} [S_z, S_-] &= \left[\frac{1}{2} \left(-\Omega_j + \sum_{m'} a_{jm'}^\dagger a_{jm'} \right), \sum_{m>0} (-)^{j-m} a_{j-m} a_{jm} \right] \\ &= \frac{1}{2} \sum_{m'} \sum_{m>0} (-)^{j-m} \left(a_{jm'}^\dagger a_{jm'} a_{j-m} a_{jm} - a_{j-m} a_{jm} a_{jm'}^\dagger a_{jm'} \right). \end{aligned} \quad (7.10)$$

上式最后一步右边括号内第二项为

$$\begin{aligned}
 & a_{j-m} a_{jm} a_{jm'}^\dagger a_{jm'} = a_{j-m} (\delta_{mm'} - a_{jm'}^\dagger a_{jm}) a_{jm'} \\
 &= \delta_{mm'} a_{j-m} a_{jm'} - a_{j-m} a_{jm'}^\dagger a_{jm} a_{jm'} \\
 &= \delta_{mm'} a_{j-m} a_{jm'} - (\delta_{-mm'} - a_{jm'}^\dagger a_{j-m}) a_{jm} a_{jm'} \\
 &= \delta_{mm'} a_{j-m} a_{jm'} - \delta_{-mm'} a_{j-m} a_{jm} a_{jm'} + a_{jm'}^\dagger a_{j-m} a_{jm} a_{jm'} .
 \end{aligned}$$

把上式代入式(7.10) 得到

$$[S_z, S_-] = \frac{1}{2} \left[- \sum_{m>0} (-)^{j-m} a_{j-m} a_{jm} + \sum_{m>0} (-)^{j-m} a_{jm} a_{j-m} \right] = -S_- \quad (7.11)$$

令 $S_+ = S_x + iS_y$, $S_- = S_x - iS_y$, $\vec{S} = \vec{e}_x S_x + \vec{e}_y S_y + \vec{e}_z S_z$. 我们由式(7.7)、(7.9)、(7.11) 容易证明

$$\vec{S} \times \vec{S} = i\vec{S}, \quad (7.12)$$

即 \vec{S} 满足角动量对易式. 例如我们有

$$\begin{aligned}
 [S_x, S_y] &= \frac{1}{4i} [S_+ + S_-, (S_+ - S_-)] = \frac{1}{4i} ([S_+, -S_-] + [S_-, -S_+]) \\
 &= \frac{1}{4i} (-2S_z - 2S_z) = iS_z .
 \end{aligned} \quad (7.13)$$

如前所述, S_z 作用到一个态上的本征值为 $(N_j - \Omega_j)/2$, 是半整数或整数. 因为这些原因, 人们常把这样定义的 \vec{S} 称为准自旋算符. 我们有

$$S_+ S_- = (S_x + iS_y)(S_x - iS_y) = S_x^2 + S_y^2 - i[S_x, S_y] = \vec{S}^2 - S_z^2 + S_z. \quad (7.14)$$

S_z 是 \vec{S} 的一个分量, 本征值为 $\frac{N_j - \Omega_j}{2}$, 一般情况我们考虑 $N < \Omega_j$ (核子数填充前半壳) 情况, 而 $N > \Omega_j$ 时作空穴处理, 因此 S_{\min} 取 $\frac{\Omega_j - N_j}{2}$. 另一方面, 我们可以把 \vec{S} 写为

$$\vec{S} = \sum_m \vec{S}^{(m)}, \quad \vec{S}_+^{(m)} = (-)^{j-m} a_{jm}^\dagger a_{j-m}^\dagger, \quad \vec{S}_-^{(m)} = \left(\vec{S}_+^{(m)} \right)^\dagger.$$

可以证明 $\vec{S}^{(m)}$ 对应 $\frac{1}{2}$ 自旋, 因此 S_{\max} 为 $\frac{\Omega_j}{2}$. 基于这些讨论我们知道, S 的取值为

$$S = \frac{\Omega_j - N_j}{2}, \frac{\Omega_j - N_j}{2} + 1, \frac{\Omega_j - N_j}{2} + 2, \dots, \frac{\Omega_j}{2}.$$

我们可以换一种标记方法

$$S = \frac{\Omega_j}{2}, \frac{\Omega_j - 2}{2}, \frac{\Omega_j - 4}{2}, \dots, \frac{\Omega_j - v}{2}, \dots, \frac{\Omega_j}{2}.$$

v 称为seniority 量子数. 下面我们将看到, v 对应非 S 对的核子个数.

利用seniority 量子数, 我们得到关于 S_+S_- 的本征方程

$$\begin{aligned} & S_+S_- \left(\left| S = \frac{\Omega - v}{2}, S_z = \frac{\Omega - N}{2} \right. \right) \\ &= \frac{\Omega - v}{2} \left(\frac{\Omega - v}{2} + 1 \right) \\ &\quad - \frac{\Omega - N}{2} \left(\frac{\Omega - N}{2} + 1 \right) \left(\left| S = \frac{\Omega - v}{2}, S_z = \frac{\Omega - N}{2} \right. \right). \end{aligned} \quad (7.15)$$

7.2 单轨道情形下对力哈密顿量和波函数

我们强调, 原子核内核子之间的相互作用主要是短程吸引, 所以常用 δ 相互作用来近似. δ 势极好地表述核力的短程性, 给出的结果与真实相互作用的结果在许多情况下都很相似, 如图5.1 所示. 两同类核子处 $J = 0$ 最低, 在 $J = 0\text{-}2$ 之间有一个很大的能隙后, $J = 2, 4, 6 \dots$ 随着角动量增加, 能量依次增加, $J = 4, 6, 8$ 几个态基本上能量的绝对值很小, 即能量接近于零.

尽管 δ 力已经比较简单, 然而实际计算也不容易. 因为两体矩阵元上面提到的这种性质, 沿着这个方面的一个简化是对力. 与 δ 势类似的是, 对力是当两核子只有在波函数重叠特别大时才存在. 对力对应的组态能量为: 只有 $J = 0$ 的能量被降低, 其它态不受影响. 对力是模拟两个全同核子处于 $|j^2, J = 0\rangle$ 的组态时很强的吸引势, 可以看做 δ 力一个粗略的近似. 我们定义

$$\langle j_1 j_2 J | V_{\text{pairing}} | j_3 j_3 J' \rangle = -G \sqrt{(j_1 + 1/2)(j_2 + 1/2)} \delta_{j_1 j_2} \delta_{j_3 j_4} \delta_{J0} \delta_{J'0}, \quad (7.16)$$

称为对力相互作用; 注意这个定义允许“非对角”作用, 即把一个轨道的 $J = 0$ 配对变成另外一个轨道的 $J = 0$ 配对. 这对于偶偶核 $J = 0$ 基态和第一个 $J^{\text{parity}} = 2^+$ 态之间配对能隙以及对力关联是重要的. 对力取这种形式的理由是受到 δ 相互作用的启发, 我们在两体相互作用的讨论中知道

$$\begin{aligned} & \langle j^2, J = 0 | -V_0 \delta(\vec{r}_1 - \vec{r}_2) | (j')^2, J = 0 \rangle \\ &= - \left(\frac{V_0}{4\pi} (-)^{l+l'} \int R_{nlj}^2(r) R_{n'l'j'}^2(r) r^2 dr \right) \sqrt{(j + 1/2)(j' + 1/2)}. \end{aligned}$$

这里我们假定

$$G = \frac{V_0}{4\pi} (-)^{l+l'} \int R_{nlj}^2(r) R_{n'l'j'}^2(r) r^2 dr ,$$

与轨道无关; 除了相因子以外, 径向积分只要对于轨道不敏感上述假定就是很好的. 因此我们说, 对力可以看作为 δ 力的近似. 在单轨道情况下下, 对力定义为

$$\langle j^2 J | V_{\text{pairing}} | j^2 J' \rangle = -\frac{G}{2} (2j+1) \delta_{J0} \delta_{J'0} . \quad (7.17)$$

把上式代入壳模型哈密顿量式(5.143)中, 得到对力哈密顿量为

$$\begin{aligned} H_{\text{pairing}} &= \langle j^2 J = 0 | V | j^2 J = 0 \rangle A(jj)^{(0)\dagger} A(jj)^{(0)} \\ &= -\frac{G}{2} (2j+1) \delta_{J0} \frac{1}{\sqrt{2}} (a_j^\dagger a_j)^{(0)} (-) \frac{1}{\sqrt{2}} (a_j a_j)^{(0)} \\ &= \frac{1}{4} G \sum_{mm'} (-)^{j-m} (-)^{j-m'} a_{jm}^\dagger a_{j-m}^\dagger a_{jm'} a_{j-m'} \\ &= -G \sum_{m>0, m'>0} (-)^{j-m} (-)^{j-m'} a_{jm}^\dagger a_{j-m}^\dagger a_{j-m'} a_{jm'} \\ &= -GS_+ S_- . \end{aligned} \quad (7.18)$$

这是在教科书中最常见的对力哈密顿量的形式(如Greiner 教科书、Lawson 教科书、Ring 教科书、Heyde 教科书、Casten 书). 其它形式于此有很小的差异, 例如Talmi fat book(相差2倍因子).

设 $|0\rangle$ 为价核子真空态, 因为 $H_{\text{pairing}}|0\rangle = 0$, 我们有

$$\begin{aligned} H_{\text{pairing}}(S_+)^n |0\rangle &= [H_{\text{pairing}}, (S_+)^n] |0\rangle + (S_+)^n H_{\text{pairing}} |0\rangle \\ &= [H_{\text{pairing}}, (S_+)^n] |0\rangle . \end{aligned} \quad (7.19)$$

我们计算对易式

$$[H_{\text{pairing}}, S_+] , [H_{\text{pairing}}, (S_+)^2] , \dots , [H_{\text{pairing}}, (S_+)^n] .$$

利用式(7.6) 我们得到

$$[H_{\text{pairing}}, S_+] = -GS_+ [S_-, S_+] = -GS_+ (\Omega_j - N_j) . \quad (7.20)$$

$$\begin{aligned} [H_{\text{pairing}}, (S_+)^2] &= [H_{\text{pairing}}, S_+] S_+ + S_+ [H_{\text{pairing}}, S_+] \\ &= -GS_+ (\Omega_j - N_j) S_+ - G(S_+)^2 (\Omega_j - N_j) . \end{aligned} \quad (7.21)$$

类似地,

$$\begin{aligned}
 & [H_{\text{pairing}}, (S_+)^n] \\
 = & [H_{\text{pairing}}, S_+] (S_+)^{n-1} + S_+ [H_{\text{pairing}}, S_+] (S_+)^{n-2} \\
 & + (S_+)^2 [H_{\text{pairing}}, S_+] (S_+)^{n-3} + \cdots + (S_+)^{n-1} [H_{\text{pairing}}, S_+] . \quad (7.22)
 \end{aligned}$$

由式(7.19) 和上式我们得到

$$\begin{aligned}
 & H_{\text{pairing}}(S_+)^n |0\rangle \\
 = & -GS_+(\Omega_j - N_j)(S_+)^{n-1} |0\rangle - G(S_+)^2(\Omega_j - N_j)(S_+)^{n-2} |0\rangle \\
 & -G(S_+)^3(\Omega_j - N_j)(S_+)^{n-3} |0\rangle - \cdots - G(S_+)^n(\Omega_j - N_j) |0\rangle \\
 = & -G[(\Omega_j - 2(n-1)) + (\Omega_j - 2(n-2)) + (\Omega_j - 2(n-3)) \\
 & + \cdots + (\Omega_j - 4) + (\Omega_j - 2) + (\Omega_j - 0)](S_+)^n |0\rangle \\
 = & -G[n\Omega_j + (n-1)n](S_+)^n |0\rangle = -Gn(\Omega_j - n + 1)(S_+)^n |0\rangle . \quad (7.23)
 \end{aligned}$$

在上式中我们利用了

$$N_j(S_+)^n |0\rangle = 2n(S_+)^n |0\rangle . \quad (7.24)$$

上式的结论是很明显的, 因为 N_j 是粒子数算符, $(S_+)^n |0\rangle$ 态上有 $2n$ 个粒子. 当然有些教科书(如Greiner 教科书)中还附带了一些练习, 如在Greiner 教科书中证明了 $[S_+, N_j] = -2S_+$, 即 $N_j S_+ = S_+(N_j + 2)$, 也可以由此证明上式; 但没有带来更多的改进.

在 $(S_+)^n |0\rangle$ 状态中, 所有核子都两两耦合角动量为零. 我们把这种状态称为 seniority $v = 0$ 的状态, 在中文教科书中把这个 v 量子数按照英文意思称为先辈数、或按照发音翻译为辛弱数, 其原文vetek来自于希伯来语, 英文意思为seniority. 在 l^n 组态的seniority 方法是Racah 在1943年引入的[51], 而在 j^n 组态中的seniority 方法是Racah 在1952 年[55]、Flowers 在1952 年[56]独立引入的.

下面我们计算seniority $v = 0$ 的状态 $(S_+^\dagger)^n |0\rangle$ 的归一化系数, 即

$$|j^{2n}, v = 0, I = 0\rangle = \Lambda_n (S_+^\dagger)^n |0\rangle , \quad \Lambda_n^{-2} = \langle 0 | (S_-^\dagger)^n (S_+^\dagger)^n |0\rangle .$$

由此我们有

$$\begin{aligned}
 H_{\text{pairing}} B_J^\dagger |0\rangle &= [H_{\text{pairing}}, B_J^\dagger] |0\rangle \\
 &= -GS_+ \left(\sum_{m>0} \sum_{m'>0} C_{jm',j-m'}^{00} C_{jm,j-m}^{J0} \delta_{mm'} (1 - a_{j-m}^\dagger a_{j-m'} - a_{jm}^\dagger a_{jm'}) \right) |0\rangle \\
 &= -GS_+ \sum_m C_{jm,j-m}^{00} C_{jm,j-m}^{J0} |0\rangle = -GS_+ \delta_{0J} |0\rangle = 0,
 \end{aligned} \tag{7.27}$$

上式第一步利用了 $S_-|0\rangle = 0$, 第二步利用式(7.4)-(7.5) 的结果, 第三步利用了 a_{jm} 作用于 $|0\rangle$ 的结果为零, 第四步利用了 Clebsch-Gordan 系数的正交性, 最后一步利用了 $J \neq 0$. 上式其实可以这样理解, 对力算符仅对 $J = 0$ 的两个核子起作用, 如果 $J \neq 0$ 则没有作用, 或者说能量为零.

由算符 B_J^\dagger 以及 $(S_+)^n$ 我们可以构造出一系列 seniority 量子数 $v = 2$ (有且只有两个核子耦合为 $J \neq 0$) 的态,

$$B_J^\dagger |0\rangle, S_+ B_J^\dagger |0\rangle, (S_+)^2 B_J^\dagger |0\rangle, (S_+)^3 B_J^\dagger |0\rangle, \dots, (S_+)^{(n-1)} B_J^\dagger |0\rangle. \tag{7.28}$$

利用式(7.20)、(7.21)、(7.22), 我们得到对力哈密顿量 H_{pairing} 作用在 seniority 等于 2 的状态上的结果为

$$\begin{aligned}
 H_{\text{pairing}} B_J^\dagger |0\rangle &= 0, \\
 H_{\text{pairing}} S_+ B_J^\dagger |0\rangle &= -GS_+(\Omega_j - N_j) B_J^\dagger |0\rangle = -G(\Omega_j - 2) S_+ B_J^\dagger |0\rangle, \\
 H_{\text{pairing}} (S_+)^2 B_J^\dagger |0\rangle &= [-GS_+(\Omega_j - N_j) S_+ - G(S_+)^2 (\Omega_j - N_j)] B_J^\dagger |0\rangle \\
 &= -G(\Omega_j - 4 + \Omega_j - 2) B_J^\dagger (S_+)^2 B_J^\dagger |0\rangle,
 \end{aligned}$$

与式(7.23)类似, 我们得到

$$\begin{aligned}
 H_{\text{pairing}} (S_+)^{(n-1)} B_J^\dagger |0\rangle &= [H_{\text{pairing}}, (S_+)^{(n-1)}] B_J^\dagger |0\rangle \\
 &= [H_{\text{pairing}}, (S_+)] (S_+)^{(n-2)} B_J^\dagger |0\rangle + S_+ [H_{\text{pairing}}, (S_+)] (S_+)^{(n-3)} B_J^\dagger |0\rangle \\
 &\quad (S_+)^2 [H_{\text{pairing}}, (S_+)] (S_+)^{(n-4)} B_J^\dagger |0\rangle + \dots + (S_+)^{(n-2)} [H_{\text{pairing}}, (S_+)] B_J^\dagger |0\rangle \\
 &= -GS_+ [(\Omega_j - N_j)(S_+)^{(n-2)} + S_+(\Omega_j - N_j)(S_+)^{(n-3)} \\
 &\quad (S_+)^2 (\Omega_j - N_j)(S_+)^{(n-4)} + \dots + (S_+)^{(n-2)} (\Omega_j - N_j)] B_J^\dagger |0\rangle \\
 &= -G[\Omega_j - 2(n-1) + \Omega_j - 2(n-2) + \dots + \Omega_j - 2] (S_+)^{(n-1)} B_J^\dagger |0\rangle \\
 &= -G(n-1)(\Omega_j - n) (S_+)^{(n-1)} B_J^\dagger |0\rangle.
 \end{aligned} \tag{7.29}$$

利用式(7.6), 我们得到

$$\begin{aligned}
& \langle 0 | \left(S_-^\dagger \right)^n \left(S_+^\dagger \right)^n | 0 \rangle = \langle 0 | \left(S_-^\dagger \right)^{n-1} \left[\Omega_j - \hat{N}_j + S_+ S_- \right] \left(S_+^\dagger \right)^{n-1} | 0 \rangle \\
= & \langle 0 | \left(S_-^\dagger \right)^{n-1} \left[(\Omega_j - (2n-2)) \left(S_+^\dagger \right)^{n-1} | 0 \rangle \right. \\
& \quad \left. + \left(S_+ (\Omega_j - \hat{N}_j) + (S_+)^2 S_- \right) \left(S_+^\dagger \right)^{n-2} | 0 \rangle \right] \\
= & \langle 0 | \left(S_-^\dagger \right)^{n-1} \left[(\Omega_j - (2n-2)) \left(S_+^\dagger \right)^{n-1} | 0 \rangle \right. \\
& \quad \left. + ((\Omega_j - 2n+4) S_+ + (S_+)^2 S_-) \left(S_+^\dagger \right)^{n-2} | 0 \rangle \right] \\
= & \langle 0 | \left(S_-^\dagger \right)^{n-1} [\Omega_j - (2n-2) + \Omega_j - (2n-4) + \cdots + \Omega_j] \left(S_+^\dagger \right)^{n-1} | 0 \rangle \\
= & \langle 0 | \left(S_-^\dagger \right)^{n-1} n [\Omega_j - (n-1)] \left(S_+^\dagger \right)^{n-1} | 0 \rangle .
\end{aligned}$$

重复这个过程, 我们可得

$$\begin{aligned}
& \langle 0 | \left(S_-^\dagger \right)^n \left(S_+^\dagger \right)^n | 0 \rangle \\
= & n [\Omega_j - (n-1)] \cdot (n-1) [\Omega_j - (n-2)] \cdots 1 [\Omega_j - 0] \\
= & n! \frac{(2j+1)!!}{2^n (2j+1-2n)!!} .
\end{aligned}$$

由此得到归一化的seniority $v = 0$ 的波函数形式为

$$| j^{2n}, v = 0, I = 0 \rangle = \sqrt{\frac{2^n (2j+1-2n)!!}{n! (2j+1)!!}} \left(S_+^\dagger \right)^n | 0 \rangle . \quad (7.25)$$

我们定义

$$B_J^\dagger = \frac{1}{2} \sum_m C_{jm,j-m}^{J0} a_{jm}^\dagger a_{j-m}^\dagger = \sum_{m>0} C_{jm,j-m}^{J0} a_{jm}^\dagger a_{j-m}^\dagger . \quad (7.26)$$

B_J^\dagger 把两个核子耦合为总角动量为 J ($J \neq 0$) 的状态. 由 $[S_+, B_J^\dagger] = 0$, 我们得到

$$[H_{\text{pairing}}, B_J^\dagger] = -G S_+ \sum_{m>0} \sum_{m'>0} C_{jm',j-m'}^{00} C_{jm,j-m}^{J0} \left[a_{jm'} a_{j-m'}, a_{jm}^\dagger a_{j-m}^\dagger \right] .$$

上式表明, $(S_+)^{(n-1)}B_J^\dagger|0\rangle$ 也是对力哈密顿量的本征态, 这些态上seniority 量子数 $v = 2$.

类似于处理seniority $v = 0$ 的情况, 我们求 $v = 2$ 波函数的归一化系数, 为此先求重叠

$$\langle 0 | B_J(S_-)^{(n-1)}(S_+)^{(n-1)}B_J^\dagger | 0 \rangle .$$

此时已经有了两个核子占据在 m_1 和 m_2 上, 因为 S 对是由两个 m 相反的核子给出, 因此核子只能占据 $m \neq \pm|m_1|, m \neq \pm|m_2|$ 态上, 因此 $2j + 1$ 变为 $2j + 1 - 4$, n 变为 $n - 1$. 因此我们得到归一化的 $v = 2$ 波函数为

$$\sqrt{\frac{2^{n-1}(2j-1-n)!!}{(n-1)!(2j-3)!!}}(S_+)^{(n-1)}B_J^\dagger|0\rangle .$$

采用seniority 量子数, 我们把粒子数等于 $2n$, seniority 为 v 的状态标记为 $|N = 2n, v, \alpha, J\rangle$, 这里 α 为附加量子数. 对于 $v = 0, 2$ 单轨道情况, 不需要附加量子数.

$$\begin{aligned} v = 0, \quad & |N = 2n, v = 0, \alpha, J\rangle = (S_+)^n|0\rangle , \\ v = 2, \quad & |N = 2n, v = 2, \alpha, J\rangle = (S_+)^{(n-1)}B_J^\dagger|0\rangle . \end{aligned}$$

我们重复上面过程, 构造 $(B_J^\dagger B_{J'}^\dagger)'|0\rangle$. 这里我们在括号上打了一个撇号, 表示考虑了过完备(overcompleteness)、正交性等. 我们证明 $[H_{\text{pairing}}, (B_J^\dagger B_{J'}^\dagger)']|0\rangle = 0$, 容易得到

$$\begin{aligned} H_{\text{pairing}}B_{J_1}^\dagger B_{J_2}^\dagger|0\rangle &= [H_{\text{pairing}}, B_{J_1}^\dagger B_{J_2}^\dagger]|0\rangle \\ &= [H_{\text{pairing}}, B_{J_1}^\dagger]B_{J_2}^\dagger|0\rangle + B_{J_1}^\dagger[H_{\text{pairing}}, B_{J_2}^\dagger]|0\rangle \\ &= -GS_+\left(\frac{1}{2}\sum_m C_{jm,j-m}^{00}C_{jm,j-m}^{J0}B_{J_2}^\dagger|0\rangle\right) \\ &\quad -GS_+\left(\frac{1}{2}\sum_m C_{jm,j-m}^{00}C_{jm,j-m}^{J0}(-N_j)\right)B_{J_2}^\dagger|0\rangle + 0 = 0 , \end{aligned}$$

上式第三步利用了式(7.27) 第二步的结果. 从这个过程可以知道

$$H_{\text{pairing}}\left(B_{J_1}^\dagger B_{J_2}^\dagger \cdots B_{J_t}^\dagger\right)'|0\rangle \equiv 0 . \quad (7.30)$$

这也是很容易理解的, 因为对力仅作用在 $J = 0$ 的核子配对上, $J \neq 0$ 时没有作用, 即本征值等于 0.

重复式(7.29)的过程, 我们得到

$$H_{\text{pairing}}(S_+)^{(n-2)} \left(B_{J_1}^\dagger B_{J_2}^\dagger \right)' |0\rangle = -G(n-2)(\Omega-n-1)(S_+)^{(n-2)} B_{J_1}^\dagger B_{J_2}^\dagger |0\rangle, \quad (7.31)$$

更一般情况, 对于 $v = 2t$ 时

$$\begin{aligned} & H_{\text{pairing}}(S_+)^{(n-t)} B_{J_1}^\dagger \cdots B_{J_t}^\dagger |0\rangle \\ &= -G(n-t)(\Omega-n-t+1)(S_+)^{(n-t)} B_{J_1}^\dagger \cdots B_{J_t}^\dagger |0\rangle, \end{aligned} \quad (7.32)$$

seniority 为 v 的态与 $v = 0$ 的态之间能量差为

$$E(v = 2t) - E(v = 0) = Gt(\Omega_j - t + 1).$$

注意同一个 seniority 的所有状态是能量兼并的, 与 J 和附加量子数无关. $v = 2$ 时,

$$E(v = 2) - E(v = 0) = G\Omega_j.$$

如上面所述,

$$\begin{aligned} S_z|N = v, v, \alpha, J\rangle &= \frac{N_j - \Omega}{2}|N = v, v, \alpha, J\rangle, \quad S_-|N = v, v, \alpha, J\rangle = 0, \\ \vec{S}^2|N = v, v, \alpha, J\rangle &= [S_+S_- + S_z(S_z - 1)]|N = v, v, \alpha, J\rangle \\ &= \frac{\Omega_j - v}{2} \left(\frac{\Omega_j - v}{2} + 1 \right) |N = v, v, \alpha, J\rangle = S_v^2|N = v, v, \alpha, J\rangle. \end{aligned}$$

下面为方便我们令 $v = 2t$, 这说明 $|N = v, v, \alpha, J\rangle$ 是 \vec{S}^2 和 S_z 的共同本征函数. 因为 S_+ 与 \vec{S}^2 对易, 在上式中两边作用算符 $(S_+)^{(n-t)}$, 我们有

$$\begin{aligned} & (S_+)^{(n-t)} \vec{S}^2 |N = v, v, \alpha, J\rangle = \vec{S}^2 (S_+)^{(n-t)} |N = v, v, \alpha, J\rangle \\ &= \frac{\Omega_j - v}{2} \left(\frac{\Omega_j - v}{2} + 1 \right) (S_+)^{(n-t)} |N = v, v, \alpha, J\rangle. \end{aligned}$$

即 $(S_+)^{(n-t)} |N = v, v, \alpha, J\rangle$ 也是 \vec{S}^2 的本征态, 并且本征值不变. 当然 S_z 作用在 $(S_+)^{(n-t)} |N = v, v, \alpha, J\rangle$ 的本征值变化了; 其本征值由 $\frac{2t-\Omega_j}{2}$ 变为 $\frac{2n-\Omega_j}{2}$. 所以

然后做变分

$$\delta\langle S^n J | H | S^n J \rangle = 0.$$

这里的 S 成分不象单粒子能级简并情形下那么容易得到, 变分无法得到解析结果; 而这种变分却是现在配对理论得到 S 配对结构系数标准做法之一.

一个出路是凝聚态物理中关于超导体的BCS 理论. 当BCS 理论在1957 年提出后, A. Bohr, B. R. Mottelson 和D. Pines 在1958 年、 Soloviev 在1958年、 Belyaev 在1959人提出可以用BCS 理论近似给出单满壳偶偶核基态. 这里试探波函数为

$$\psi = \prod_{j m>0} \left[u_j + (-)^{j-m} v_j a_{jm}^\dagger a_{j-m}^\dagger \right] |0\rangle. \quad (7.33)$$

式中试探波函数不满足粒子数守恒, 这是这种方法的最大弱点. 在金属超导现象中因为电子库珀对(Cooper pair)很多, 这个不守恒带来的影响是可以忽略的, 正如正则系综在统计物理中一样. 然而在核物理中价核子数比较小, 粒子数不守恒带来的影响比较严重. 上式中的 u_j 、 v_j 通过变分得到, 下面我们将看到这些系数的意义. 我们首先看看这个试探波函数的特点.

首先所有粒子都是 S 配对. 为了看到这一点, 我们考虑一个 j 轨道, 令 $j = 3/2$, 我们有

$$\begin{aligned} & \prod_{m>0} \left[u + (-)^{\frac{3}{2}-m} v a_m^\dagger a_{-m}^\dagger \right] |0\rangle \\ &= \left[u + (-)^{\frac{3}{2}-\frac{3}{2}} v a_{\frac{3}{2}}^\dagger a_{-\frac{3}{2}}^\dagger \right] \left[u + (-)^{\frac{3}{2}-\frac{1}{2}} v a_{\frac{1}{2}}^\dagger a_{-\frac{1}{2}}^\dagger \right] |0\rangle \\ &= \left[u^2 + uv(a_{\frac{3}{2}}^\dagger a_{-\frac{3}{2}}^\dagger - a_{\frac{1}{2}}^\dagger a_{-\frac{1}{2}}^\dagger) - v^2 a_{\frac{3}{2}}^\dagger a_{-\frac{3}{2}}^\dagger a_{\frac{1}{2}}^\dagger a_{-\frac{1}{2}}^\dagger \right] |0\rangle \\ &= \left[u^2 + uv S_{\frac{3}{2}}^\dagger + \frac{v^2}{2!} (S_{\frac{3}{2}}^\dagger)^2 \right] |0\rangle. \end{aligned} \quad (7.34)$$

上式中我们省略了 $j = \frac{3}{2}$ 角标, 这里的 $S_{\frac{3}{2}}^\dagger$ 定义与前面seniority 中形式相同. 注意我们处理的是费米子, 每个 $|jm\rangle$ 态上最多可以容纳一个粒子. 从这个意义上确实BCS 波函数是seniority 为零的状态, 它对应这样的状态, u^4 几率没有任何核

我们得到

$$\begin{aligned}
& H_{\text{pairing}} (S_+)^{(n-t)} |N = v, v, \alpha, J\rangle \\
&= -G \left[\vec{S}^2 - S_z(S_z - 1) \right] (S_+)^{(n-t)} |N = v, v, \alpha, J\rangle \\
&= -G \left[\frac{\Omega_j - 2t}{2} \left(\frac{\Omega_j - 2t}{2} + 1 \right) - \frac{2n - \Omega_j}{2} \left(\frac{2n - \Omega_j}{2} - 1 \right) \right] \\
&\quad \cdot (S_+)^{(n-t)} |N = v, v, \alpha, J\rangle \\
&= -G \left[\left(\frac{\Omega_j}{2} - t \right) \left(\frac{\Omega_j}{2} - t + 1 \right) - \left(\frac{\Omega_j}{2} - n \right) \left(\frac{\Omega_j}{2} - n + 1 \right) \right] \\
&\quad \cdot (S_+)^{(n-t)} |N = v, v, \alpha, J\rangle \\
&= -G(n-t)(\Omega - n - t + 1)(S_+)^{(n-t)} B_{J_1}^\dagger \cdots B_{J_t}^\dagger |0\rangle ,
\end{aligned}$$

与式(7.15)、(7.32) 结果一致. 可见准自旋表象中的 $v = 2t$ 正是系统的未配对核子数, 或者称作非 S 配对的核子数.

7.3 BCS 理论

前面讨论了单轨道的seniority 理论, 实际上seniority 方法的应用不限于 j^N 组态. 如果满壳外有几个近似简并的单粒子 j 轨道, seniority 方法可以推广. 不过对于远离满壳情况, 原子核存在稳定形变时, 单粒子能级差不多有点均匀分布, 这种方法就不再适用了. 多轨道配对一个最有名的实例是偶偶的Sn 同位素链, 从Sn-102 到Sn-130 的第一个 2^+ 激发态能量近似一个常量(1.2 MeV). 人们发展了推广的seniority 方法、BCS 方法、broken pair 近似、配对理论等.

作为一个试探, $N = 2n$ 个粒子配对基态为

$$|S^n\rangle = \left(\sum_j \alpha_j S_j^\dagger \right)^n |0\rangle = \left(\sum_j \alpha_j (a_j^\dagger a_j^{(0)}) \right)^n |0\rangle .$$

然后做变分

$$\delta \langle S^n | H | S^n \rangle = 0 .$$

从而得到系数 α_j . 同样我们可以做

$$|S^{n-1}J\rangle = \left(\sum_j \alpha_j S_j^\dagger \right)^{n-1} \sum_{j_1 j_2} \beta_{j_1 j_2} (a_{j_1}^\dagger a_{j_2}^\dagger)^{(J)} |0\rangle .$$

子、 $2u^2v^2$ 几率有两个核子、而 v^4 几率占据四个核子. 对于任意 j 我们类似有

$$\begin{aligned} & \prod_{m>0} \left[u_j + (-)^{j-m} v_j a_{jm}^\dagger a_{j-m}^\dagger \right]^n |0\rangle \\ &= \sum_{n=0}^{\Omega_j} \frac{u_j^{\Omega_j-n}}{n!} \left(S_j^\dagger \right)^n |0\rangle = u_j^{\Omega_j} \exp \left(\frac{v_j}{u_j} S_j^\dagger \right) |0\rangle . \end{aligned} \quad (7.35)$$

我们把式(7.33) 写为

$$\psi = \prod_j \left[u_j^{\Omega_j} \exp \left(\frac{v_j}{u_j} S_j^\dagger \right) \right] |0\rangle = \left[\prod_j u_j^{\Omega_j} \right] \left[\exp \left(\sum_j \frac{v_j}{u_j} S_j^\dagger \right) \right] |0\rangle . \quad (7.36)$$

我们下面解释式(7.33) 中 u_j 和 v_j 的意义. 我们为了方面仍然以 $j = 3/2$ 壳为例, 由归一化条件

$$\begin{aligned} 1 &= \langle \psi | \psi \rangle \\ &= \langle 0 | \left(u - va_{\frac{1}{2}} a_{-\frac{1}{2}} \right) \left(u + va_{\frac{3}{2}} a_{-\frac{3}{2}} \right) \left(u + va_{\frac{1}{2}}^\dagger a_{-\frac{3}{2}}^\dagger \right) \left(u - va_{\frac{1}{2}}^\dagger a_{-\frac{1}{2}}^\dagger \right) |0\rangle \\ &= \langle 0 | \left(u - va_{\frac{1}{2}} a_{-\frac{1}{2}} \right) \left(u - va_{\frac{1}{2}}^\dagger a_{-\frac{1}{2}}^\dagger \right) |0\rangle \langle 0 | \left(u + va_{\frac{3}{2}} a_{-\frac{3}{2}} \right) \left(u + va_{\frac{1}{2}}^\dagger a_{-\frac{3}{2}}^\dagger \right) |0\rangle \\ &= (u^2 + v^2)^2 . \end{aligned} \quad (7.37)$$

可见, $u_j^2 + v_j^2 = 1$ 是BCS 波函数归一化条件. 我们下面计算粒子数算符在BCS 基态上的期望值,

$$\begin{aligned} & a_{j'm'}^\dagger a_{j'm'} |\psi\rangle \\ &= \prod'_{j m>0} \left(u_j + (-)^{j-m} v_j a_{jm}^\dagger a_{j-m}^\dagger \right) a_{j'm'}^\dagger a_{j'm'} \left(u_{j'} + (-)^{j-m} v_{j'} a_{j'm'}^\dagger a_{j'-m'}^\dagger \right) |0\rangle \\ &= (-)^{j-m} v_{j'} a_{j'm'}^\dagger a_{j'-m'}^\dagger \prod'_{j m>0} \left(u_j + (-)^{j-m} a_{jm}^\dagger a_{j-m}^\dagger \right) |0\rangle , \end{aligned}$$

式中连乘号的撇号 \prod' 表示连乘中不包含 $j'm'$. 我们由上式得到

$$\langle \psi | a_{j'm'}^\dagger a_{j'm'} | \psi \rangle = v_{j'}^2 . \quad (7.38)$$

由此可见, v_j^2 为 j 轨道占据的几率, 而 $u_j^2 = 1 - v_j^2$ 自然而然就对应于 j 轨道没有核子的几率.

式中连乘号上双撇号指的是连乘中不包括 $j_2, m_2 > 0$. 上式中因为 S_{j_2} 和 $S_{j_1}^\dagger$ 中分别自带了相因子 $(-)^{j_2-m_2}$ 和 $(-)^{j_1-m_1}$ 使得 v_{j_1}, v_{j_2} 前的相因子消掉了. 上式的做法是 S_{j_2} 作用于右边的 $|\psi\rangle$, 而 $S_{j_1}^\dagger$ 作用于左边的 $\langle\psi|$. 正如式(7.37) 那样, 上式右边那些连乘号内的那些都变成 $u^2 + v^2 = 1$ 而消去: 上式因为第二个连乘号内少了 j_2m_2 的配对产生算符, 因此对应的 $u_{j_1} + (-)^{j_1-m_1}v_{j_1}a_{j_1m_1}a_{j_1-m_1}$ 无法消去, 类似地, 第一个连乘号内少了 j_1m_1 的配对产生算符, 对应的 $u_{j_1} + (-)^{j_1-m_1}v_{j_1}a_{j_1m_1}^\dagger a_{j_1-m_1}^\dagger$ 也无法消去; 因此上式变为

$$\begin{aligned} & \langle\psi| - G \sum_{j_1 j_2} S_{j_1}^\dagger S_{j_2} |\psi\rangle \\ = & -G \sum_{j_1 j_2} \sum_{m_1 > 0, m_2 > 0} v_{j_1} v_{j_2} \langle 0 | (u_{j_2} + (-)^{j_2-m_2} v_{j_2} a_{j_2-m_2} a_{j_2m_2}) \\ & \quad \left(u_{j_1} + (-)^{j_1-m_1} v_{j_1} a_{j_1m_1}^\dagger a_{j_1-m_1}^\dagger \right) |0\rangle. \end{aligned}$$

上式容易化简为

$$\begin{aligned} & \langle\psi| - G \sum_{j_1 j_2} S_{j_1}^\dagger S_{j_2} |\psi\rangle \\ = & -G \sum_{j_1 j_2} \sum_{m_1 > 0, m_2 > 0} v_{j_1} v_{j_2} u_{j_1} u_{j_2} - G \sum_j \sum_{m > 0} v_j^4 \\ = & -G \left(\sum_j \Omega_j v_j u_j \right)^2 - G \sum_j \Omega_j v_j^4. \end{aligned}$$

定义 $\Delta = \sum_j \Omega_j u_j v_j$, 总结上面的结果, 我们有

$$\begin{aligned} \langle\psi|\mathcal{H}|\psi\rangle &= \sum_j (2j+1)(\epsilon_j - \lambda)v_j^2 - \frac{1}{G}\Delta^2 - G \sum_j \sum_{m > 0} v_j^4 \\ &= 2 \sum_j \Omega_j (\epsilon_j - \lambda)v_j^2 - \frac{1}{G}\Delta^2 - G \sum_j \Omega_j v_j^4. \end{aligned} \tag{7.42}$$

下面我们看式(7.39), 首先由 $u_j^2 + v_j^2 = 1$ 我们得到

$$\frac{\partial u_j}{\partial v_j} = -\frac{v_j}{u_j},$$

由 Δ 的定义, 我们有

$$\frac{\partial \Delta}{\partial v_j} = G \Omega_j \left(u_j + \frac{\partial u_j}{\partial v_j} v_j \right) = G \Omega_j \frac{u_j^2 - v_j^2}{u_j} = G \Omega_j \frac{1 - 2v_j^2}{u_j}.$$

下面我们利用变分方法求BCS 基态. 此时系统的哈密顿量形式为

$$H = \sum_{jm} \epsilon_j a_{jm}^\dagger a_{jm} - G \sum_{j_1 j_2} S_{j_1}^\dagger S_{j_2} .$$

为了求粒子数限定的哈密顿量能量极小, 我们引入拉格朗日乘子, 计算

$$\mathcal{H} = H - \lambda \sum_j N_j$$

的期望值. 办法是不断改变 v_j 的值, 使得

$$\frac{\partial}{\partial v_j} \langle \psi | \mathcal{H} | \psi \rangle = 0 , \quad (7.39)$$

假如有 k 个轨道, 那么就有 k 个方程, 这加上粒子数条件

$$\langle \psi | \sum_j N_j | \psi \rangle = \sum_j v_j^2 = N , \quad (7.40)$$

共有 $n + 1$ 个方程, 决定 n 个 v_j 和拉格朗日乘子 λ (化学势). 其中 \mathcal{H} 单体部分的计算很直接

$$\mathcal{H}_1 = \langle \psi | \sum_{jm} (\epsilon_j - \lambda) a_{jm}^\dagger a_{jm} | \psi \rangle = \sum_j (2j + 1)(\epsilon_j - \lambda) v_j^2 . \quad (7.41)$$

为了计算 \mathcal{H} 两体部分, 我们先看

$$\begin{aligned} & a_{j_2-m_2} a_{j_2 m_2} \prod_{j m>0} \left[u_j + (-)^{j-m} v_j a_{jm}^\dagger a_{j-m}^\dagger \right] |0\rangle \\ &= (-)^{j_2-m_2} v_{j_2} \prod'_{j m>0} \left[u_j + (-)^{j-m} v_j a_{jm}^\dagger a_{j-m}^\dagger \right] |0\rangle , \end{aligned}$$

式中连乘号上的撇号是指连乘中不包含 $j_2 m_2 > 0$. 两体部分计算结果为

$$\begin{aligned} & \langle \psi | -G \sum_{j_1 j_2} S_{j_1}^\dagger S_{j_2} | \psi \rangle \\ &= -G \sum_{j_1 j_2} \sum_{m_1 > 0, m_2 > 0} v_{j_1} v_{j_2} \langle 0 | \prod''_{j' m'>0} \left[u_{j'} + (-)^{j'-m'} v_{j'} a_{j'm'}^\dagger a_{j'-m'}^\dagger \right] \\ & \quad \prod'_{j m>0} \left[u_j + (-)^{j-m} v_j a_{jm}^\dagger a_{j-m}^\dagger \right] |0\rangle . \end{aligned}$$

因此式(7.39)变为

$$\frac{\partial}{\partial v_j} \langle \psi | \mathcal{H} | \psi \rangle = 4\Omega_j(\epsilon_j - \lambda)v_j - 2\Delta\Omega_j \frac{1 - 2v_j^2}{u_j} - 4G\Omega_j v_j^3 = 0.$$

上式两边消去 $2\Omega_j$, 并乘以 u_j , 变为

$$2(\epsilon_j - \lambda)u_j v_j - \Delta(1 - 2v_j^2) - 2G\Omega_j u_j v_j^3 = 0. \quad (7.43)$$

因为 $u_j^2 + v_j^2 = 1$, 因此这是一个关于 v_j 的一元方程. 如果有 n 个能级, 那么就有 n 个这样的一元方程. 在数值上求解时, 首先令 v_j^3 项等于零; v_j^3 项的影响其实可以通过调整 λ 的值补偿; 在此假定下, 上式两边平方, 得到

$$4(\epsilon_j - \lambda)^2 v_j^2 (1 - v_j^2) = \Delta^2 (1 - 4v_j^2 + 4v_j^4). \quad (7.44)$$

把上式改写为

$$[(\epsilon_j - \lambda)^2 + \Delta^2] (v_j^2)^2 - [\Delta^2 + (\epsilon_j - \lambda)^2] (v_j^2) + \frac{\Delta^2}{4} = 0.$$

这个关于 v_j^2 的一元二次方程,

$$\begin{aligned} v_j^2 &= \frac{[(\epsilon_j - \lambda)^2 + \Delta^2] \pm \sqrt{[\Delta^2 + (\epsilon_j - \lambda)^2]^2 - [\Delta^2 + (\epsilon_j - \lambda)^2] \Delta^2}}{2[(\epsilon_j - \lambda)^2 + \Delta^2]} \\ &= \frac{1}{2} \left(1 \pm \frac{\epsilon_j - \lambda}{\sqrt{(\epsilon_j - \lambda)^2 + \Delta^2}} \right). \end{aligned} \quad (7.45)$$

上式 v_j 有两个解, 括号内分数前面的正负号有不确定性; 这种不确定性来源于我们在式(7.43)中忽略 v_j^3 后两边做了平方而导致的. 为了消除这个不确定性, 我们不妨把这两个解代入式(7.43) [忽略忽略 v_j^3]. 当上式中± 取正号时,

$$2(\epsilon_j - \lambda)u_j v_j = -\Delta \frac{\epsilon_j - \lambda}{\sqrt{(\epsilon_j - \lambda)^2 + \Delta^2}}.$$

两边消去 $(\epsilon_j - \lambda)$, u_j 、 v_j 都取正数, 上式不成立, 因此我们在 v_j^2 的解括号内只能取负号. 由此得到

$$v_j^2 = \frac{1}{2} \left(1 - \frac{\epsilon_j - \lambda}{\sqrt{(\epsilon_j - \lambda)^2 + \Delta^2}} \right), \quad u_j^2 = \frac{1}{2} \left(1 + \frac{\epsilon_j - \lambda}{\sqrt{(\epsilon_j - \lambda)^2 + \Delta^2}} \right). \quad (7.46)$$

上式的解代入粒子数的定义, 得到

$$N = \sum_j \Omega_j \left(1 - \frac{\epsilon_j - \lambda}{\sqrt{(\epsilon_j - \lambda)^2 + \Delta^2}} \right). \quad (7.47)$$

把上面的 u_j 、 v_j 代入到 Δ 的定义中, 得到

$$\begin{aligned} \Delta &= G \sum_j \Omega_j \sqrt{\frac{1}{2} \left(1 - \frac{\epsilon_j - \lambda}{\sqrt{(\epsilon_j - \lambda)^2 + \Delta^2}} \right) \cdot \frac{1}{2} \left(1 + \frac{\epsilon_j - \lambda}{\sqrt{(\epsilon_j - \lambda)^2 + \Delta^2}} \right)} \\ &= \frac{G}{2} \sum_j \Omega_j \sqrt{1 - \frac{(\epsilon_j - \lambda)^2}{(\epsilon_j - \lambda)^2 + \Delta^2}} = \frac{G}{2} \sum_j \Omega_j \frac{\Delta}{\sqrt{(\epsilon_j - \lambda)^2 + \Delta^2}}. \end{aligned}$$

上式两边消去 Δ , 得到

$$\frac{G}{2} \sum_j \frac{\Omega_j}{\sqrt{(\epsilon_j - \lambda)^2 + \Delta^2}} = 1. \quad (7.48)$$

从式(7.47) 和(7.48) 这两个二元方程求出 Δ 和 λ , 然后我们可以从(7.46) 得到 u_j 和 v_j . 式(7.43) 可以写为

$$2[\epsilon_j - \lambda'] u_j v_j - \Delta(1 - 2v_j^2) = 0, \quad \lambda' = \lambda + Gv_j^2.$$

即(7.43)中被忽略的 $-2G\Omega_j u_j v_j^3$ 项, 可以改变 λ 来等效地考虑进来. 反正 λ 是未知的, 把 λ 的值上加一项没有关系, 变成 λ' 没有关系. 换句话说, 我们如果通过式(7.47) 和(7.48) 得到 λ , 这个 λ 的结果不是我们在式(7.43)中的 λ , 而是 $\lambda' = \lambda + Gv_j^2$. 真正的化学势 λ 等于这样的 λ 减去 Gv_j^2 .

有了 u_j 和 v_j 以后, 就可以利用BCS 波函数计算基态的能量. 显然, 结果为

$$E_0 = \langle \psi | H | \psi \rangle = \sum_j (2j+1)\epsilon_j v_j^2 - \Delta^2/G - G \sum_j \Omega_j v_j^4. \quad (7.49)$$

7.3.1 BCS 理论可靠性

下面我们检验BCS 方法的近似程度. 我们处理一个简单系统, 令所有的单粒子能级简并, 此时可以得到对力哈密顿量的解, 然后与BCS 的结果进行比较. 单粒子能级简并的对力哈密顿量的形式为

$$H = \epsilon \sum_j N_j - GS_+ S_-, \quad S_{\pm} = \sum_j S_{\pm}(j).$$

首先看严格的解。这个对力方程在单粒子能级简并情形下seniority 理论适用。可以直接用seniority 结果推广得到，也就是说，单轨道情况下seniority 方法的所有推导都可以直接用于单粒子能量简并的对力哈密顿量情况。此时容易验证

$$[S_+ S_-] = N - \Omega, \quad N = \sum_j N_j, \quad \Omega = \sum_j \Omega_j,$$

式中 $N = 2n$ 总的价核子数算符。上式与式(7.6) 形式上完全一样。因为对力只对于自旋为零的核子对(seniority 等于零)贡献一个负的能量，系统基态seniority一定为零，基态波函数为

$$\psi = \sqrt{\frac{2^N (2\Omega - N)!!}{N!! (2\Omega!!)}} (S_+)^n |0\rangle. \quad (7.50)$$

对应的基态能量为

$$E_0(\text{seniority}) = \langle \psi | H | \psi \rangle = N\epsilon - \frac{G}{4} N (2\Omega - N + 2). \quad (7.51)$$

上面两式分别可以从式(7.25) 和(7.23) 得到；当然也可以按照那里的套路再直接求解一遍。

下面看BCS 的结果。根据式(7.46)， v_j 是与 j 无关的常量，根据式(7.40)， $v_j^2 = N_j/(2j+1) = \frac{N}{2\Omega}$ ，因此 $u_j = [(1 - N/(2\Omega))]$ 。我们容易计算 Δ 的值，

$$\begin{aligned} \Delta^2 &= \left(G \sum_j \sqrt{\frac{N}{2j+1} \cdot \frac{(2j+1)-N}{2j+1}} \right)^2 = G^2 \Omega^2 \frac{N}{2\Omega} \left(1 - \frac{N}{2\Omega} \right) \\ &= \frac{G^2 N \Omega}{2} \left(1 - \frac{N}{2\Omega} \right). \end{aligned} \quad (7.52)$$

把这些结果代入BCS 基态能量公式(7.49)中，

$$\begin{aligned} E_0(\text{BCS}) &= \epsilon N - \frac{G^2 N \Omega}{2} \left(1 - \frac{N}{2\Omega} \right) \cdot \frac{1}{G} - G \Omega \left(\sqrt{\frac{N}{2\Omega}} \right)^4 \\ &= \epsilon N - \frac{GN\Omega}{2} \left(1 - \frac{N}{2\Omega} \right) - G \Omega \left(\frac{\Omega}{2N} \right)^2 \\ &= \epsilon N - \frac{GN}{4} \left(2\Omega - N + \frac{N}{\Omega} \right). \end{aligned}$$

比较上式和式(7.51) 能量差异, 两体部分的相对偏离结果为

$$\frac{E_0(\text{BCS}) - E_0(\text{seniority})}{\frac{G}{4}N(2\Omega - N + 2)} = \frac{2 - \frac{N}{\Omega}}{2\Omega - N + 2}.$$

可以看出, 当 N 小于半满壳时, 分母值比较大而分子上的值一直不大, 所以这相对误差不大的. 上式中我们忽略了单粒子项, 因为单粒子项的对比根本没有什么意思, 该项的结果总归是完全一致的.

再看BCS 波函数, 式(7.35)的 ψ 不满足粒子数守恒, 其中包含了0个核子、2个核子、4个核子……、 2Ω 个核子的成分, 其中粒子为 $N = 2n$ 的状态为

$$\begin{aligned}\psi &= \prod_j u_j^{\Omega_j} \exp \left(\sum_j \frac{v_j}{u_j} S_j^\dagger \right) |0\rangle \\ &\rightarrow \left(\sqrt{1 - \frac{N}{2\Omega}} \right)^{\Omega} \left(\sqrt{\frac{N}{2\Omega - N}} S_+ \right)^n |0\rangle \\ &= \left(\sqrt{1 - \frac{N}{2\Omega}} \right)^{\frac{\Omega-n}{2}} \left(\frac{N}{2\Omega} \right)^{n/2} (S_+)^n |0\rangle.\end{aligned}\quad (7.53)$$

除了归一化系数差异外(上式右边没有归一化, 我们仅仅考虑了总波函数中 N 个粒子成分) 完全一致. 换句话说, 我们计算能量时给出误差的唯一来源是因为粒子数不守恒造成的. Kerman 等人指出, 即使单粒子能量不简并, 这个结论也很好地成立. 对于一般情况下的 G 参数, BCS 波函数对应的基态能量与精确结果的误差在 500 keV 以内. 特别是如果我们考虑了确定的粒子数之后再计算基态能量, 那么得到的能量与精确结果非常接近. 因此BCS 波函数是处理对力哈密顿量一个很好的方法.

我们需要说明的是, 在seniority 理论中, seniority 量子数 v 相同的态具有相同的能量, 是简并的. 在实际问题中则并非如此, 其原因是对力哈密顿量太简单了, 下面我们将讨论, BCS 理论还是能用来处理这些比较真实的情况.

7.4 准粒子方法

BCS 波函数很好地给出单满壳的偶偶核基态, 我们可以把它看作准粒子的“真空态”. 准粒子消灭算符的定义为

$$\alpha_{jm} |\psi(\text{BCS})\rangle = 0. \quad (7.54)$$

准粒子算符是核子产生和消灭算符的一个线性组合,

$$\alpha_{jm} = Aa_{jm} + Ba_{j-m}^\dagger. \quad (7.55)$$

把上式代入式(7.54) 中,

$$\begin{aligned} 0 &= \alpha_{j_1 m_1} |\psi(\text{BCS})\rangle \\ &= \prod'_{jm} \left(u_j + (-)^{j-m} v_j a_{jm}^\dagger a_{j-m}^\dagger \right) \alpha_{j_1 m_1} \left(u_{j_1} + (-)^{j_1-m_1} v_{j_1} a_{j_1 m_1}^\dagger a_{j_1-m_1}^\dagger \right) |0\rangle \\ &= \prod'_{jm} \left(u_j + (-)^{j-m} v_j a_{jm}^\dagger a_{j-m}^\dagger \right) (Bu_{j_1} + (-)^{j_1-m_1} Av_{j_1}) a_{j_1-m_1}^\dagger |0\rangle, \end{aligned}$$

上式成立所需要的条件是

$$(Bu_{j_1} + (-)^{j_1-m_1} Av_{j_1}) a_{j_1-m_1}^\dagger |0\rangle = 0.$$

上式中我们如果取 $A = u_{j_1}$, $B = -(-)^{j_1-m_1} v_{j_1}$ 显然能满足这一条件. 我们就取这个 A 、 B 值. 把这个结果代入式(7.56), 我们得到准粒子消灭算符形式为

$$\alpha_{jm} = u_j a_{jm} - (-)^{j-m} v_j a_{j-m}^\dagger. \quad (7.56)$$

上式的厄米共轭给出准粒子产生算符形式

$$\alpha_{jm}^\dagger = u_j a_{jm}^\dagger - (-)^{j-m} v_j a_{j-m}. \quad (7.57)$$

我们可以把这两个算符作逆变换, 即用准粒子算符表示粒子算符,

$$a_{jm}^\dagger = u_j \alpha_{jm} + (-)^{j-m} v_j \alpha_{j-m}, \quad (7.58)$$

$$a_{jm} = u_j \alpha_{jm} + (-)^{j-m} v_j \alpha_{j-m}^\dagger. \quad (7.59)$$

容易验证

$$\alpha_{jm}^\dagger \alpha_{j'm'}^\dagger + \alpha_{j'm'}^\dagger \alpha_{jm}^\dagger = 0,$$

$$\alpha_{jm} \alpha_{j'm'} + \alpha_{j'm'} \alpha_{jm} = 0,$$

$$\alpha_{jm}^\dagger \alpha_{j'm'} + \alpha_{jm}^\dagger \alpha_{j'm'}^\dagger = (u_j^2 + v_j^2) \delta_{jj'} \delta_{mm'} = \delta_{mm'}.$$

可见, 准粒子的对易关系和一般费米子对易关系在形式上完全一致, 这正是其名称来源.

我们可以证明, 一个准粒子态对应seniority 量子数等于1 的本征态.

$$\begin{aligned}
& \alpha_{j_1 m_1}^\dagger |\psi(\text{BCS})\rangle \\
= & \prod'_{jm} \left(u_j + (-)^{j-m} v_j a_{jm}^\dagger a_{j-m}^\dagger \right) \left(u_j \alpha_{jm}^\dagger - (-)^{j-m} v_j \alpha_{j-m}^\dagger \right) \\
& \quad \left(u_{j_1} + (-)^{j_1-m_1} v_{j_1} a_{j_1 m_1}^\dagger a_{j_1-m_1}^\dagger \right) |0\rangle \\
= & \prod'_{jm} \left(u_j + (-)^{j-m} v_j a_{jm}^\dagger a_{j-m}^\dagger \right) (u_{j_1}^2 + v_{j_1}^2) a_{j_1 m_1}^\dagger |0\rangle \\
= & \frac{1}{u_{j_1}} \prod_{jm} \left(u_j + (-)^{j-m} v_j a_{jm}^\dagger a_{j-m}^\dagger \right) |0\rangle, \tag{7.60}
\end{aligned}$$

式中连乘号上撇号指的是连乘中不包括 $j_1, m_1 > 0$, 上式倒数第二步利用了 $a_{j-m} a_{j-m}^\dagger |0\rangle = |0\rangle$, 最后一步利用了Pauli 原理. 从上式看到, 一个准粒子态有一个未配对核子, seniority 量子数为1, 可以近似描写奇质量数原子核seniority 为1 的态.

类似地我们可以证明, 二个准粒子态当总角动量不为零时对应于seniority 量子数等于2 的态, 当角动量为零时对应于seniority 等于零的状态. 应用式(7.60)我们可得

$$\begin{aligned}
& \alpha_{j_2 m_2}^\dagger \alpha_{j_1 m_1}^\dagger |\psi(\text{BCS})\rangle \\
= & \prod''_{jm} \left(u_j + (-)^{j-m} v_j a_{jm}^\dagger a_{j-m}^\dagger \right) a_{j_2 m_2}^\dagger a_{j_1 m_1}^\dagger |0\rangle, \tag{7.61}
\end{aligned}$$

式中连乘号上双撇号指的是连乘中不包括 $j_1, m_1 > 0$ 和 $j_2, m_2 > 0$, $(j_1 m_1) \neq (j_2 m_2)$. 上式为非耦合表象, 因为系统总角动量是好量子数, 因此上式结果为

$$\begin{aligned}
& \alpha_{j_2 m_2}^\dagger \alpha_{j_1 m_1}^\dagger |\psi(\text{BCS})\rangle \\
= & \sum_{IM} C_{j_1 m_1, j_2 m_2}^{IM} \prod''_{jm} \left(u_j + (-)^{j-m} v_j a_{jm}^\dagger a_{j-m}^\dagger \right) (a_{j_2}^\dagger a_{j_1}^\dagger)_M^{(I)} |0\rangle. \tag{7.62}
\end{aligned}$$

$I = 0$ 时上式为seniority 量子数为零、 $I \neq 0$ 时为seniority 量子数等于2. 多 j 轨道存在时, 直接做壳模型计算比较麻烦, 利用seniority 量子数为2 的方法构造基矢, 可以近似得到哈密顿量的本征态.



Nucleon-pair approximation to the nuclear shell model



Y.M. Zhao ^{a,*}, A. Arima ^{a,b}

^a Department of Physics and Astronomy, Shanghai Jiao Tong University, Shanghai 200240, China

^b Musashi Gakuen, 1-26-1 Toyotamakami Nerima-ku, Tokyo 176-8533, Japan

ARTICLE INFO

Article history:

Accepted 4 July 2014

Available online 14 July 2014

editor: M. Ramsey-Musolf

Keywords:

The nuclear shell model

Low-lying states

Collective nucleon pairs

Truncation scheme

ABSTRACT

Atomic nuclei are complex systems of nucleons—protons and neutrons. Nucleons interact with each other via an attractive and short-range force. This feature of the interaction leads to a pattern of dominantly monopole and quadrupole correlations between like particles (i.e., proton–proton and neutron–neutron correlations) in low-lying states of atomic nuclei. As a consequence, among dozens or even hundreds of possible types of nucleon pairs, very few nucleon pairs such as proton and neutron pairs with spin zero, two (in some cases spin four), and occasionally isoscalar spin-aligned proton–neutron pairs, play important roles in low-energy nuclear structure. The nucleon-pair approximation therefore provides us with an efficient truncation scheme of the full shell model configurations which are otherwise too large to handle for medium and heavy nuclei in foreseeable future. Furthermore, the nucleon-pair approximation leads to simple pictures in physics, as the dimension of nucleon-pair subspace is always small. The present paper aims at a sound review of its history, formulation, validity, applications, as well as its link to previous approaches, with the focus on the new developments in the last two decades. The applicability of the nucleon-pair approximation and numerical calculations of low-lying states for realistic atomic nuclei are demonstrated with examples. Applications of pair approximations to other problems are also discussed.

© 2014 Elsevier B.V. All rights reserved.

Contents

1. Introduction.....	2
2. Formulation of the nucleon pair approximation.....	4
2.1. The nucleon-pair basis	4
2.2. The nuclear shell model Hamiltonian	6
2.3. Matrix elements in the coupled nucleon-pair basis	7
2.4. Special cases of the nucleon-pair approximation.....	8
2.4.1. Integrable models: seniority scheme and Richardson pairing model.....	8
2.4.2. The broken pair approximation	9
2.4.3. The Ginocchio model.....	9
2.4.4. The fermion dynamical symmetry model.....	10
2.4.5. Nucleon-pair approximation in the deformed basis	10
2.4.6. The multi-step shell model	10
2.4.7. The NPA with isospin symmetry	11
2.5. Summary of this section.....	11

* Corresponding author.

E-mail address: ymzhao@sjtu.edu.cn (Y.M. Zhao).

3.	Validity of the NPA	11
3.1.	The NPA for a single- j shell	12
3.1.1.	Quadrupole-quadrupole interaction.....	12
3.1.2.	Monopole plus quadrupole interaction.....	13
3.1.3.	Schematic cases: J -pairing interaction	14
3.2.	Validity of the NPA for many- j shells	16
3.2.1.	Semi-magic nuclei $^{43,45}\text{Ca}$ with effective interactions	16
3.2.2.	Validity of the NPA for open shells	17
3.3.	Summary of this section.....	18
4.	Application of the NPA.....	21
4.1.	Brief survey	21
4.2.	$A \sim 130\text{--}150$ region	21
4.2.1.	FDSM description.....	21
4.2.2.	SD pairs with the surface-delta interaction	22
4.2.3.	Low-lying states with SD nucleon pairs	23
4.2.4.	Backbending in yrast states of even-even nuclei	23
4.2.5.	Negative parity levels of even-even nuclei	24
4.2.6.	Chiral bands in odd-odd nuclei	24
4.2.7.	$B(E2)$ and g factors of even-even Tin isotopes	24
4.3.	Other regions.....	25
4.3.1.	$A \sim 80\text{--}100$	25
4.3.2.	$A \sim 200\text{--}210$	25
4.4.	Ioscalar nucleon-pair approximations.....	25
4.5.	Exemplification: a few nuclei around ^{208}Pb	26
4.6.	Other applications	28
4.6.1.	Shape phase transitions in the nucleon-pair approximations.....	30
4.6.2.	Nucleon-pair approximation with random interactions	31
4.7.	Current status of applications	32
4.8.	Future theoretical applications	34
4.9.	Summary of this section	35
5.	Summary	35
	Acknowledgments	36
	Appendix A. Mathematical notations	36
	Appendix B. Fundamental formulas of the NPA	37
	Appendix C. The NPA with isospin symmetry	40
	References.....	41

1. Introduction

Atomic nuclei are very complex systems consisted of nucleons, i.e., neutrons and protons. Each nucleon is a composite particle including three constituent quarks. In low-energy (usually up to a few MeV) nuclear structure physics, one can ignore the internal structure of nucleons, and take nucleons as the fundamental building blocks in studies of the nuclear structure. Nucleons interact with each other via strong interactions, and the quantum chromo-dynamics (QCD for short) is the fundamental theory to describe such interactions. However, it is not yet possible to derive unambiguously the strong interactions used for low-energy phenomena of nuclei from the QCD. The interactions in use are usually determined by nucleon-nucleon scattering experiments and the properties of the deuteron nucleus.

Assuming that low-lying states of atomic nuclei are given by nucleons interacting through two-body interactions, we should solve the non-relativistic many-body Schrödinger equation, but this cannot be performed exactly. Therefore we have to resort to various models of the nuclear structure. A breakthrough along this line was made in 1949 by Mayer and Jensen. They suggested the nuclear shell model (NSM) [1–3] in 1949, and received the Nobel Award in physics in 1963 (shared with E.P. Wigner) owing to this achievement. The NSM explains elegantly the magic numbers, 2, 8, 20, 28, 50, 82, for both proton number Z and neutron number N , and additionally 126 for neutron number N . Furthermore it makes understandable a vast amount of experimental data.

The level schemes for nuclei with one extra valence nucleon (or one nucleon hole) with respect to the doubly closed shell cores are well explained by the NSM. According to the NSM, the extra valence nucleon moves in a spherical and static potential, which includes a strong spin-orbit interaction leading to large splittings between the single-particle orbits $j = l + 1/2$ and $j = l - 1/2$ for large l . For systems with several nucleons outside closed shells, we must consider the mutual interactions between valence nucleons as well as the single-particle energies, and solve the Schrödinger equation for valence nucleons in the active shells. Here we need to know the input which includes the single-particle energies and the two-body matrix elements of effective interactions; with the input we solve the many-body Schrödinger equation for valence nucleons in given shells. The NSM has been successful in both describing and predicting low-lying states of atomic nuclei, and is regarded as the “standard” framework of the nuclear structure theory [4,5]. For comprehensive reviews and current status of the NSM, see Refs. [6–8].

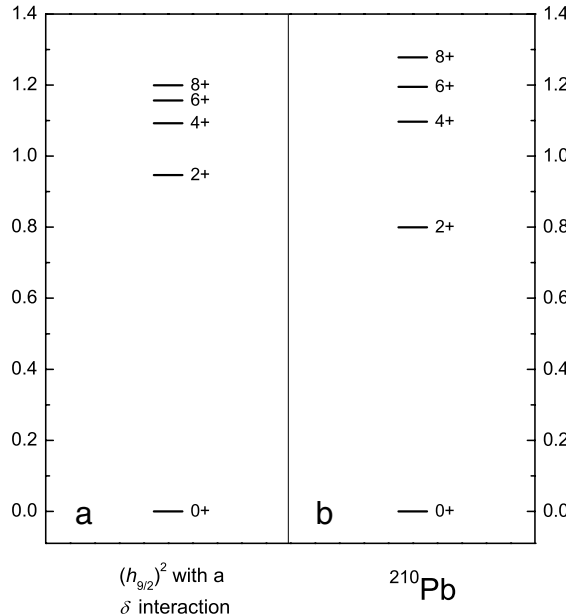


Fig. 1. (a) Energies of two identical nucleons in a $j = 9/2$ orbit for a zero-range interaction, $V(|\vec{r}_1 - \vec{r}_2|) = V_0 \delta(\vec{r}_1 - \vec{r}_2)$. Here we take the integral $\frac{V_0}{4\pi} \int R_{nl}^4 r^2 dr = -0.25$ MeV, and $R_{nl}(r)$ is the radial function of one nucleon in a $h_{9/2}$ orbit. (b) The low-lying states of ^{210}Pb . In both cases the spins of the lowest states are zero, and those of the first excited states are two.

Unfortunately, the dimension of the NSM configuration space grows explosively as going from the lightest to heavier nuclei, even if we restrict ourselves in one major shell for valence protons and neutrons. Exact diagonalization of the NSM Hamiltonian is prohibitively difficult, although impressive progresses have been made with the fast developments of computational power. Truncations of the NSM configurations are therefore indispensable.

Sagacious truncations of the NSM model space are even more pressing in the studies of nuclear structure for atomic nuclei far from the stability line. In the last two decades, with the new generation of the radioactive beam facilities all over the world, the territory of the nuclear structure physics has expanded from stable to unstable nuclei, in the light-mass region as well as in medium and heavy mass regions [9]. Many fascinating and exotic phenomena, e.g., halo structure, α -particle correlation, two-proton and two-neutron emissions, unbound states, new magic numbers, shape-coexistence and etc., have been observed in the expedition to the borders of proton and neutron drip lines in the nuclear chart. It has been generally realized that many more single-particle orbits are involved in the low-lying states of exotic nuclei, in comparison with those of stable nuclei. Therefore the NSM configuration space in this case is much larger than that for low-lying states of “normal” nuclei which could often be interpreted within one major-shell space. Proper truncation schemes of NSM space for exotic nuclei become more challenging, and the nucleon-pair approximation (NPA) to the NSM is among one of the practical approaches along this line.

Clearly, as to be explained in this review, the NPA has been proved to be both efficient and reliable. More importantly, the dimension of the collective nucleon-pair subspace is small, therefore the NPA provides us with simple pictures in physics. The validity of the NPA is ascribed to the strong pairing property of identical valence nucleons into spin-zero (denoted by S) pairs. This pairing feature is easily understood based on the short-range and attractive nature of the effective nucleon-nucleon interaction. Let us approximate the attractive short-range (in comparison with the spatial distribution of single-nucleon wave functions) interaction between two valence nucleons by a zero-range interaction, i.e., delta potential. This delta potential was assumed and studied in 1950 by Mayer [10] who concluded “The assumption of short-range attractive forces between identical nucleons in the $j-j$ coupling model of nuclear structure is in agreement with the empirically observed spins”. For two nucleons in a single- j shell with the attractive delta interaction, the $J = 0$ state has the lowest energy, see Fig. 1(a) for example. If the interactions between valence nucleons were given uniquely by the monopole pairing interaction, the ground states of even-even nuclei would be given by the S -pair condensation, the lowest excited states would be constructed by breaking one of the S pairs, and consequently, higher excited states have more non- S nucleon pairs. The experimental hallmarks of pairing phenomena in nuclei are the odd-even staggering of binding energies, the gap in the excitation spectrum of even-even nuclei, and the compressed quasiparticle spectrum in odd-mass and odd-odd nuclei [11]. For a comprehensive review of pairing in nuclear systems, see Ref. [12].

Let us begin our discussion with a very brief historical survey of the NPA. This approach is actually an old idea. It can be traced back to the seniority scheme (seniority quantum number, usually denoted by v in the literature, is equal to the number of particles unpaired to zero spin) suggested by Racah. The seniority scheme was introduced to classify atomic energy levels [13] and later was applied in nuclear structure by Racah and independently by Flowers [14,15], soon after the shell

model was established. The seniority scheme was applied to nuclei a few years before the Bardeen–Cooper–Schrieffer (BCS) theory [16] of superconductivity in condensed matter physics was invented. Soon after the BCS theory, Bohr, Mottelson, and Pines [17], and independently, Belyaev and collaborators [18], and Midgal [19], suggested the nucleon-pair correlations in nuclei. For a single- j shell, there is an equivalent and very elegant formulation of the pairing theory, called the quasi-spin theory [20,21]. The quasispin formulation of seniority scheme was generalized to many- j shells and extensively studied by Ichimura and Arima [22], and also by Ginocchio [23]. The seniority scheme was generalized from single- j shell to many- j shells by Talmi in Ref. [24], and has been successfully applied to single-closed shell (or called semi-magic in some references) nuclei, for which the attractive pairing interaction is much stronger in comparison with other components in the effective interactions. The success of the seniority coupling scheme in nuclei (in particular, semi-magic nuclei) stimulated a number of nucleon-pair truncated schemes, e.g., the broken pair approximation [25,26].

In 1970s the interacting boson model (IBM) was suggested by Arima and Iachello [27–32]. In the IBM the building blocks of the configurations and the Hamiltonian are interacting spin-zero and spin-two bosons, denoted by s and d , respectively. These two types of bosons were suggested to be mapping “images” of collective S pairs and spin-two (denoted by D) nucleon pairs [33–35]. The IBM has been proved to be very successful in describing the collective motions in nuclei, e.g., vibrational and rotational motion, and the low-lying states of the *gamma*-unstable nuclei, on the same footing. Thousands of papers addressed various issues of the IBM and its applications to low-lying states of atomic nuclei. The great success of the IBM stimulated many studies and discussions of the SD nucleon-pair approximation to the full nuclear shell model space. The dominant role played by S and D nucleon pairs in low-lying states of atomic nuclei is also understood from the matrix elements of a delta force for two identical nucleons in the same orbit. While the energy with $J = 0$ is the lowest for two identical nucleons in a single- j orbit interacting by a delta force, the energy with $J = 2$ is always the second lowest, see Fig. 1(a). A very good example to learn the dominant role played by S and D nucleon pairs is the low-lying spectrum of ^{210}Pb , which has two additional valence neutrons outside the doubly-closed-shell core, the ^{208}Pb nucleus. One finds that its $J^\pi = 0^+$ ground state is much lower than all other states, the first excited state with $J^\pi = 2^+$ arises at 0.8 MeV, then excited states with $J^\pi = 4^+, 6^+$ and 8^+ arise around 1.1 MeV, see Fig. 1(b). Empirically, one also learns such SD -pair dominance from the systematics of the low-lying states in even–even nuclei: the ground states of even–even nuclei are always zero without exception, and with very few exceptions the first excited states have spin two. Thus SD nucleon pairs are always the dominant bricks in constructing low-lying states in nucleus, although in some cases additional nucleon pairs should be also considered.

In 1990s Chen derived recursive formulas of calculating the matrix elements of the phenomenological shell model Hamiltonian in pair basis, and called this approach the nucleon-pair shell model (NPSM) [36]. This NPSM method was refined in Ref. [37] and called the nucleon-pair approximation (NPA) to the shell model. The NPSM and NPA have been used interchangeably in the literature. In recent years, the validity of the NPA was extensively investigated, and many NPA calculations were preformed to study the low-lying states of atomic nuclei.

This paper aims at a sound review of the NPA. It is organized as follows. In Section 2 we give a short introduction to the nuclear shell model, and define the shell model Hamiltonian. Then we introduce the formulation of the NPA. We also discuss its links to previous theories including the broken pair approximation (BPA) [25,26], the fermion dynamical symmetry model (FDSM) [38–44], and some interesting results of single- j shell. In Section 3 we discuss on its validity. We compare the calculated results by using the NPA and those calculated by exact shell model diagonalizations, for both schematic and realistic cases. In Section 4 we discuss its applications to low-lying states of realistic nuclei, with a few typical examples for nuclei in the mass number $A \sim 210$ region. We also discuss its application to other problems such as random interactions and quantum phase transitions, and future perspectives. In Section 5 we summarize this paper and conclude on the NPA. In Appendices A–C we present mathematical notations and useful formulas.

2. Formulation of the nucleon pair approximation

In this section we present a brief introduction to the formulation of the NPA. We begin with the nucleon pair basis and the NSM Hamiltonian. Then we present a simple example on how to evaluate the matrix elements in the NPA. The links of the present formulation with previous theories are also discussed.

Readers who are interested in a self-contained formulation of the NPA are warmly invited to Appendices B and C, where all relevant formulas of calculating the overlaps, one-body and two-body interactions of the shell model Hamiltonian in nucleon-pair basis are given. One can go directly to Refs. [36,37,45] for details.

2.1. The nucleon-pair basis

We use ψ_{nljm_j} to denote the three-dimensional oscillator wave function,

$$\psi_{nljm_j} = R_{nl}(r) (Y_l(\theta, \phi) \chi_{1/2})_{m_j}^{(j)} \equiv R_{nl}(r) \sum_{m_l, m_s} C_{lm_l, sm_s}^{jm_j} Y_{lm_l}(\theta, \phi) \chi_{m_s}.$$

The $nljm_j$ represent the number of radial nodes in $R_{nl}(r)$, orbital angular momentum, total angular momentum of a given single-particle orbit, and z-axis projection of j , respectively. $Y_{lm_l}(\theta, \phi)$ is the spherical harmonic function, χ_{m_s} is the spin

eigenfunction, and $C_{lm_l, sm_s}^{jm_j}$ is the Clebsch–Gordan coefficient, with the coupling order $\vec{l} + \vec{s} = \vec{j}$. The parity of ψ_{nljm_j} is given by $(-)^l$. In atomic nuclei there are two types of nucleons, i.e., neutrons and protons. One introduces the isospin quantum number t , which is mathematically similar to spin s , with $t = 1/2$ and $m_t = \pm 1/2$ corresponding to protons and neutrons, respectively. Because t is the same for both protons and neutrons, one can suppress t and keep only m_t to label the single-particle states. The single-particle energies for protons and neutrons are different due to the Coulomb force, with the proton ones higher (in particular when proton number Z becomes large). For all single-particle states within one major shell, the value of each j is unique, one usually suppresses the quantum numbers nl and uses only the total angular momentum j to label a certain single-particle level, without confusion. In this paper, we also use the letters a, b to denote the total angular momentum of a single-particle orbit.

A collective proton or neutron pair with angular momentum r and projection m_r is defined by

$$A_{mr}^{r\dagger} = \sum_{ab} y(abr) A_{mr}^{r\dagger}(ab), \quad A_{mr}^{r\dagger}(ab) = \left(C_a^\dagger \times C_b^\dagger \right)_{mr}^{(r)} \equiv \sum_{m_am_b} C_{am_a, bm_b}^{rmr} C_{am_a}^\dagger C_{bm_b}^\dagger, \quad (1)$$

where $C_{am_a}^\dagger$ is the operator of creating a nucleon in the a orbit. $y(abr)$ are called structure coefficients of the collective pair, which must be determined properly for each nucleus. The Pauli principle leads to the following symmetry of $y(abr)$:

$$y(abr) = -\theta(abr)y(bar), \quad \theta(abr) = (-)^{a+b+r}.$$

The phase convention of the time reversal of annihilation operator C_{am_a} is taken to be

$$\tilde{C}_{am_a} = (-)^{a-m_a} C_{a-m_a}.$$

The time reversal of the operator $A_{mr}^{r\dagger}$ is

$$\tilde{A}_{mr}^r = - \sum_{ab} y(abr) \left(\tilde{C}_a \times \tilde{C}_b \right)_{mr}^{(r)}. \quad (2)$$

For an even- A system with $2N$ valence protons or neutrons, all these valence nucleons are coupled to collective pairs. Our collective nucleon-pair subspace is constructed by coupling N collective pairs r_1, \dots, r_N stepwise,

$$A_{M_N}^{J_N\dagger}(r_1 r_2 \cdots r_N, J_1 J_2 \cdots J_N) |0\rangle \equiv A_{M_N}^{J_N\dagger} |0\rangle = \left(\cdots \left(\left((A^{r_1\dagger} \times A^{r_2\dagger})^{(J_2)} \times A^{r_3\dagger} \right)^{(J_3)} \times \cdots \times A^{r_N\dagger} \right)^{(J_N)} \right)_{M_N} |0\rangle.$$

Similarly, for an odd- A system with $2N + 1$ valence protons or neutrons, valence nucleons are paired except one nucleon which may occupy any single-particle level j of the shell in consideration. Our nucleon-pair subspace is given by successively coupling N nucleon pairs to the unpaired nucleon in the j orbit, with J_i (half-integer) being the total angular momentum for the first $2i + 1$ nucleons,

$$A_{M_N}^{J_N\dagger}(j r_1 r_2 \cdots r_N, J_1 J_2 \cdots J_N) |0\rangle \equiv A_{M_N}^{J_N\dagger} |0\rangle = \left(\cdots \left(\left(\left(C_j^\dagger \times A^{r_1\dagger} \right)^{(J_1)} \times A^{r_2\dagger} \right)^{(J_2)} \times A^{r_3\dagger} \right)^{(J_3)} \times \cdots \times A^{r_N\dagger} \right)^{(J_N)} \right)_{M_N} |0\rangle.$$

The basis for even and odd numbers of valence nucleons can be unified as below,

$$\begin{aligned} A_{M_N}^{J_N\dagger}(\tau) |0\rangle &\equiv A_{M_N}^{J_N\dagger}(r_0 r_1 r_2 \cdots r_N, J_1 J_2 \cdots J_N) |0\rangle \\ &= \left(\cdots \left(\left(\left(A^{r_0\dagger} \times A^{r_1\dagger} \right)^{(J_1)} \times A^{r_2\dagger} \right)^{(J_2)} \times A^{r_3\dagger} \right)^{(J_3)} \times \cdots \times A^{r_N\dagger} \right)^{(J_N)} \right)_{M_N} |0\rangle, \end{aligned} \quad (3)$$

where $A^{r_0\dagger} = C_j^\dagger$ for a nucleus with an odd number of valence nucleons and $A^{r_0\dagger} = 1$ for a nucleus with an even number of valence nucleons. The time reversal of the operator $A_{M_N}^{J_N\dagger}(\tau)$ in Eq. (3) is

$$\begin{aligned} \tilde{A}_{M_N}^{J_N}(\tau) &= \tilde{A}_{M_N}^{J_N}(r_i, J_i) = \tilde{A}_{M_N}^{J_N}(r_0 r_1 r_2 \cdots r_N, J_1 J_2 \cdots J_N) \\ &= \left(\cdots \left(\left(\left(\tilde{A}^{r_0} \times \tilde{A}^{r_1} \right)^{(J_1)} \times \tilde{A}^{r_2} \right)^{(J_2)} \times \tilde{A}^{r_3} \right)^{(J_3)} \times \cdots \times \tilde{A}^{r_N} \right)^{(J_N)} \right)_{M_N}. \end{aligned} \quad (4)$$

In this paper we use the abbreviation $|\tau, J_N\rangle = A_{M_N}^{J_N\dagger}(r_0 r_1 r_2 \cdots r_N, J_1 J_2 \cdots J_N) |0\rangle$.

If one considers both valence protons and neutrons, the nucleon-pair basis is given by

$$\begin{aligned} A_{M_N M_T}^{J_N T_N \dagger}(\tau) |0\rangle &\equiv A_{M_N M_T}^{J_N T_N \dagger}(r_0 t_0, r_1 t_1, r_2 t_2, \dots, r_N t_N; J_1 T_1, J_2 T_2, \dots, J_N T_N) |0\rangle \\ &= \left(\cdots \left(\left((A^{(r_0 t_0) \dagger} \times A^{(r_1 t_1) \dagger})^{(J_1 T_1)} \times A^{(r_2 t_2) \dagger} \right)^{(J_2 T_2)} \times A^{(r_3 t_3) \dagger} \right)^{(J_3 T_3)} \times \cdots \times A^{(r_N t_N) \dagger} \right)^{(J_N T_N)}_{M_N M_T} |0\rangle. \end{aligned} \quad (5)$$

Here the pair creation operator is defined by

$$\begin{aligned} A_{M_{r_i} M_{t_i}}^{(r_i t_i) \dagger} &= \sum_{ab} y(ab r_i t_i) \left(C_a^\dagger \times C_b^\dagger \right)^{(r_i t_i)} = \sum_{ab} y(ab r_i t_i) A_{M_{r_i} M_{t_i}}^{(r_i t_i) \dagger}(ab) \\ &= \sum_{ab} y(ab r_i t_i) \sum_{m_a m_b m_{t_a} m_{t_b}} (am_a, bm_b | r_i M_{r_i}) (tm_{t_a}, tm_{t_b} | t_i M_{t_i}) C_{am_a, m_{t_a}}^\dagger C_{bm_b, m_{t_b}}^\dagger. \end{aligned} \quad (6)$$

Here $t = 1/2$, r_i and t_i is the total angular momentum and isospin for the i th collective pair in Eq. (5). The couplings are two-folded: one corresponds to angular momentum coupling, and the other corresponds to the isospin coupling.

In many calculations, however, the nucleon-pair basis with both valence protons and valence neutrons is usually taken as

$$|\tau_\nu J_\nu, \tau_\pi J_\pi : JM\rangle = \sum_{M_\nu M_\pi} C_{J_\nu M_\nu J_\pi M_\pi}^{JM} |\tau_\nu J_\nu M_\nu\rangle |\tau_\pi J_\pi M_\pi\rangle, \quad (7)$$

without considering the isospin symmetry, where π is for protons and ν is for neutrons. The reason is that the NPA has been applied mainly to medium and heavy mass nuclei, for which valence protons and neutrons usually belong to different major shells. Even if the valence protons and neutrons are in the same shells, e.g., for ^{132}Te , the valence protons are particle-like and the neutrons are hole-like, and the isospin quantum number is not used for simplicity.

2.2. The nuclear shell model Hamiltonian

One feature of atomic nuclei is that the residual interaction between the valence nucleons, i.e., the part of the interaction which cannot be covered by the mean-field part, is very strong, and plays an important role. The residual interaction leads to strong configuration mixings. Therefore, one needs to diagonalize the NSM Hamiltonian in the shell model space to obtain the eigenvalues and wave functions.

The general form of the shell model Hamiltonian includes a one-body term

$$H_1 = \sum_{am_a m_t} \epsilon_{am_t} C_{am_a, m_t}^\dagger C_{am_a, m_t} = - \sum_{a_\pi} \hat{a}_\pi \epsilon_{a_\pi} \left(C_{a_\pi}^\dagger \times \tilde{C}_{a_\pi} \right)^{(0)} - \sum_{a_\nu} \hat{a}_\nu \epsilon_{a_\nu} \left(C_{a_\nu}^\dagger \times \tilde{C}_{a_\nu} \right)^{(0)}, \quad (8)$$

and a two-body term

$$H_2 = \frac{1}{4} \sum_{abcd, JT} \sqrt{(1 + \delta_{ab})(1 + \delta_{cd})} G_{JT}(ab, cd) \sum_{M_J M_T} A_{M_J M_T}^{JT\dagger}(ab) A_{M_J M_T}^{JT}(cd), \quad (9)$$

where

$$A_{M_J M_T}^{JT}(cd) = \left(A_{M_J M_T}^{JT\dagger}(cd) \right)^\dagger, \quad \hat{a} = \sqrt{2a + 1}.$$

$J(T)$ in $A_{M_J M_T}^{JT}(ab)$ is the total spin (isospin) resulting from angular momentum (isospin) couplings of two nucleons, one in the a orbit and the other in the b orbit. $G_{JT}(ab, cd)$'s are two-body matrix elements defined by

$$G_{JT}(ab, cd) = \langle 0 | A_{M_J M_T}^{JT}(ab) | V | A_{M_J M_T}^{JT\dagger}(cd) | 0 \rangle, \quad (10)$$

for a two-body interaction, V . $G_{JT}(ab, cd)$'s are independent of M_J or M_T . The Hamiltonian of Eq. (9) respects parity conservation, which means that the parity product for the four orbits in $G_{JT}(ab, cd)$ of Eq. (9) is positive. The Hamiltonian Eq. (9) also respects rotational and time-reversal invariance, which means that V in Eq. (10) is a scalar and takes real values. When we consider systems in which there is only one type of valence particles (i.e., neutrons or protons), T can be suppressed. For a single- j shell ($a = b = c = d \equiv j$) labels a , b , c , d , and T are suppressed, and we denote the two-body matrix elements by G_j (the allowed values of J are $J = 0, 2, \dots, 2j - 1$). The number of non-zero G_j 's of identical nucleons in a single- j shell is $j + \frac{1}{2}$.

In addition to the above general NSM Hamiltonian, another phenomenological and separable form is widely used. This separable form is easy to handle, and many NPA calculations are carried out by assuming this form. The Hamiltonian H in

this approach consists of two parts, namely $H^{\text{like nucleons}}$, which includes the interactions between like nucleons, and $H_{\pi\nu}$, which describes the interactions between neutrons and protons.

$$H^{\text{like nucleons}} = H_1 + H_2, \quad (11)$$

where H_1 is the one-body part, taken to be the spherical single-particle energy

$$H_1 = \sum_{j\sigma} \epsilon_{j\sigma} C_{j\sigma}^\dagger C_{j\sigma},$$

where $\sigma = \pi, \nu$. The values of $\epsilon_{j\sigma}$ are usually assumed to be the excited energies of the lowest j state of only one nucleon outside the nearest doubly-closed core. H_2 in Eq. (11) is the two-body part. It is expanded in terms of the particle-particle type (H_P) and particle-hole type (V_{ph}) interactions.

$$H_P = V_0 + V_2 + \dots \quad (12)$$

Here

$$\begin{aligned} V_0 &= G_0 \mathcal{A}^{\dagger(0)} \mathcal{A}^{(0)}, & \mathcal{A}^{\dagger(0)} &= \sum_j \frac{\sqrt{2j+1}}{2} (C_j^\dagger \times C_j^\dagger)_0^{(0)}, \\ V_2 &= G_2 \sum_M \mathcal{A}_M^{\dagger(2)} \mathcal{A}_M^{(2)}, & \mathcal{A}_M^{\dagger(2)} &= \sum_{j_1 j_2} q(j_1 j_2) (C_{j_1}^\dagger \times C_{j_2}^\dagger)_M^{(2)}, \end{aligned} \quad (13)$$

with

$$\begin{aligned} \mathcal{A}^{(0)} &= (\mathcal{A}^{\dagger(0)})^\dagger, & \mathcal{A}_M^{(2)} &= (\mathcal{A}_M^{\dagger(2)})^\dagger, \\ q(j_1 j_2) &= \frac{(-)^{j_1-1/2} \hat{j}_1 \hat{j}_2}{\sqrt{20\pi}} \frac{1 + (-)^{l_1+l_2}}{2} C_{j_1 1/2, j_2 -1/2}^{20} \langle nl_1 | r^2 | nl_2 \rangle. \end{aligned} \quad (14)$$

Here $\hat{j} \equiv \sqrt{2j+1}$.

The particle-hole interaction V_{ph} takes the form

$$V_{ph} = \kappa Q^{(t)} \cdot Q^{(t)} = \kappa (-)^t \hat{t} (Q^{(t)} \times Q^{(t)})^{(0)} = \kappa \sum_M (-)^M Q_M^{(t)} Q_{-M}^{(t)}, \quad (15)$$

where $Q_M^{(t)}$ is called the multipole operator, defined by the second quantization of the operator $r^t Y_{tM}$; and for $t = 2$, $Q_M^{(2)}$ is the quadrupole operator:

$$Q_M^{(2)} = \sum_{cd} q(j_1 j_2) (C_{j_1}^\dagger \times \tilde{C}_{j_2})_M^{(2)}, \quad (16)$$

where $q(j_1 j_2)$ is the same as that in the definition of $A_M^{\dagger(2)}$.

The phenomenological and separable form of the neutron-proton interaction is given by

$$H_{\nu\pi} = \sum_t \kappa_{\nu\pi}^{(t)} Q_\nu^{(t)} \cdot Q_\pi^{(t)}. \quad (17)$$

In many NPA calculations, the shell model Hamiltonian for like valence particles is assumed to consist of single-particle, monopole and quadrupole pairing, and quadrupole-quadrupole interactions, and the interaction between valence protons and neutrons is assumed to be of simple quadrupole-quadrupole type, i.e.,

$$H = H_1 + \sum_\sigma \left(\sum_{s=0,2} G_{s\sigma} \mathcal{A}^{s\sigma\dagger} \cdot \mathcal{A}^{s\sigma} + \kappa_\sigma Q_\sigma \cdot Q_\sigma \right) + \kappa_{\pi\nu} Q_\nu \cdot Q_\pi. \quad (18)$$

This separable form of the shell model Hamiltonian was extensively studied in Refs. [46,47]. $G_{s\sigma}$ is in unit of MeV; $G_{2\sigma}$, κ_σ and $\kappa_{\pi\nu}$ are in unit of MeV/ r_0^4 . The r_0 comes from the matrix element of $\langle nl | r^2 | nl \rangle$, and $r_0^2 = 1.012 A^{1/3} \text{ fm}^2$.

2.3. Matrix elements in the coupled nucleon-pair basis

The key technique of the NPA is the Wick theorem of coupled nucleon pairs developed in Refs. [48,49]. In Refs. [50–52], Piepenbring and collaborators used this technique and presented explicit formulas of one-body and two-body operators in the pair basis up to four non-collective pairs. Very recently, the same method has been also applied in developing the recurrence relations which permit computations of matrix elements of one-body and two-body operators in the generalized seniority scheme [53–55].

For compactness of this review, formulas to calculate one- and two-body matrix elements in the NPA by using the generalized Wick theorem for nucleon pairs are explained and given in Appendices B and C. These formulas are self-contained, with an introduction of commutators between coupled operators, from an elementary level of quantum mechanics. Details to derive these formulas can be found in Refs. [36,37,45].

Here we give only one simple example by using the single-particle energy term H_0 of Eq. (18), to explain the essence of the NPA formulation. We rewrite H_0 as $H_0 = -\sum_a \hat{a}\epsilon_a (\tilde{C}_a^\dagger \times \tilde{C}_a)^0$, and obtain

$$\langle jr_1 \cdots r_N, J_1 \cdots J_N | H_0 | j_0 s_1 \cdots s_N, J'_1 \cdots J'_N \rangle = \sum_{k=N}^0 \langle jr_1 \cdots (\mathbf{r}'_k) \cdots r_N, J_1 \cdots J_N | j_0 s_1 \cdots s_N, J'_1 \cdots J'_N \rangle, \quad (19)$$

where (\mathbf{r}'_k) represents \tilde{A}^{r_k} given by

$$\tilde{A}^{r_k} = [\tilde{A}^{r_k}, H_0] = \begin{cases} \sum_{ab} y(ab r_k)(\epsilon_a + \epsilon_b) \tilde{A}^{r_k}(ab), & 1 \leq k \leq N, \\ \epsilon_j \tilde{C}_j, & k = 0. \end{cases} \quad (20)$$

By using this formula, one can calculate the matrix elements of the single-particle energy in terms of overlaps of pair basis states. In fact, matrix elements of *any operators* can be written in terms of overlaps. In Appendix B one sees that the overlaps of N nucleon-pair basis states can be written in a recursive way, i.e., in terms of overlaps of $N - 1$ nucleon pairs, and the overlaps for $N = 1$ and 2 are analytically available. In the NPA, one avoids the snare of weight factors and phases in rearranging the order of the Clebsch–Gordan coefficients. Because the calculation in the NPA is performed in a recursive way, the NPA is applicable to any number of pairs, with no restriction on the pair structure coefficients, in principle.

Another algorithm of the NPA is to make use of the m -scheme shell model code. In this method, all calculations are carried out by using the m scheme: the basis states are expressed in terms of linear combinations of single particle Slater determinants, and the bit manipulation is used to denote each Slater determinant. The main task is the decomposition of the nucleon-pair basis states in terms of the m -scheme basis states, and the decomposition of the Hamiltonian in terms of uncoupled creation and annihilation operators, by resorting to the Clebsch–Gordan coefficients. The advantage of this method is that it makes use of the very powerful m -scheme shell model code, and that it can treat odd and even systems on the same footing without any technical distinction. One disadvantage is that one cannot use this method to handle the case where the shell model configuration space becomes too large. If one uses four-byte integers as Slater determinants, one can handle only 32 single-particle states (i.e., sum of $2j + 1$ over all orbits of the shell) which correspond to the 50–82 major shell. One needs eight-byte integers if one wants to enlarge the single particle space. Yoshinaga et al. used this scheme in their computer program of the nucleon-pair approximations, and called their method Pair-Truncated Shell Model (PTSM). The calculated results of the PTSM are precisely the same as those of the NPA, i.e., the PTSM is equivalent to the NPA (or the NPSM). Therefore the PTSM, NPA, and NPSM should be understood interchangeably.

2.4. Special cases of the nucleon-pair approximation

In this subsection we discuss a number of previous models involving the nucleon-pair approximation. Most of these models are special realizations of the NPA.

2.4.1. Integrable models: seniority scheme and Richardson pairing model

The simple seniority scheme is applicable to identical nucleons in a single- j shell. For all shells with $j \leq 7/2$, seniority scheme provides us with analytical results, whatever the two-body interactions are. The seniority violation terms arise from the $j = g_{9/2}$ shell. Recently there have been many discussions on the seniority conservation and violation effects of single- j shells, in particular, the $j = g_{9/2}$ shell [56–61]. For instance, electromagnetic transitions of some nuclear states are hindered by selection rules of seniority quantum number (such states were called “seniority isomers” in the literature [59]).

The seniority scheme of the j^n configuration was generalized to many- j shells, called the generalized seniority scheme by Talmi [24]. In the generalized seniority scheme, the pair structure coefficients of S pair are so chosen that the state $S^\dagger |0\rangle$ is an eigenstate of the Hamiltonian of two valence nucleons. If $(S^\dagger)^2 |0\rangle$ is also an eigenstate, $(S^\dagger)^N |0\rangle$ are eigenstates of H for any N . Let $D^\dagger |0\rangle$ be the lowest spin-two state of two valence protons or neutrons. If $S^\dagger D^\dagger |0\rangle$ is an eigenstate, the states $(S^\dagger)^{N-1} D^\dagger |0\rangle$ are eigenstates of H , and are assigned generalized seniority two. Simple formulas are available for eigenvalues and $B(E2)$ values of these seniority zero and two states. Reviews of the generalized seniority scheme can be found in Refs. [4,35].

The generalized seniority scheme was applied extensively to study the low-lying states of semi-magic nuclei [4,34], e.g., the Sn isotopes [62] and $N = 82$ isotones [63]. There are more than one hundred papers in *Phys. Rev. C* in which “seniority” appears in the titles and abstracts. Here we mention that, in Ref. [64] Ginocchio studied the data of pion double charge exchange on the Nickel isotopes and found a good consistence with predictions of the generalized seniority scheme; in Ref. [65] Monnoye et al. studied the odd mass Nickel isotopes in the full $pf + g_{9/2}$ shell; in Ref. [66] Engel et al. applied this approach to evaluate the double beta decay rates in ^{76}Ge , ^{82}Se and $^{128,130}\text{Te}$; and Auerbach et al. [67] and Ginocchio [68]

studied double charge exchange transition matrix elements; in Ref. [69] the yrast seniority states are compared with the corresponding shell model states of the Sn isotopes $^{104-112}\text{Sn}$, demonstrating that, for most of the cases the energies agree within a few hundred keV. Very recently, Morales, Isacker and Talmi [70] applied the generalized seniority scheme to explain the “anomalies” of experimental B(E2) values [71] for even–even $^{102-130}\text{Sn}$ nuclei: the generalized seniority scheme predicts a peak in the middle of the shell, while experimental data present a shallow minimum. The generalized seniority has been also applied to study the microscopic foundation of the IBM (e.g., see Refs. [33,34]).

For open-shell nuclei, Gai et al. applied the generalized seniority scheme to the description of band heads in a number of slightly deformed odd-mass nuclei (odd number of protons Z and even number of neutrons N) [72]. By using very simple calculations of matrix elements and wave functions, they obtained formulas which describe a large amount of data on band head energies and magnetic moments, for high- and low-spin particle states.

The Richardson equations provide us with an approach of the simplified pairing Hamiltonian. Richardson showed that the simple pairing Hamiltonian is readily solvable via a recursion procedure. In recent years many progresses have been made, by applying the Richardson solutions, in the description of various strongly correlated quantum many-body systems in condensed matter physics, nuclear physics, and the physics of confined systems. For a recent review, see Ref. [73].

2.4.2. The broken pair approximation

In atomic nuclei the attractive pairing interaction is very strong. One therefore assumes that spin-zero (S) pairs are dominant in the ground states of even–even nuclei, and the low-lying states can be approximated by configurations of breaking only one or two S pairs (or in other words, low-seniority states). This approximation is called the broken pair approximation (BPA) [25]. In the literature the BPA is also called the number-fixed BCS, or the projected quasiparticle model. The NPA is reduced to the BPA by permitting only one or two non- S pairs in the nucleon-pair basis states.

The BPA has been proved to be rather successful in studying the low-lying states of single-closed-shell even–even nuclei (as the generalized seniority scheme), for instance, the isotones with the neutron number $N = 50, 82$, and the Ni, Sn, Pb isotopes, etc. It has been also applied in studies of the electron-scattering form factors [74] and transition densities [75] for ^{88}Sr , ^{90}Zr , ^{92}Mo , ^{58}Ni , and ^{116}Sn , inelastic hadron scattering [76] for ^{88}Sr , ^{90}Zr , and ^{112}Sn . The BPA amplitudes have been used to evaluate the (p, t) and (t, p) cross sections for the even Ni isotopes [77]. Allaart and collaborators studied the lowest levels of odd semi-magic nuclei, e.g., the odd-mass $N = 50$ isotones [78] and odd Sn isotopes [79] by using the BPA with the configuration space constructed by using one unpaired nucleon, one non- S pair and S pairs for all other valence nucleons. Reasonable agreements with experimental results have been obtained for observed electromagnetic properties, electron scattering, and particle transfer data.

The BPA approach has been also applied to cases where either the proton or the neutron number of valence particles (or holes) is small (e.g., Sb, Ir, As, Zr, Mo, Ru isotopes) [80–82]. Another application of the BPA is to study microscopic foundation of the IBM. A comprehensive review of the broken pair approximation was given in Ref. [26].

2.4.3. The Ginocchio model

In Refs. [38–40] Ginocchio suggested a novel SD -pair approximation (called the Ginocchio model) in the k – i basis, in which the single-nucleon angular momentum j is decomposed into so-called pseudo orbit, k , and pseudo spin, i (One should not confuse the pseudo spin i here with the pseudo spin of the quasi-degenerate single-particle doublets discussed in Ref. [83]). $\vec{j} = \vec{k} + \vec{i}$, and $C_{jm_j}^\dagger = \sum_{mkmi} C_{km_k, im_i}^{jm} b_{km_k, im_i}^\dagger$.

In the Ginocchio model, there are two schemes for SD pairs and the multipole operators. One is called the k -active, assuming that $k = 1$ and $i = 1/2, 7/2$ couples to zero. In the k -active scheme, $S^\dagger = \sum_a \frac{1}{2} \hat{a} (C_a^\dagger \times C_a^\dagger)^{(0)}$, and $D^\dagger = -\frac{\sqrt{3}}{2} \sum_{ab} \sum_{i=1/2, 7/2} (-)^{b+i} \hat{a} \hat{b} \begin{Bmatrix} a & b & 2 \\ 1 & 1 & i \end{Bmatrix} (C_a^\dagger \times C_b^\dagger)^{(2)}$, a and $b = i+1, i, i-1$. In this scheme, the SD pair operators and multipole operators form an $SP(6)$ algebra. The other scheme is called the i -active, assuming that $k = 2$ couples to zero and $i = 3/2$. In this case $S^\dagger = \sum_a \frac{1}{2} \hat{a} (C_a^\dagger \times C_a^\dagger)^{(0)}$, and $D^\dagger = \sum_{ab} (-)^{a+\frac{3}{2}} \hat{a} \hat{b} \begin{Bmatrix} a & b & 2 \\ 3 & 3 & 2 \end{Bmatrix} (C_a^\dagger \times C_b^\dagger)^{(2)}$, a and $b = k+3/2, k+1/2, k-1/2, k-3/2$. In the i -active scheme, the SD pair operators and multipole operators form an $SO(8)$ algebra.

Assuming a shell model Hamiltonian constructed by such b_{km_k, im_i}^\dagger and b_{km_k, im_i} , one achieves a model in which the SD subspace is fully decoupled from the remaining parts of the NSM space. Ginocchio studied the chains of subgroups with dynamical symmetries which are similar to those in the IBM, e.g., $SO(8) \supset SO(6) \supset SO(5) \supset SO(3)$, $SO(8) \supset SO(7) \supset SO(5) \supset SO(3)$, $SO(8) \supset SO(5) \times SU(2) \supset SO(5) \supset SO(3)$, and so on.

The Ginocchio model is mathematically an elegant model, with its subspace constructed by symmetry-dictated fermionic SD pairs. It is therefore very useful in studies of the microscopic foundation of the IBM and energy spectra of even–even nuclei. For instance, Arima et al. applied this model to study the boson mappings of fermion systems [84] and the low-lying states of Samarium isotopes [85]. Unfortunately, the $SP(6)$ scheme and its $SU(3)$ rotational limit were abandoned, due to the fact that the Pauli principle forbids the highest $SU(3)$ representation for cases with pair number larger than $\sum_j (\frac{2j+1}{6})$.

2.4.4. The fermion dynamical symmetry model

The fermion dynamical symmetry model (FDSM) [41–44] is a further development of the Ginocchio model. Wu and collaborators established a microscopic relation between the k - i basis and the shell structure. They assumed that the normal-parity levels in a major shell must be either k or i active, and that the abnormal parity level (i.e., intruder level) coming from the next higher shell must be assigned $k = 0$, i.e., the nucleons in the abnormal parity level are assumed to be δ pairs,

$$\delta = \frac{1}{2j+1} \left(b_{0j}^\dagger b_{0j}^\dagger \right)^{(0)}.$$

For all shells with $j_{\max} < 15/2$, there is a unique k - i decomposition: either k active or i active. One important development is that the SU(3) limit of the Ginocchio model is resurrected, by assuming that the nucleons which contribute collective motion of low-lying states are those in the normal parity states. The abnormal parity levels for both proton and neutron play the role of “siphoning” off the valence nucleons, and the effective number of valence nucleons in the normal parity levels were suggested to follow an empirical formula [86].

The FDSM has been applied to many issues of the nuclear structure physics, e.g., high-spin physics [87,88], normal nuclear deformation [89] and superdeformation [90] in nuclei. A numerical program of the FDSM calculations was written by Wu and Vallieres. The advantage of the FDSM in comparison with the IBM is that it is a fermion model. It predicts a number of new symmetries beyond the IBM. Among all, the dynamical Pauli effect predicted by the FDSM has observable consequences for nuclear masses, E2 transition rates of rare-earth and actinide nuclei, and so on. The saturation and correlations of $B(E2)$ and $B(M1)$ values of even-even nuclei in rare-earth and actinide regions are explained easily. If the Pauli effect is ignored, there is a one-to-one correspondence between the generators and building blocks of the FDSM and the IBM. In the limit of large particle numbers one derives the geometric particle-rotor model. On the other hand, there were also critical discussions of the fundamental assumptions made in the FDSM [91], and controversy about the FDSM wave functions in comparison with the exact shell model results [92,93].

The NPA is reduced to the FDSM (and also the Ginocchio model) by assuming the SD pairs with special pair structure coefficients. Some of the formulas and its relation to the NPA were discussed in Ref. [36]. A comprehensive review of the FDSM has been given in Ref. [43].

2.4.5. Nucleon-pair approximation in the deformed basis

Most nucleon-pair approximations have been carried out by using the spherical shell model basis. The reason is that nucleon-pair approximations were mainly applied to study the low-lying states of nuclei with the numbers of valence protons (N_p) and valence neutrons (N_n) not large. In these cases the low-lying states are not well deformed. As $N_p N_n$ increases, nuclei become gradually deformed. The more the valence proton numbers and valence neutron numbers, the larger the deformation (before the deformation is saturated). This systematics is described by Casten's $N_p N_n$ scheme [94].

As is well-known, the conventional SD -pair truncation constructed in the spherical shell model basis is not very satisfactory in describing the low-lying states of well deformed nuclei. One convenient way to deal with the deformed nuclei is to start with an assumption that valence nucleons move in a deformed well. Here the neutron–proton interactions are first considered to obtain the deformed Nilsson single-particle diagram. With this assumption the valence nucleons are distributed in the Nilsson orbitals. Then one considers the interactions between valence protons and those between valence neutrons. One usually performs the Hartree–Fock–Bogoliubov calculation and obtains a deformed (Nilsson) pair [95]. The deformed pair does not conserve angular momentum, and can be rewritten in terms of nucleon pairs in the spherical shell model basis, with spin $J = 0, 2, 4, \dots$ (i.e., $SDG \dots$ pairs).

Many authors used nucleon-pair approximation in the deformed basis in order to investigate the validity of SD -pair approximation and the microscopic foundation of the interacting boson model [96–107]. For examples, Bes et al. [96,97] applied the Nilsson plus the BCS model to the low-lying states in strongly deformed nuclei, and pointed out the important role played by the spin-four and spin-six pairs (i.e., G and I pairs) for these states; similar results were obtained in Ref. [98] which emphasized the decisive role of $J > 2$ pairs in obtaining the many-body correlations in strongly deformed nuclei. On the other hand, Otsuka et al. showed [99] that the Cooper pairs in the Nilsson model consist mainly of SD pairs even if the quadrupole deformation is large and that the inclusion of G pairs improves the results. In Ref. [100] the number projected Hartree–Fock–Bogoliubov wave function was shown to be dominated by SD pairs before the occurrence of the back-bending. The wave functions after back-bending are essentially constructed by spin-maximum (i.e., spin-aligned) pairs coupling to SD pairs. These studies suggested the importance of SD pairs for the states with large deformation. A review of these efforts are given in Table III of Ref. [35]. The sdg boson approximation (a g boson has spin four, mapped from the G nucleon pairs) is reviewed in Ref. [108].

2.4.6. The multi-step shell model

The Multi-Step Shell Model (MSSM) was proposed by Liotta and collaborators [109–111]. In this method, one first constructs the two-particle states, and then proceeds by coupling the next two valence particles to the first two-particle states to describe a four-particle system. For a six-particle system, one couples two-particles to four-particle states obtained above. This procedure is repeated until all valence particles are exhausted (For a nucleus with an odd number of valence particles, one couples the last particle in the end). The assumption here is that only the lowest states of the two-particle systems are essential in describing the low-lying states of the four-particle system, and only the lowest states

of the two- and four-particle systems are essential in describing the low-lying states of the six-particle system. In order to improve the accuracy of predictions, energies of states obtained in each step are “renormalized” to experimental values.

Although the MSSM is not precisely the NPA, the physical picture is very similar. Earlier studies of the MSSM are restricted to low-lying states of semi-magic nuclei such as tin and lead isotopes. In Ref. [112] Sandulescu et al. further developed this idea and called it the quasi-particle multi-step shell model, with applications to low-lying states for a few even-even [113] and odd-mass [114] Sn isotopes.

2.4.7. The NPA with isospin symmetry

In the formulation of the NPA in Refs. [36,37], the isospin symmetry has not been considered. The model space is usually constructed by coupling valence proton pairs and valence neutron pairs, and the shell model Hamiltonian takes usually the separable form, accordingly. For valence protons and valence neutrons in the same shell, in particular for the $N \approx Z$ nuclei, one should consider the isospin symmetry as well.

The generalization of the NPA to considering the isospin degree of freedom is straightforward. In the presence of isospin degree of freedom, all couplings become two-folded, one originates from the angular momentum couplings and the other from the isospin couplings (the isospin of each nucleon is 1/2). The generalized version of the NPA with isospin symmetry has been recently presented [45], with one computer code developed in Fortran language and another code in Matlab language. In Ref. [115] Fu et al. applied their NPA with the isospin symmetry to studies of four and six nucleons in the pfg shell (below ^{100}Sn). Studies of the MSSM were extended to systems with both valence protons and neutrons, and in Refs. [116,117] Qi et al. performed the SM and MSSM calculations for nucleons in a single $g_{9/2}$ shell.

Special cases of the NPA with isospin were also studied in the Collective Pair Approximation (CPA), developed by Maglione and collaborators [118]. In Ref. [119] Catara et al. studied some negative parity states in the configuration space constructed by collective fermion pairs with positive parity (SD pairs) and negative parity (PF pairs). In Ref. [120] Gao et al. studied low-lying states with negative parity of ^{18}O in the configuration of collective SD pairs coupled to collective particle-hole excitations. This approach has been applied to study the low-lying states of both even- and odd-mass $1s0d$ - and $1p0f$ -shell nuclei, by Kwasniewicz and collaborators [121]. In their calculations, the structures of their collective pairs are fixed by diagonalizing the nuclear shell model Hamiltonian of two nucleons outside the closed shells. Their Hamiltonian includes the one-body and two-body terms. They were able to include both $T = 1$ pairs and $T = 0$ pairs in their calculations. According to their calculations [121], the lowest $T = 0$ pairs are of minor significance for low-lying states of mass number $A = 60\text{--}62$ nuclei; and the low-lying states of these nuclei are well represented by the lowest $T = 1$ pairs instead.

2.5. Summary of this section

In this section we have presented a brief introduction to the nucleon-pair approximation to the shell model. We have defined the nuclear shell model Hamiltonian H which includes one-body and two-body interactions, with both the general and schematic forms. The general form of two-body interactions is defined by two-body matrix elements, $\langle j_1j_2, JT | V | j_3j_4, JT \rangle$. The schematic form of two-body interactions is defined by multipole pairing interactions and multipole-multipole interactions, usually with a separable form for valence protons and neutrons.

We have defined the nucleon-pair basis. For even-even nuclei the basis is constructed by step-wise coupling of coherent nucleon pairs. For odd-mass nuclei, the basis is given by stepwise coupling the nucleon-pairs to the unpaired nucleon. Please be noted that the coupling scheme of odd-mass nuclei is different from the conventional coupling scheme in which one couples the unpaired nucleon to the even-even nuclei. The nucleon-pair basis is in general neither orthogonal nor normalized. If the valence protons and neutrons are not in the same shells, the nucleon-pair basis is constructed by coupling valence proton-pair basis to valence neutron-pair basis. For nuclei near $Z \approx N$ with both valence protons and neutrons, one should consider the isospin invariance as well.

For the compactness of this review, we put all the explicit formulas for calculating matrix elements of one-body and two-body operators, such as the shell model Hamiltonian and transition operators, in Appendix B, instead of inserting them into this section. Those formulas are sufficient to code the computer program for the NPA calculations. As usual, one obtains the energy level scheme of low-lying states, and evaluates electromagnetic transition rates, after diagonalizing the shell model Hamiltonian. An extension of the NPA with the isospin symmetry is straightforward. All couplings become two-folded (i.e., both angular momentum coupling and isospin coupling), instead of only one-folded coupling (i.e., angular momentum coupling). Useful formulas of the NPA with the isospin symmetry are given in Appendix C, and computer codes of the isospin-dictated NPA have been recently developed in Fortran and Matlab languages.

We have very briefly discussed a few special cases of the NPA, including the generalized seniority scheme, the broken pair approximation, the Ginocchio model, the fermion dynamical symmetry model, the NPA by the m -scheme shell model code, in a deformed basis, with isospin, and the multi-step shell model. Details of these models can be found in Refs. [24,26, 32,40,43,73,95,109].

3. Validity of the NPA

The dimension of the NPA is drastically smaller than that of the exact shell model. This leads to the simplicity of the NPA in which the physics exhibited in numerical calculations is much more transparent. Therefore its validity is crucial—the NPA

would not be useful if the agreement between calculated results by using the NPA and those by using exact shell model diagonalizations were not good. There have been a large amount of efforts to study the validity of the NPA in various cases, e.g., for both a single- j and many- j shells, for both schematic and realistic interactions, for both semi-magic nuclei with only one type of valence particles and open-shell nuclei in the presence of both valence protons and valence neutrons.

The validity of S -pair approximation has been well-known, owing to many discussions and applications of the generalized seniority scheme for semi-magic nuclei. In the seniority scheme, the ground states of even–even nuclei are given by S pair condensates. The validity of SD -pair approximations has been mainly motivated by the microscopic foundation of the interacting boson model (IBM). Many of these studies were carried out by using the spherical shell model basis [33,34,122–129]. There have been also many studies which address the issue whether SD - or SDG -pair truncated subspace is a good approximation to the full shell model space (e.g., [95–107]) by using the deformed Nilsson single-particle diagram. In recent years one is able to diagonalize the shell model Hamiltonian in the nucleon pair basis for configuration dimension up to $10^{4–5}$ by using desktop computers. This new development allows an explicit comparison between wave functions obtained by the exact shell model calculation and those by the nucleon-pair truncated shell model calculation.

In this section we discuss the validity of the NPA in the presence of both schematic and effective interactions. We use the conventional spherical shell model basis.

3.1. The NPA for a single- j shell

The validity of the NPA for a single- j shell has been studied in many papers. For a single- j shell, a pair with spin J is uniquely defined, and calculations in a single- j shell are much easier than for many- j shells. Thus the NPA in a single- j shell serves as a prototype of complicated many- j shells, with the virtue of simplicity.

For a single- j shell, seniority is defined exactly. If the interaction between like valence nucleons is simply an attractive pairing interaction, the shell model states are classified by the seniority quantum number. The ground states of even–even nuclei have the lowest seniority, i.e., seniority equals zero. If one considers other interactions, say, quadrupole pairing interaction, the seniority is in principle not a good quantum number for some of the states of nucleons in a single- j shell. It is found, however, that seniority continues to serve as a very useful quantum number for a wide range of interactions, as discussed in Ref. [56].

In this subsection we discuss validity of the NPA for a single- j shell, with quadrupole–quadrupole interaction, and pairing plus quadrupole interactions, as well as a few schematic cases such as J -pairing and J_{\max} -pairing interactions.

3.1.1. Quadrupole–quadrupole interaction

In Ref. [128], Halse studied identical fermions in a $j = 13/2$ shell with a quadrupole–quadrupole interaction. He calculated the overlaps between the wave functions in the SD -pair subspace and the exact solutions, and found that the lowest levels are very well represented by the SD -pair subspace. In Ref. [129], Halse et al. investigated the pair approximation for rotational states in a single $j = 17/2$ shell of identical nucleons again with a quadrupole–quadrupole interaction. They found that the number of different pairs necessary for a good agreement with the exact shell model results are state dependent: the SD pairs are the dominant building blocks of low-spin states in the ground band, and the contribution from the G pair is very important for the low-spin states in the lowest $K = 2$ band states. The moment of inertia is about 30% lower than the exact result.

In Ref. [130] Yoshinaga et al. studied six nucleons in a single- j shell ($j = 23/2$) with the quadrupole–quadrupole interaction, in the SDG -pair subspace. The results could be improved by considering the effects from pairs beyond the SDG subspace. This was achieved by using a so-called H^n -cooling method suggested by Nakada and Otsuka [131], who diagonalized the Hamiltonian in the following basis: $|\tau_i, J_N\rangle = A_{M_N}^{Jn\dagger}(r_0 r_1 r_2 \cdots r_N, J_1 J_2 \cdots J_N)|0\rangle, H|\tau_i, J_N\rangle, H^2|\tau_i, J_N\rangle, \dots, H^n|\tau_i, J_N\rangle$. They picked up the lowest state wave function of these $(n+1)$ -dimensional space and denote this state by Φ_i . Supposing the $(SDG)^N$ subspace is N -dimensional, they performed the above $(n+1)$ -dimensional diagonalization for each $|\tau_i, J_N\rangle$ and obtained new N -dimensional subspace, Φ_i (the lowest state in energy given in each diagonalization). These Φ_i ($i = 1, 2, \dots, N$) form the new pair-basis states. The H^n -cooling procedure was refined as follows. One first diagonalizes the Hamiltonian H in the SDG -pair subspace represented by $|\tau_i, J_N\rangle$ ($i = 1, 2, \dots, N$), and obtains the eigen-functions, $\Phi^{(0)}(i)$. Next one constructs the $(n+1)$ dimensional subspace $\Phi^{(0)}(i), H\Phi^{(0)}(i), H^2\Phi^{(0)}(i), \dots, H^n\Phi^{(0)}(i)$, and diagonalizes H in the $(n+1)$ dimensional subspaces. This is repeated for N successive times (i.e., for different i), and in each time the lowest eigen function, denoted by $\Phi^{(1)}(i)$, is selected. The N eigen-functions, $\Phi^{(1)}(i), i = 1, 2, \dots, N$ form the new basis states. Yoshinaga found [132] that the SDG pair basis with the H^n -cooling such modified is very good.

There is an interesting result of pair approximation for a single- j shell with a quadrupole–quadrupole interaction, obtained by Chen and collaborators [133]. They studied four identical nucleons in a $j = 21/2$ shell, with only the attractive quadrupole–quadrupole force. Unexpectedly, they found that the subspace constructed by using pairs with the highest spin (i.e., the J_{\max} pairs, $J_{\max} = 2j - 1$) are very good approximation to the full SM space, namely, the J_{\max} pairs are much better building blocks than the low-spin pairs (such as SDG pairs). Furthermore, the bands can be elegantly classified by using these J_{\max} pairs. On the other hand, the SDG -pair subspace can reproduce fairly well the yrast band, but is not sufficient for the higher bands. Thus for low-lying states in this special case, the J_{\max} pair approximation provides us with a more economic basis. Unfortunately, the J_{\max} -pair approximation loses its virtue of simplicity when the number of particles increases. For

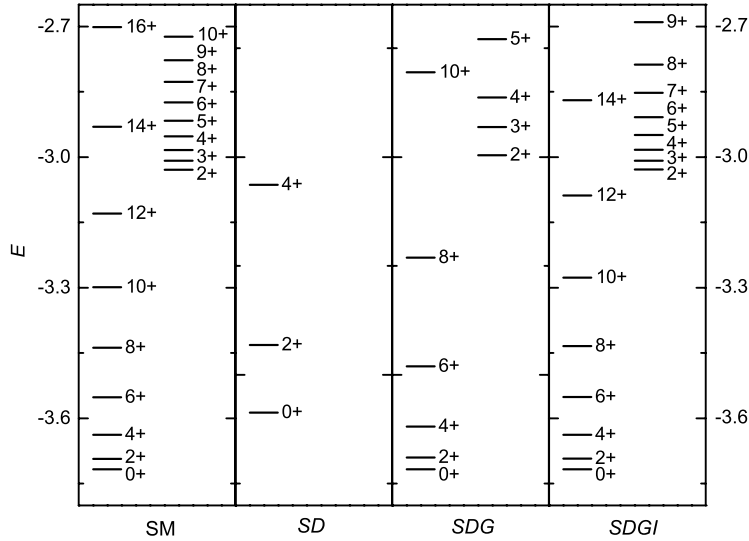


Fig. 2. Calculated energy levels of six nucleons in a single- j ($j = 19/2$) shell, with an attractive quadrupole-quadrupole interaction ($\kappa = 1/q^2(jj)$, $q(jj)$ is defined in Eq. (14)). The panel “SM” corresponds to the exact shell model calculation, “SD” the SD-pair calculation, “SDG” the SDG-pair calculation, and “SDGI” the SDGI-pair calculation. One sees that the inclusion of G and I pairs improves the agreement between the SM results and the SD-pair results substantially.

Table 1

Overlaps between wave functions calculated in the SD-, SDG- or SDGI-pair truncated subspaces and those in the full shell model space, for a system of six nucleons in a $j = 19/2$, under an attractive quadrupole-quadrupole interaction, corresponding to Fig. 2.

	SD	SDG	SDGI
0_1^+	0.965	1.000	1.000
2_1^+	0.917	0.999	1.000
4_1^+	0.793	0.995	1.000
6_1^+	0.538	0.973	1.000
8_1^+		0.907	0.999
10_1^+		0.760	0.991
2_2^+	0.592	0.988	1.000
3_1^+	0.446	0.967	1.000
4_2^+	0.302	0.936	1.000
5_1^+		0.870	0.999
6_2^+		0.814	0.996
7_1^+		0.670	0.986
8_2^+		0.586	0.969
9_1^+		0.378	0.926

three pairs in a $j = 21/2$ shell, the $J = 20$ pair approximation is not as good as it is for a two-pair system. The overlap between the ground state wave function calculated by using the $J = 20$ pair approximation and that calculated by the exact shell model calculations is only around 0.60.

In Fig. 2 we show an example with six nucleons in a single- j ($j = 19/2$) shell, with an attractive quadrupole-quadrupole interaction. One sees that the SD-pair subspace presents a rotational spectrum of the ground band, with a much larger moment of inertia. Inclusion of G pairs substantially improves the results, as pointed out by Halse [129]. In order to have a good agreement with the SM results for the lowest spin-ten state, inclusion of I pairs is necessary. A comparison of wave functions calculated in the SD-, SDG- and SDGI-pair subspaces with respect to the shell model wave functions is given in Table 1. One sees that the SD pairs provide a reasonable result for the 0_1^+ and 2_1^+ states but not for higher excited states, the SDG pairs present a reasonable truncation scheme for most of the low-lying states, and that SDGI pair subspace presents an excellent description of the full shell model results.

3.1.2. Monopole plus quadrupole interaction

In Ref. [130] Yoshinaga considered arbitrary combinations of the monopole pairing and quadrupole-quadrupole interactions. He used the seniority scheme to evaluate some of the matrix elements in the pair basis, and his results indicated

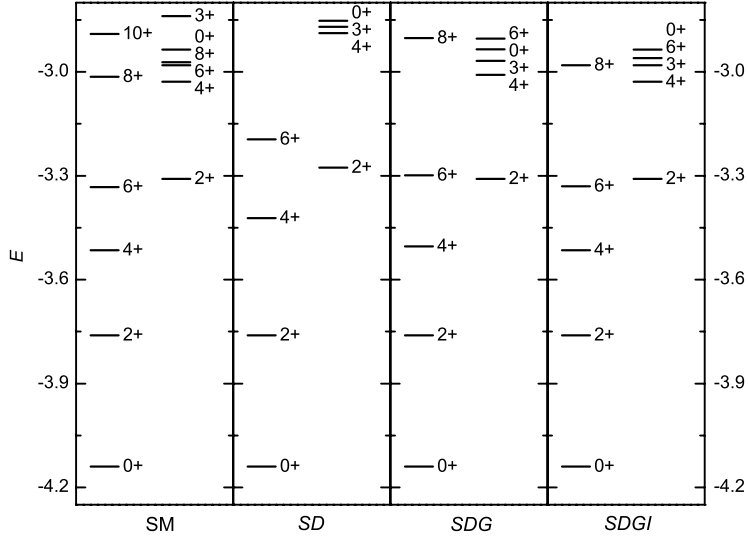


Fig. 3. Calculated energy levels of six nucleons in a single- j ($j = 19/2$) shell, with an attractive monopole and quadrupole pairing plus a quadrupole-quadrupole interaction. Here $G_0 = 0.15$ MeV, $G_2 = \kappa = 0.008$ (MeV/ r_0^4), and $n = 0$, $l = 10$. The notations “SM”, “SD”, “SDG”, and “SDGI”, are the same as in Fig. 2. One sees that for the cases with considerably strong pairing interaction all these truncations reproduce the SM results very well.

Table 2

Overlaps between wave functions calculated in pair-truncated subspaces and those in the full SM space, for a system of six nucleons in a $j = 19/2$ shell, under an attractive monopole and quadrupole pairing plus a quadrupole-quadrupole interaction with “typical” strength parameters, corresponding to Fig. 3.

	SD	SDG	SDGI
0_1^+	1.000	1.000	1.000
2_1^+	1.000	1.000	1.000
4_1^+	0.937	0.996	1.000
6_1^+	0.891	0.982	0.999
8_1^+		0.801	0.958
0_2^+	0.978	1.000	1.000
2_2^+	0.988	1.000	1.000
3_2^+	0.934	0.996	1.000
4_2^+	0.916	0.992	1.000
6_2^+		0.852	0.995

that the “renormalized” SD-pair subspace essentially incorporates the contribution of G pair. For both the vibrational and rotational motions, SDG-pair subspace reasonably reproduces the energy levels of shell model results.

In Ref. [134] a set of two-body interaction parameters are taken to simulate a typical vibrational nucleus, for a $j = 11/2$ shell with both valence proton and neutron numbers changing from zero to six. “Reasonable” strengths of two-body interaction parameters were assumed. In all these cases, the total binding energies are almost perfectly reproduced in the small SD-pair configurations. The low-lying energy levels (in particular the ground state and the first excited state) as well as E2 transition rates between these low-lying states are reasonably described by the SD pairs. We should note that the good agreement in Ref. [134] is partly because moderate pairing strength is assumed and j is not large. In case of deformed nuclei where quadrupole-quadrupole interaction is very strong and j value is large, the results are not so good [129].

In Fig. 3 we show six nucleons in a single- j ($j = 19/2$) shell with an attractive monopole and quadrupole pairing plus a quadrupole-quadrupole interaction. $G_0 = 0.15$ MeV, $G_2 = \kappa = 0.008$ (MeV/ r_0^4), and $n = 0$, $l = 10$. One sees that SD pairs reproduce the lowest 0^+ , 2^+ , 4^+ and 6^+ states quite well. In order to reasonably describe the states with higher spins, one should consider other pairs such as G and I pairs, which improve the agreement between the SM results and those in the pair-truncated subspaces. In Table 2 the overlaps between wave functions in pair-truncated subspaces and those in the shell model space are presented explicitly, demonstrating the validity of these pair approximations in low-lying states.

3.1.3. Schematic cases: J -pairing interaction

There are a few very interesting results of the pair approximation with J -pairing interaction, i.e., $H = H_J = -G_J \sum_M A_M^{(J)} A_M^{(J)}$. Because G_J is the unique interaction strength parameter and serves as the energy scale of the energy levels, we take $G_J = 1$ (in an arbitrary unit) for simplicity. For $n = 3$, it was shown [135] that there is only one non-zero eigenvalue

for each spin I of the three nucleons. The wave function of this state is constructed by J -pair basis, i.e., $|jj, I\rangle/\sqrt{K_{jj}}$ (here J means a pair with spin J and the factor in the denominator is the normalization factor), and its eigenvalue equals

$$-K_{jj} = -1 - 2(2J + 1) \begin{Bmatrix} j & j & I \\ J & j & j \end{Bmatrix}.$$

Therefore in this case the states constructed by using one spin- J pair coupled with an unpaired nucleon provide us with the exact solution.

For $n = 4$, the J -pairing truncation is usually not an exact solution, yet it survives as a reasonable approximation to the full shell model space. See the numerical results and discussions of Ref. [136]. In Ref. [137] it was shown that for $n = 4$ nucleon pairs with spin J and isospin T provide us with a good approximation for the JT -pairing Hamiltonian for the lowest isoscalar states.

Another interesting result is for $H = H_{J\max}$, i.e., $G_J = -\delta_{J\max J}$. In this case there are many states which have eigenvalues asymptotically equal to -1 or -2 , ..., which corresponds to states with one J_{\max} pair, two or more J_{\max} pairs. The wave functions of such states are very well represented by various clustering pictures, for example, the J_{\max} pair is one of the possible “clusters” which are favored in the system.

To understand these “integer” eigenvalues let us consider the pair basis of four nucleons

$$|j^4(r_1 r_2)I, M\rangle = \frac{1}{\sqrt{N_{r_1 r_2; r_1 r_2}^{(I)}}} (A^{r_1 \dagger} \times A^{r_2 \dagger})_M^{(I)} |0\rangle, \quad (21)$$

where $N_{r_1 r_2; r_1 r_2}^{(I)}$ is the diagonal matrix element of the normalization matrix

$$\begin{aligned} N_{r'_1 r'_2; r_1 r_2}^{(I)} &= \langle 0 | (A^{r'_1} \times A^{r'_2})_M^{(I)} (A^{r_1 \dagger} \times A^{r_2 \dagger})_M^{(I)} | 0 \rangle \\ &= \delta_{r_1, r'_1} \delta_{r_2, r'_2} + (-)^I \delta_{r_1, r'_2} \delta_{r_2, r'_1} - 4 \hat{r}_1 \hat{r}_2 \hat{r}'_1 \hat{r}'_2 \begin{Bmatrix} j & j & r_1 \\ j & j & r_2 \\ r'_1 & r'_2 & I. \end{Bmatrix}, \end{aligned} \quad (22)$$

where \hat{r}_1 is the short hand notation for $\sqrt{2r_1 + 1}$. In general this basis is overcomplete and the normalization matrix may have zero eigenvalues for a given I . The matrix elements of H_j are

$$\langle j^4(r'_1 r'_2)I, M | H_j | j^4(r_1 r_2)I, M \rangle = -\frac{1}{\sqrt{N_{r_1 r_2; r_1 r_2}^{(I)} N_{r'_1 r'_2; r'_1 r'_2}^{(I)}}} \sum_{J'=\text{even}} N_{r_1 r_2; J J'}^{(I)} N_{r'_1 r'_2; J J'}^{(I)}. \quad (23)$$

There are two terms in $N_{r_1 r_2; J J'}^{(I)}$: the second term is a nine- j coefficient which is usually much less than unity in magnitude, in particular when J is large and I not large [136]. Neglecting this very small nine- j symbol, the allowed states are $|j^4(r_1 r_2)I, M\rangle \approx (A^{r_1 \dagger} \times A^{r_2 \dagger})_M^{(I)} |0\rangle$ for $r_2 < r_1$, and $|j^4(r_1 r_1)I, M\rangle \approx \frac{1}{\sqrt{2}} (A^{r_1 \dagger} \times A^{r_1 \dagger})_M^{(I)} |0\rangle$, I even only, and the Hamiltonian matrix becomes

$$\langle j^4(r'_1 r'_2)I, M | H_j | j^4(r_1 r_2)I, M \rangle \approx -\frac{(\delta_{r_1, r'_1} \delta_{r_2, r'_2} + (-)^I \delta_{r_1, r'_2} \delta_{r_2, r'_1})}{\sqrt{1 + (-1)^I \delta_{r_1, r_2}}} \frac{(\delta_{r_1, J} + \delta_{r_2, J})}{\sqrt{1 + (-1)^I \delta_{r'_1, r'_2}}}. \quad (24)$$

One sees that the matrix is diagonal which validates the pair approximation. The eigenvalues are either 0 , -1 , or -2 with their corresponding wave functions having 0 , 1 or 2 pairs with angular momentum J , respectively. Therefore, the integer eigenvalues of many I states originate from both the asymptotic properties of the above nine- j symbols and the validity of J -pair truncation. From the J -pair coupling scheme, the number of $|j^4(r_1 r_2)I, M\rangle$ with $r_1 = r_2 = 2j - 1$ is $\frac{1+(-)^I}{2}$, and the number of $|j^4(r_1 r_2)I, M\rangle$ with $r_1 = 2j - 1$, $r_2 < r_1$ and $I < 2j - 1$ is $\lfloor \frac{I}{2} \rfloor$ (the largest integer not exceeding $\frac{I}{2}$). Thus the number of states with eigenvalues $\simeq -2$ is $\frac{1+(-)^I}{2}$ and the number of states with eigenvalues $\simeq -1$ is $\lfloor \frac{I}{2} \rfloor$. All these are readily confirmed by numerical experiments. We note that such “integer” eigenvalues appear not only in even- A systems but also in odd- A systems.

Eigenvalues not close to integers are also worth mentioning. For $n = 4$, the “non-integer” eigenvalues are found to be almost the same for the $2j - 8 \leq I \leq 4j - 12$ states. These non-zero eigenvalues are given, asymptotically but very accurately, by one of three-particle clusters with $I^{(3)} \sim I_{\max}^{(3)}$ coupled to a single- j particle. Such picture was confirmed by investigating the wave functions [135]. Similar results were found for $n = 5$ and 6 systems.

The low-lying states of identical particles (fermions or bosons) in a single- j shell interacting by an attractive $H = H_{J\max}$ thus favor a clustering structure, where each cluster has a maximum (or close to maximum) angular momentum. The coupling between the constituent clusters (including pairs and spectators) are very weak and negligible, therefore we can obtain both their approximate wave functions and eigenvalues, which are simple couplings of these clusters. As is well

known, the existence of degeneracy indicates that the Hamiltonian has a certain symmetry. The degeneracy for the J_{\max} pairing interaction, however, is not exact. It would be interesting to explore the broken symmetry hidden in the J_{\max} pairing interaction. It would be also interesting to discuss the modification of the J_{\max} pairing interaction in order to recover the exact degeneracy.

3.2. Validity of the NPA for many- j shells

In Ref. [138] Lei et al. studied the validity of the NPA by using the schematic Hamiltonian in Eq. (18) for ^{46}Ca (semi-magic nucleus); and in Ref. [139] the same authors compared the wave functions of low-lying states in truncated nucleon-pair subspaces and those of the full shell model spaces for $^{43–46}\text{Ca}$ (both even- and odd-mass nuclei), by investigating the energy spectra and overlaps between these two sets of wave functions, by using effective interactions. In Refs. [54,55] Caprio et al. used the GXPF1 and FPD6 interactions, in studies of the validity of the NPA for semi-magic nuclei in the pf shell. They compared the energy levels, occupation, and electromagnetic observables for low-lying states in the seniority scheme with the full shell model results, under the restriction of seniority number ≤ 3 .

In Ref. [140] Lei et al. studied the case for $^{130–131}\text{Te}$ and ^{132}I , i.e., a few systems with both valence protons and valence neutrons, by the schematic interaction in Eq. (18). Validity of the NPA with effective interactions for open shell nuclei has been studied for a few $N = Z$ nuclei ($A = 92, 94, 96$) [115], by using the JUN45 interaction. The isoscalar spin-aligned pairs are shown to be dominant configuration for some of the low-lying states (see Section 4).

In this subsection we exemplify the results of semi-magic nuclei $^{43,45}\text{Ca}$ presented in Ref. [139] in which effective interactions are used, and ^{130}Te (open-shell nucleus) presented in Ref. [140] in which a phenomenological shell model Hamiltonian is used.

3.2.1. Semi-magic nuclei $^{43,45}\text{Ca}$ with effective interactions

Here we exemplify the results of semi-magic nuclei $^{43,45}\text{Ca}$, i.e., three or five valence neutrons in the pf shell. The calculated results are based on Ref. [139], where the single particle (s. p.) energies are assumed to take the values -8.6240 , -5.6793 , -1.3829 and -4.1370 MeV for the $f_{7/2}$, $p_{3/2}$, $f_{5/2}$ and $p_{1/2}$ orbits, respectively. As the s. p. energies of the $j \neq 7/2$ orbits are much higher than that of the $j = 7/2$ orbit, it is likely that for low-lying states unpaired valence neutrons other than $f_{7/2}$ do not play an important role (they contribute to high excited states). For simplicity, we therefore do not take into account configurations in which the unpaired nucleon is not in the $f_{7/2}$ orbit. For two-body interaction parameters, we use the matrix elements of the GXPF1A interaction [141].

The structure coefficients of the collective pairs are obtained via the following procedure: we first diagonalize our Hamiltonian H in the space $(S_j^\dagger S_{j_2}^\dagger \cdots S_{j_n}^\dagger)^N |0\rangle$, with $S_j^\dagger = (a_j^\dagger \times a_j^\dagger)^0$ and j running over all s. p. levels. We then obtain the structure coefficients $y(jj0)$ by maximizing the overlap between the ground state from this diagonalization and a state $(S^\dagger)^N |0\rangle$. In order to obtain $y(j_1 j_2 r)$ for non- S pairs, e.g. D and G pairs, we diagonalize the same H in the $(S^\dagger)^{N-1} A_{j_1 j_2}^{r\dagger} |0\rangle$ space, with j_1, j_2 running over all s.p. levels.

The calculations are performed in the following spaces: the shell model space, denoted by “SM”; the space constructed by coupling the unpaired $f_{7/2}$ valence neutron to SD pairs, denoted by “ $SDf_{7/2}$ ”; the space constructed coupling by the unpaired $f_{7/2}$ valence neutron to SDG pairs, denoted by “ $SDGf_{7/2}$ ”, and so on. The number of states for the SM space and various NPA spaces are shown in Table 3.

The calculated energies of low-lying states are presented in Fig. 4. We see that the $SDf_{7/2}$ approximation is able to reproduce very well the lowest five SM states (below two MeV in excitation energy). However, this small subspace is not sufficient to describe higher spin states and non-yrast states for ^{43}Ca and ^{45}Ca . For example, the calculated $(\frac{7}{2})_2^-$ state of ^{43}Ca in the $SDf_{7/2}$ basis is much higher than that of the shell model calculation and the $(\frac{3}{2})_2^-$ state of ^{45}Ca is likewise not reproduced in the $SDf_{7/2}$ basis. Inclusion of one G or I pair substantially improves the agreement for higher spin states and non-yrast states of ^{43}Ca and ^{45}Ca . For ^{43}Ca nucleus, the G pair makes an important contribution to the $(\frac{3}{2})_2^+$ state, and the I pair makes an important contribution to the $(\frac{5}{2})_2^+$ state. Similarly, in ^{45}Ca the G pair makes an important contribution to the $(\frac{19}{2})_1^+$ state. In general, most of the low-lying energy levels of the shell-model space are well reproduced in the $SDGf_{7/2}$, $SDIf_{7/2}$ and $SDGI_{7/2}$ subspaces, with the $SDGI_{7/2}$ subspace the best among them.

The overlaps between the wave functions of a few low-lying states in the pair subspaces and those in the shell-model space are presented in Table 4. One sees that the overlaps for the five lowest states obtained in the pair-truncated subspaces all exceed 0.94. Inclusion of G and I pairs improves the description of higher states, except for the $(\frac{1}{2})_1^-$ state of ^{43}Ca . For ^{43}Ca , all yrast states are nicely reproduced in the $SDGI_{7/2}$ subspace, except for the $(\frac{1}{2})_1^-$ state. For ^{45}Ca , both the I_1^+ states and the I_2^+ states are reasonably well reproduced, as almost all of the calculated low-lying states in the $SDGI_{7/2}$ subspace overlap with those in the SM space at the level of ≥ 0.92 . The only exception is the $(\frac{7}{2})_2^+$ state in the $SDGI_{7/2}$ subspace, for which the wave function overlap is 0.88.

The calculated $B(E2, I_1^+ \rightarrow (I-2)_1^+)$ values (between yrast states) and $B(E2, I_2^+ \rightarrow (I-2)_1^+)$ values (i.e., E2 transitions from the second lowest I states to the first I states) versus I are shown in Fig. 5. According to Fig. 5(a), the $B(E2)$ values between the $(\frac{17}{2})_1^-$ and $(\frac{13}{2})_1^-$ states and between the $(\frac{7}{2})_1^-$ and $(\frac{3}{2})_1^-$ states calculated in the pair subspaces for the ^{43}Ca nucleus deviate from those of the SM calculation, even though the overlaps between pair-truncated wave functions

Table 3

Dimensions of given spin states in different model spaces for ^{43}Ca and ^{45}Ca . Notations "SM", " $SDf_{7/2}$ ", " $SDGf_{7/2}$ ", " $SDIf_{7/2}$ " and " $SDGI_{f7/2}$ " are the same as in Fig. 4.

	SM	$SDf_{7/2}$	$SDGf_{7/2}$	$SDIf_{7/2}$	$SDGI_{f7/2}$
^{43}Ca					
$1/2^-$	12		1		1
$3/2^-$	25	1	2	1	2
$5/2^-$	28	1	2	2	3
$7/2^-$	27	2	3	3	4
$9/2^-$	23	1	2	2	3
$11/2^-$	16	1	2	2	3
$13/2^-$	8		1	1	2
$15/2^-$	5		1	1	2
$17/2^-$	1			1	1
^{45}Ca					
$1/2^-$	107	1	5	3	9
$3/2^-$	198	3	10	7	18
$5/2^-$	253	3	12	10	24
$7/2^-$	271	5	15	13	29
$9/2^-$	252	3	13	12	29
$11/2^-$	211	3	13	12	29
$13/2^-$	153	1	9	10	25
$15/2^-$	105	1	8	9	20
$17/2^-$	58		4	6	15
$19/2^-$	29		3	4	11
$21/2^-$	11		1	2	6

and the SM wave functions are very close to one. This means that the $B(E2)$ values are extremely sensitive to details of wave functions, a very small (5%) difference may lead to a difference in magnitude of E2 transitions by a factor two or three.

In Fig. 5(b), we note large deviations for the $B(E2)$ values involving $(\frac{5}{2})_2^- \rightarrow (\frac{1}{2})_1^-$ and $(\frac{11}{2})_2^- \rightarrow (\frac{7}{2})_1^-$ transitions. These large deviation can be understood in terms of the relatively small overlaps for the $(\frac{1}{2})_1^-$ state and the $(\frac{11}{2})_2^-$ state in the pair subspaces. In Fig. 5(a') and (b'), we see that most E2 transition rates calculated in the SM space are well described in the pair subspaces, and especially in the $SDGI_{f7/2}$ subspace. This is consistent with the large wave function overlaps for the " $SDGI_{f7/2}$ " configurations seen in Table 4.

Assuming the same set of interactions, comparisons between the calculated results by using the SM and those by using the NPA for $^{44,46}\text{Ca}$ have been also made in Ref. [139], to which one refers for details. Through these examples, one sees that although the dimensions in the nucleon-pair approximation are much smaller than those of the shell model, the nucleon-pair approximation nevertheless provides a reasonable approximation to the shell model for low-lying states. G and I pairs were found to be important in higher spin and non-yrast states of the low-energy region. As the number of pairs increases, one obtains better agreement with the SM results in a truncated pair basis.

3.2.2. Validity of the NPA for open shells

Microscopic foundation of the IBM has sparked off many studies of the SD -pair and SDG pair approximations for open-shell nuclei [35]. For example, Halse studied [142] SD -pair approximation for $^{56,58}\text{Fe}$ by assuming the $1f_{7/2}$ shell for valence protons and $2p_{3/2}, 1f_{5/2}2p_{1/2}$ shell for valence neutrons. He showed that the SD subspace gives a reasonable description of some low-energy eigenstates with low spin. In Ref. [134] a quadrupole-quadrupole interaction was assumed for six valence neutrons and six protons in the sd , pf and sdg shells, where it was shown that the rotational features remain in the ground band while the moment of inertia becomes smaller and smaller as the shell model space expands (i.e., from sd to sdg shells).

Here we exemplify the validity of the NPA for nuclei in open shells, by using the ^{130}Te nucleus [140]. The SM configuration space is constructed by using valence protons outside the proton number $Z = 50$ closed shell, and valence neutron holes with respect to the neutron number $N = 82$ closed shell. The single-particle energies and interaction parameters are taken to be the same as Ref. [143].

It is useful to investigate the energy levels of ^{134}Te and ^{130}Sn , with only two valence protons or two valence neutron holes with respect to the doubly-closed shell nucleus, ^{132}Sn . Their low-lying states are instructive to predict which pairs are favored in low-lying states of their neighboring nuclei. One sees that two valence protons with $\text{spin}^{\text{parity}} = 0^+, 2^+, 6^+, 4^+$, and two valence neutron holes with $\text{spin}^{\text{parity}} = 0^+, 2^+, (4^-, 5^-), 6^-, 7^-$ achieve low energies. It is noted that the contribution of the 4^-_v and 5^-_v pairs can be essentially represented by the 6^-_v and 7^-_v pairs in low-lying states of the ^{130}Te nucleus, and are therefore not included. Besides collective proton pairs with $\text{spin}^{\text{parity}} = 0^+, 2^+, 4^+, 6^+$, and collective pairs of neutron holes with $\text{spin}^{\text{parity}} = 0^+, 2^+, 6^-, 7^-$, one should also consider a few non-collective favored pairs constructed by the proton $g_{7/2}$ and neutron $h_{11/2}$ orbits, because they are the lowest in energy: $[g_{7/2}g_{7/2}]_{\pi}^{(2,4,6)}$, and $[h_{11/2}h_{11/2}]_{v}^{(2,4,6,8,10)}$.

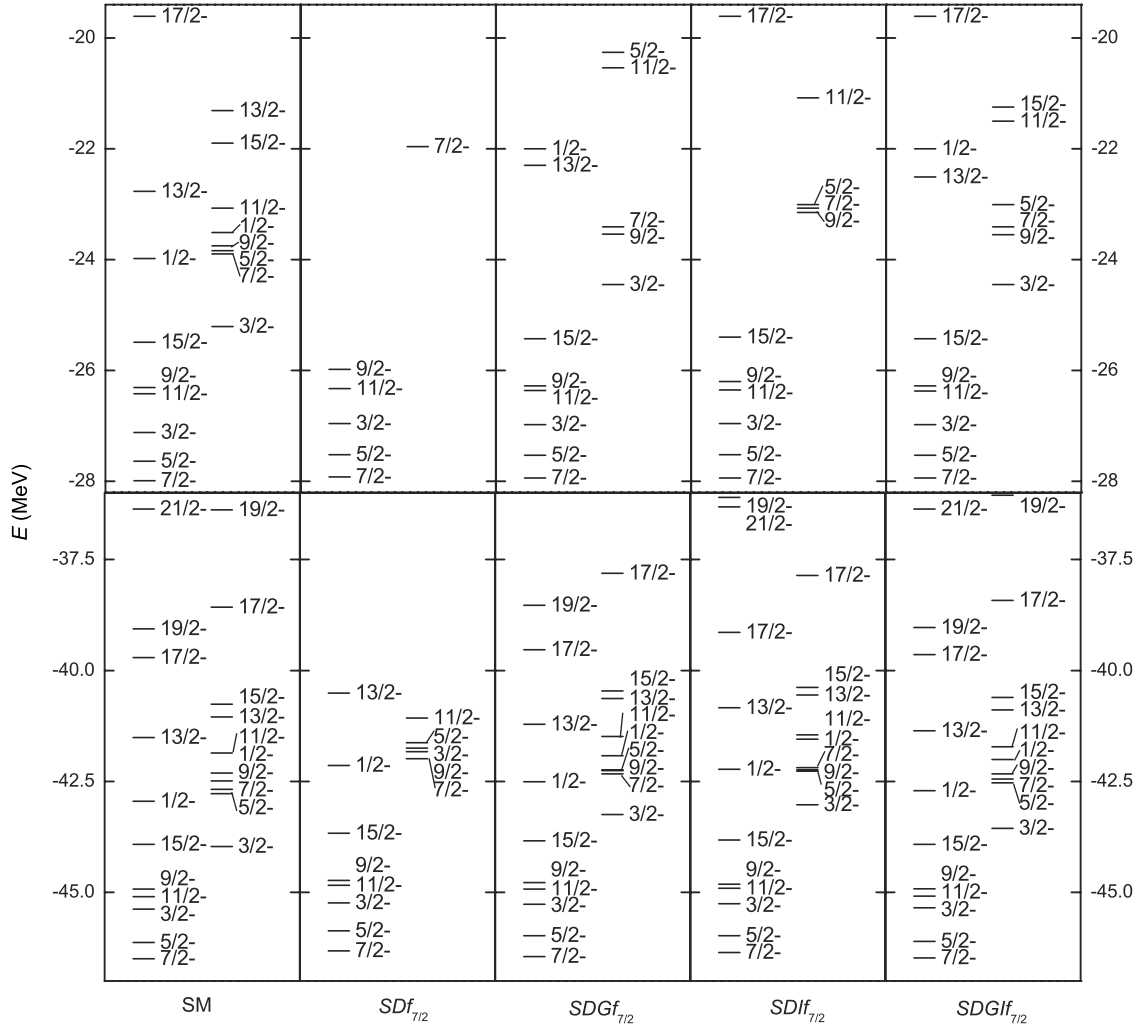


Fig. 4. The low-lying spectra of ^{43}Ca and ^{45}Ca calculated by using both the SM and the NPA. The interaction employed here is the effective GXPF1A interaction. The upper panels correspond to ^{43}Ca and the lower ^{45}Ca . The panel “SM” corresponds to the exact SM calculation, “ $\text{SD}f_{7/2}$ ” the SD pairs coupled to an unpaired neutron in the $f_{7/2}$ orbit, “ $\text{SDG}f_{7/2}$ ” the SDG pairs coupled to an unpaired neutron in the $f_{7/2}$ orbit, and so on.

These pairs are important for some of the low-lying states, for which the overlaps between the NPA wave functions and the SM wave functions would be below 0.9 without them.

For the ^{130}Te nucleus, the dimensions of the SM configurations are $\sim 10^4$. The dimensions of the SD -pair truncation for this even-even nucleus are less than 10. The dimensions of the above favored-pair subspaces are $\sim 10^2$, which are only about 1% of the full SM spaces. See Table 5 for details. Now let us see whether or not these small subspaces with much smaller dimensions are able to well reproduce the results of the full SM space.

Fig. 6 shows energy levels of ^{130}Te . The calculated ground state energy of ^{130}Te with respect to ^{132}Sn is -5.325 , -5.135 and -5.192 (MeV) in the SM space, the SD subspace, and the favored-pair subspace for ^{130}Te , respectively. From Fig. 6 one sees that the SD subspace reproduces the ground state 0^+ and the first 2^+ state reasonably well, and the favored-pair subspace nicely reproduces all low-lying states (except the 1_1^+ state) including the so-called yrare band states.

The above comments are also readily confirmed by comparing the wave functions in different spaces. Table 6 presents overlaps between the SM wave functions and the NPA wave functions. One sees that the overlaps between wave functions calculated in the shell model calculations and those in the favored-pair approximations are, in most cases, larger than 0.9.

3.3. Summary of this section

In this section we have discussed the validity of the NPA for both schematic single- j shells and more realistic many- j shells, for both semi-magic and open shell nuclei. Although the NPA configuration space is much smaller than the exact SM configuration space, yet good agreements are obtained between them for low-lying states.

Table 4

Overlaps between wave functions calculated in the NPA subspaces and those the full SM space, for low-lying (both yrast and non-yrast) states of ^{43}Ca and ^{45}Ca , with excitation energies from the lower to the higher.

	$SDf_{7/2}$	$SDGf_{7/2}$	$SDIf_{7/2}$	$SDGIf_{7/2}$
^{43}Ca				
$7/2_1^-$	0.994	0.996	0.996	0.996
$5/2_1^-$	0.989	0.990	0.989	0.990
$3/2_1^-$	0.972	0.976	0.972	0.976
$11/2_1^-$	0.993	0.996	0.993	0.995
$9/2_1^-$	0.944	0.998	0.990	0.998
$15/2_1^-$		0.996	0.993	0.996
$1/2_1^+$		0.784		0.784
$13/2_1^-$		0.925	0.022	0.959
$17/2_1^-$			1	1
$3/2_2^-$		0.820		0.820
$5/2_2^-$		0.045	0.815	0.814
$7/2_2^-$	0.428	0.821	0.515	0.803
$9/2_2^-$		0.983	0.926	0.984
$11/2_2^-$		0.380	0.633	0.782
$13/2_2^-$				0.119
$15/2_2^-$				0.944
^{45}Ca				
$7/2_1^-$	0.990	0.997	0.991	0.999
$5/2_1^-$	0.975	0.986	0.990	0.999
$3/2_1^-$	0.984	0.985	0.985	0.997
$11/2_1^-$	0.977	0.987	0.987	1.000
$9/2_1^-$	0.983	0.986	0.992	0.999
$15/2_1^-$	0.979	0.996	0.995	1.000
$1/2_1^+$	0.714	0.935	0.814	0.975
$13/2_1^-$	0.058	0.937	0.711	0.977
$17/2_1^-$		0.982	0.898	0.995
$19/2_1^-$		0.931	0.528	0.998
$21/2_1^-$		0.955	0.996	1.000
$3/2_2^-$	0.566	0.847	0.670	0.925
$5/2_2^-$	0.743	0.846	0.890	0.970
$7/2_2^-$	0.434	0.842	0.697	0.884
$9/2_2^-$	0.896	0.966	0.976	0.988
$11/2_2^-$	0.643	0.957	0.873	0.981
$13/2_2^-$		0.909	0.668	0.972
$15/2_2^-$		0.570	0.098	0.987
$17/2_2^-$		0.891	0.337	0.985
$19/2_2^-$		0.870	0.540	0.970

Table 5

Dimensions of the shell-model space (denoted by “SM”), the SD-pair subspace (denoted by “SD”), and the subspace constructed by using SD coupled to a few “favored” pairs (denoted by “FP”) for ^{130}Te . Our favored pairs of ^{130}Te includes G_π (the lowest $J^\text{parity} = 4^+$ pair), the first $J^\text{parity} = 6_v^-, 7_v^-$ pair, and a few non-collective pairs: $[g_{7/2}g_{7/2}]_\pi^{(2,4,6)}$ and $[h_{11/2}h_{11/2}]_v^{(2,4,6,8,10)}$, in addition to SD pairs. See the text for details.

spin ^{parity}	SM	SD	FP	spin ^{parity}	SM	SD	FP	spin ^{parity}	SM	FP
0^+	8 316	4	64	1^+	23 471	2	99	1^-	20 739	129
2^+	37 219	7	213	3^+	47 159	3	225	3^-	43 955	284
4^+	54 190	4	307	5^+	57 032	1	289	5^-	56 931	392
6^+	57 309		336	7^+	54 503		295	7^-	56 842	428
8^+	50 319		313	9^+	44 439		260	9^-	46 199	392
10^+	38 242		257							

For a single- j shell we have discussed systems with a few special interactions: J -pairing interaction, J_{\max} -pairing interaction, quadrupole-quadrupole interaction, and pairing plus quadrupole interactions. For J -pairing interaction, J -pair truncation is reasonable. Attractive J_{\max} -pairing interaction favors dominantly the spin- J_{\max} pairs and a very few other clusters with total spin I close to the maximum in low-lying states. The SD-pair approximation is very good for systems with pairing plus quadrupole-quadrupole interactions (if pairing interaction strength is considerably large), but is not good for pure quadrupole-quadrupole interaction. The inclusion of additional G pairs in the pair subspace improves the NPA substantially.

For many- j shells, we have discussed its validity for a semi-magic nuclei $^{43,35}\text{Ca}$ in the pf shell, and an open-shell nucleus ^{130}Te , by using schematic interactions. The overlaps between the SM and NPA wave functions, as well as energy levels and E2

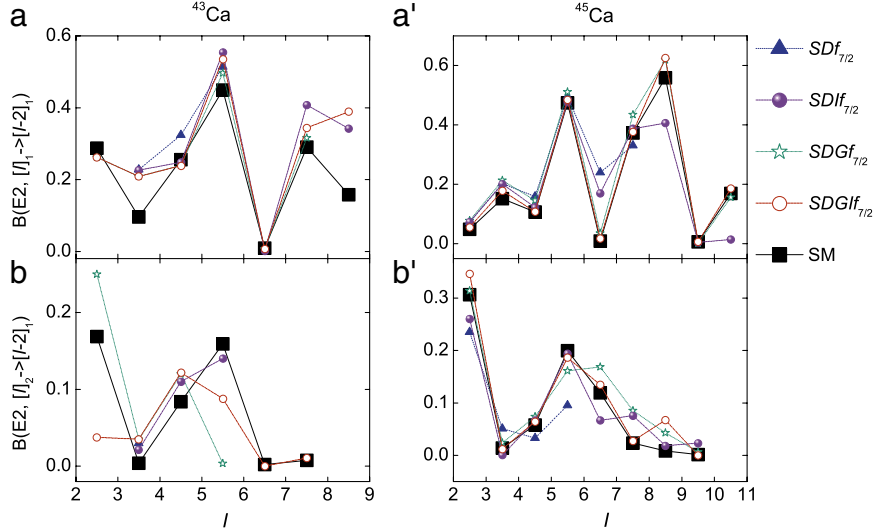


Fig. 5. (Color online) $B(E2)$ values (in unit of W. u.) for low-lying states of ^{43}Ca and ^{45}Ca . In panels (a) and (a') we plot $B(E2, I_1^+ \rightarrow (I-2)_1^+)$ (i.e., between yrast states) versus I , and in (b) and (b') we plot $B(E2, I_2^+ \rightarrow (I-2)_1^+)$ (i.e., E2 transition rates from the second lowest I states to the first I states) versus I . Notations “ $SDf_{7/2}$ ”, “ $SDGf_{7/2}$ ”, etc., are the same as in Fig. 4. The effective charge of valence neutrons is taken to be 0.5e.

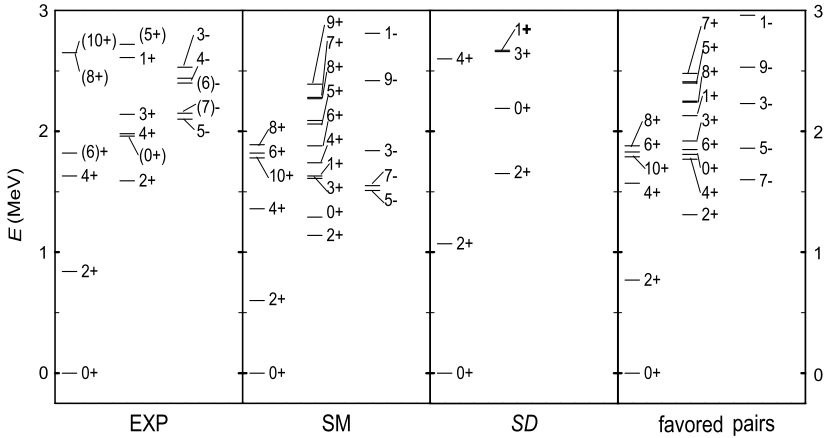


Fig. 6. The low-lying states of ^{130}Te . The panels from the left to the right are based on experimental data [144] (denoted by “EXP”), the shell-model calculations (denoted by “SM”), the SD -pair approximation (denoted by “ SD ”) and the calculations in the subspace constructed by SD and a few additional favored nucleon pairs (called “favored-pair subspace” in this paper and denoted by “favored pairs”, see the text for details). The calculated ground state energies in the SM space, the SD subspace and the favored-pair subspace are -5.325 , -5.135 and -5.192 (MeV), respectively.

Table 6

Overlaps between wave functions in the SM space and those in the SD -pair subspace or the favored-pair subspace for the ^{130}Te nucleus. Notations “ SD ” and “favored pairs” are the same as in Fig. 6.

spin ^{parity}	SD	Favored pairs	spin ^{parity}	SD	Favored pairs
0_1^+	0.961	0.980	2_2^+	0.209	0.585
2_1^+	0.813	0.945	3_1^+	0.021	0.842
4_1^+	0.533	0.903	1_1^+	0.038	0.116
6_1^+	0.046	0.956	4_2^+	0.212	0.845
8_1^+		0.961	6_2^+		0.956
10_1^+	0.965		5_1^+	0.080	0.925
			8_2^+		0.927
7_1^-		0.936	7_1^+		0.944
5_1^-		0.828	9_1^+		0.934
3_1^-		0.730	10_2^+		0.942
9_1^-		0.904			
1_1^-		0.555			

transition rates between low-lying states are presented. One sees that although the NPA subspaces are much smaller than the full SM space, essential physics is reasonably reproduced in the subspaces constructed by only a few “favored” pairs including S and D pairs. Similar comment also holds for their neighboring odd-mass and odd-odd nuclei, see Ref. [140] for details.

One might gain intuition on the “favored” pairs based on the single-particle energies (also see next section) or by diagonalizing the shell model Hamiltonian for two nucleons in the shell (as for ^{130}Te in this section). Another practical way is to select “favored” pairs by the numerical experiments. In Ref. [145] Zhang et al. studied the relevance of collective pairs with spin $J = 1, 3, 4, 6, 8, 10$, for both neutron and proton degree of freedom, for a number of physical quantities of low-lying states of the ^{130}Xe nucleus. If there is substantial difference between the calculated results by using SD pairs and those by using collective SD pairs and spin- J pairs, one conjectures that the collective nucleon pairs with spin J are relevant pairs of corresponding states. However, one must keep in mind that relevant “favored pairs” cannot be identified prior to diagonalization of the Hamiltonian. Misidentification of favored pairs leads possibly to unreliable results due to non-optimal valence spaces. Clearly, this would be the case for increasing valence space toward the midshell which is very likely to contain important favored pairs that are not coming low in energy near shell closures. How to identify favored pairs for nuclei in which the full model calculations are prohibitively difficult is an open problem.

Another important issue in the NPA is the determination of pair structure coefficients, $y(abr)$ in Eq. (1). There are various ways to determine $y(abr)$. Roughly speaking, the $y(abr)$ obtained by different methods are very close to each other for S pairs, and structure coefficients for S pair change smoothly and slowly with pair numbers. The simplest way to obtain structure coefficients of S pair is to solve the BCS equation. However, structure coefficients of non- S pairs obtained by different methods are usually quite different. Therefore, it is important to investigate the “optimal” D pairs and other non- S pairs. In Ref. [146] Lei et al. studied the pair number dependence of pair structure coefficients obtained via variation procedure. They found that D pair structure coefficients change considerably with pair numbers. In Refs. [147,148], Yang and Lu defined modified D pairs with the virtue of commutation with S pairs. They studied the pair structure of such pairs for the valence neutron shell $N = 50\text{--}82$. There is an algorithm to compute the pair structure coefficients by projecting pairs with spin zero, two, and four, from the deformed (Nilsson) pair in the HFB calculations.

The study of the NPA validity should be extended to rotational motion in realistic nuclei in future.

4. Application of the NPA

As is well known, when both valence protons and valence neutrons are present, the shell model configuration space for a heavy nucleus is mostly too gigantic to handle by exact diagonalizations. The dimension of the NPA subspace is usually very small (usually below a hundred for even-even nuclei, or ten thousand for odd-odd nuclei), and thus is a proper tool in studying the low-lying states of transitional nuclei, with medium and heavy masses, and both valence neutrons and protons less than eight. The NPA calculated results include binding energies, energy levels of low-lying states, $B(\text{E}2)$ and $B(\text{M}1)$ transition rates between these levels, electric quadrupole moments and magnetic dipole moments.

In this section we summarize the numerical calculations of the NPA. In studies of low-lying states for nuclei with the number of protons considerably smaller than that of neutrons, we do not need to consider the isospin symmetry, as valence protons and neutrons are dominantly not in same orbits. In the case of $N \sim Z$, isospin symmetry should be considered. In addition to the studies of realistic nuclei, we also discuss the applications of NPA to the studies of phase transitions of collective motions and regularities of low-lying states in nuclei with random interactions.

4.1. Brief survey

First we present a short survey of these calculations. See Table 7 for a list of these papers.

4.2. $A \sim 130\text{--}150$ region

Many calculations have been performed on low-lying states of Sb, Te, I, Xe, Cs, Ba, La, and Ce nuclei with mass around 130–150 [91,143,151–165], these studies were partly motivated by the fact that even-even Xe, Ba and Ce nuclei with $A \sim 130$ exhibit the pattern of the $O(6)$ symmetry [174] predicted in the IBM. It is therefore of interest to investigate whether or not one is able to describe such $O(6)$ symmetry by using a basis constructed from the shell model configurations.

4.2.1. FDSM description

In Ref. [152], Pan et al. used the $\text{SO}(8)$ -symmetry dictated nucleon pairs, and an $\text{SO}(8) \supset \text{SO}(6) \supset \text{SO}(3)$ Hamiltonian of the FDSM, to describe low-lying states of even-even and even-odd nuclei $^{126\text{--}132}\text{Xe}$ and $^{131\text{--}137}\text{Ba}$. They showed that low-lying energy levels of these nuclei can be reasonably described by a unified and analytical expression, with only two or three parameters of the FDSM Hamiltonian. The states of even-even and odd- A nuclei are given by the vector and spinor representations, respectively, of the same $\text{SO}(8)$ group. Analytical expressions are given for wave functions and for $B(\text{E}2)$ values which agree reasonably well with available experimental data. The suppression of energy levels of the $\text{SO}(5)$ quantum number was explained in terms of a perturbation of pairing interaction on the $\text{SO}(6)$ -symmetric Hamiltonian. Because

Table 7Numerical calculations using the NPA since 1995. v represents the seniority number.

References	Collective pairs	Nuclei
Caprio, Luo et al. [54]	$v \leq 3$	even and odd $^{21-39}\text{Ca}$.
Caprio, Luo et al. [55]	$v_\pi \leq 2, v_v \leq 2$	even-even $^{42-58}\text{Ca}$, even-even $^{44-60}\text{Ti}$, even-even $^{46-62}\text{Cr}$, ^{92}Mo , ^{94}Ru , ^{96}Pd .
Rowe, Rosensteel [56]	$v = 0, 2, 4$	odd-mass $^{57-69}\text{Ni}$.
Monnoye, Pittel et al. [65]	$v_\pi \leq 2, v_v \leq 3$	even-even $^{104-112}\text{Sn}$.
Sandulescu, Blomqvist et al. [69]	$S^N + S^{N-1}D$	even-even $^{102-130}\text{Sn}$.
Morales, Isacker et al. [70]	$S^N + S^{N-1}D$	^{92}Pd .
Qi, Blomqvist et al. [116]	$(g_9/2g_{9/2})^{(9)}, T = 0$	^{92}Pd , ^{94}Ag , ^{96}Cd .
Xu, Qi et al. [117]	$(g_9/2g_{9/2})^{(9)}, T = 0$	^{92}Pd , ^{94}Ag , ^{96}Cd .
Fu, Shen et al. [115]	$(g_9/2g_{9/2})^{(9)}, T = 0$ and SD, $T = 1$	$A = 59 - 62$ nuclei, with $T = 0$ and 1.
Kwasniewicz, Brzostowski et al. [121]	$SS'D'D''G$	even and odd mass $^{134-142}\text{Sn}$.
Kartamyshev, Engeland et al. [149]	$v \leq 2$	even-even $^{202-206}\text{Pb}$, $^{204-210}\text{Po}$, $^{212-206}\text{Rn}$, $^{214-208}\text{Ra}$,
Xu, Lei et al. [150]	$SD + G_\pi I_\pi K_\pi G_\nu$	odd-A $^{203-207}\text{Bi}$, $^{205-211}\text{At}$, $^{209-213}\text{Fr}$, odd-A $^{203,205}\text{Pb}$, $^{205-209}\text{Po}$, $^{207-211}\text{Rn}$, $^{211,213}\text{Ra}$.
Jia, Zhang et al. [143,151]	SD	both even and odd- A $^{124-139}\text{Sn}$, $^{126-142}\text{Te}$, $^{128-144}\text{Xe}$, both even and odd- A $^{130-146}\text{Ba}$, $^{132-148}\text{Ce}$, odd-mass $^{125-141}\text{Sb}$, $^{127-143}\text{I}$, $^{129-145}\text{Cs}$, $^{129-145}\text{La}$, $^{126-132}\text{Xe}$, $^{131-137}\text{Ba}$.
Jia, Zhang et al. [151]	SD	even-even $^{128-134}\text{Xe}$, $^{130-136}\text{Ba}$, $^{126-132}\text{Te}$, $^{132-138}\text{Ce}$.
Pan, Ping et al. [152]	SO(6)-SD	^{134}Ba .
Chen, Luo et al. [153,154]	SD	^{126}Xe , ^{128}Ba .
Luo, Zhang et al. [155]	SD	even-even $^{124-140}\text{Sn}$, $^{126-132}\text{Te}$, $^{128-144}\text{Xe}$, $^{130-136}\text{Ba}$, $^{132-138}\text{Ce}$.
Meng, Wang et al. [156]	SD	even-even $^{126-134}\text{Xe}$, $^{128-136}\text{Ba}$, $^{130-138}\text{Ce}$, $^{132-140}\text{Nd}$, odd-mass $^{129-133}\text{Xe}$, $^{131-135}\text{Ba}$, $^{133-137}\text{Ce}$.
Zhao, Yamaji et al. [157]	SD	^{132}Ba , $^{132,134,136}\text{Ce}$.
Yoshinaga, Higashiyama [158]	SD	even-even $^{126-134}\text{Xe}$, $^{128-136}\text{Ba}$, $^{130-138}\text{Ce}$, $^{132-140}\text{Nd}$, odd-mass $^{129-135}\text{Xe}$, $^{131-137}\text{Ba}$, $^{133-139}\text{Ce}$, $^{129-135}\text{Cs}$, odd-mass $^{131-137}\text{La}$, odd-odd $^{130,132}\text{Cs}$, $^{132,134}\text{La}$.
Higashiyama, Yoshinaga et al. [159]	$SD + (h_{\frac{1}{2}} h_{\frac{1}{2}})_v^{(j)}$	^{132}Ba .
Takahashi, Yoshinaga et al. [160]	$SD + (h_{\frac{1}{2}} h_{\frac{1}{2}})_v^{(10)}$	$^{130,132}\text{Cs}$, $^{132,134}\text{La}$.
Higashiyama, Yoshinaga [161]	SD	even-even $^{102-130}\text{Sn}$.
Lei, Xu et al. [162]	$SD + A_v^{(j-)}, J = 5, 6$	even-even $^{72-80}\text{Zn}$, odd- A $^{73-81}\text{Ga}$.
Lei, Fu et al. [163]	$SD + (h_{\frac{1}{2}} h_{\frac{1}{2}})_v^{(j)}$	even-even $^{94-100}\text{Mo}$.
Higashiyama, Yoshinaga et al. [164]	$+H^-I^-$	even-even $^{76-80}\text{Ge}$, ^{78}Se .
Jiang, Lei et al. [165]	$SD + (h_{\frac{1}{2}} h_{\frac{1}{2}})_v^{(j)}$	even-even $^{198-202}\text{Pt}$, $^{200-204}\text{Hg}$, odd-A $^{199-203}\text{Pt}$, $^{201-205}\text{Hg}$,
Jiang, Fu et al. [166]	SDG	odd-A $^{197-201}\text{Ir}$, $^{199-203}\text{Au}$, $^{201-205}\text{Tl}$, odd-odd $^{198-202}\text{Ir}$, $^{200-204}\text{Tl}$, $^{202-206}\text{Tl}$.
Zhang, Luo et al. [167]	SD	^{96}Cd .
Yoshinaga, Higashiyama et al. [168]	$SDG + (g_{9/2}g_{9/2})^{(j)}$	$^{130,132}\text{Cs}$, $^{132,134}\text{La}$.
Jiang, Shen et al. [169]	$SD + G_\nu$	$^{108,109}\text{Te}$, ^{109}I .
Zerguine, Isacker [170]	$(g_{9/2}g_{9/2})^{(9)}, T = 0$	even-even $^{102-130}\text{Sn}$, odd- A $^{101-109}\text{Sn}$ and $^{123-131}\text{Sn}$.
Higashiyama, Yoshinaga [171]	SD	
Jiang, Qi et al. [172]	SD	
Jiang, Lei et al. [173]	SD	

low-lying states for some of these nuclei are typically O(6)-symmetric, the FDSM with $\text{SO}(8) \supset \text{SO}(6) \supset \text{SO}(3)$ Hamiltonian is expected to give a reasonable description.

4.2.2. SD pairs with the surface-delta interaction

In Refs. [153–156] Luo et al. assumed a surface-delta interaction between like valence nucleons, and quadrupole-quadrupole interactions between valence protons and neutrons. They constructed the SD-pair subspace by taking the SD pairs from the first 0^+ and 2^+ wave functions of two valence nucleons interacting through the surface delta interaction. By using such SD-pair truncated configurations, they calculated energy levels and $B(\text{E}2)$ values of low-lying states in even-even $^{130-136}\text{Ba}$ nuclei, with calculated results well consistent with the experimental data. For ^{130}Ba , good agreements were achieved for nearly all energy levels up to 4 MeV. A shortcoming of these calculations is that the authors used a negative sign for interaction parameter $\kappa_{v\pi}$ (see Eq. (17)) which should be positive, because the quadrupole operator Q_v changes its sign under the particle-hole transformation. For a positive $\kappa_{v\pi}$ with the similar magnitude, the calculated results of the energy spectra do not change substantially; and one also obtains good agreement of E2 transition rates by using a negative effective charge for valence neutron holes.

4.2.3. Low-lying states with SD nucleon pairs

In Refs. [91,157] the Te, Xe, Ba, and Ce nuclei with $A \sim 130$ were studied by using the NPA. The S pair was taken to be the Bardeen–Cooper–Schrieffer (BCS) pair, and D pair was obtained by the commutator between the BCS pair and the quadrupole operator. Within the SD pair subspace such defined, the NPA calculations were carried out by using the monopole and quadrupole pairing plus quadrupole–quadrupole type interaction. In order to achieve a good agreement with experimental data, the two-body interaction parameters κ_σ and $G_{2\sigma}$ (see Eqs. (12)–(15)) were adjusted for each nucleus. In Ref. [157] $\kappa_\pi = \kappa_\nu$ and $G_{2\pi} = G_{2\nu}$ are assumed to reduce the number of adjustable parameters. The structure of energy levels for the quasi gamma band as well as the ground band was well reproduced. Other properties such as E2 transition rates and binding energies agree with experimental data very well. Predictions of the $B(E2, 0_1^+ \rightarrow 2_1^+)$ were made for neutron-rich, unstable nuclei $^{132,134}\text{Te}$. There were a number of predicted $B(E2, 0_1^+ \rightarrow 2_1^+)$ by using different theories such as the shell model and the Bohr–Mottelson phonon model. The experimental results of Ref. [175] are intermediate between the shell model and the collective model evaluations, and are very well predicted by the NPA calculations of Ref. [157], as noted in the data analysis of Ref. [175].

In Ref. [143], Jia et al. extended the NPA calculations of Sn, Te, Xe, Ba, and Ce nuclei from the $A \sim 130$ region (with neutron number N from 74 to 81) to the $A \sim 130$ –150 region (with neutron numbers from 74 to 90), and from even–even nuclei to their odd- A neighbors. In these calculations, the same types of SD nucleon pairs are assumed as in Refs. [91,157]. The parameters of monopole pairing interactions between like valence nucleons and of proton–neutron quadrupole–quadrupole interaction were fixed. The parameters of quadrupole pairing interaction and quadrupole–quadrupole interaction between like valence nucleons were fixed by single-closed shell nuclei, multiplied by a common factor given by fitting the 2_1^+ state energy. In Ref. [151] NPA calculations were generalized to the odd-mass isotopes, with the same set of interactions as those of their even–even neighboring nuclei. Many E2 transition rates, magnetic g factors, and quadrupole-moments, were reproduced or predicted in Refs. [143,151]. Some of predicted results were found to be in good agreement with experimental measurements performed in the subsequent years. For examples, measurement of g factors of excited states of the ^{132}Te nucleus in radioactive beams by the transient field technique [176], recent data analysis of g factors for $^{122,126,130,132}\text{Te}$ [177], and magnetic moments of 2_1^+ states in $^{124,126,128}\text{Sn}$ measured in Ref. [178], are well consistent with those in Ref. [143]; measurement of excited states in ^{129}I [179] yielded results of excitation energies, transition rates, electric quadrupole moments and g factors which are in very good agreement with those predicted in Ref. [151].

4.2.4. Backbending in yrast states of even–even nuclei

In Ref. [158] Yoshinaga et al. studied the Xe, Ba, Ce and Nd isotopes, with neutron number between 72 and 81. They considered the SD-pair subspace for even–even nuclei, and additionally unpaired neutron–hole for odd-mass isotopes. The SD pairs are optimized to have the lowest energy in the S pair condensation and one D-pair excitation. The form of the Hamiltonian and parameterizations are very similar to Refs. [143,151,157], with refinements of smooth changes with the number of valence protons and neutrons. In Refs. [159,160] one spin-aligned pair consisting of two neutron holes in the $h_{11/2}$ orbit (two $h_{11/2}$ neutron holes coupled to spin $r = 10$) was considered. The important role played by such spin-aligned two neutron holes in the $h_{11/2}$ orbit was conjectured from the backbending phenomenon in yrast states in the ^{132}Ba nucleus, i.e., a sudden decrease of yrast level spacing around the 10^+ isomer as well as the extremely small E2 decay rate from this isomer. Based on the magnetic moment of this isomer, the ^{132}Ba backbending was conjectured as a band crossing between the ground-state band and the Stockholm band originating from the $(\nu h_{11/2})^{-2}$ alignment [180,181]. In Ref. [161] some of the odd–odd Cs and La nuclei were discussed preliminarily. In analysis of the possible role played by the neutron pairs with spin ten in the $h_{11/2}$ orbit, Yoshinaga and collaborators re-adjusted their two-body interaction parameters (different from those for the SD-nucleon subspace) in order to obtain reasonable agreement with experimental data. The calculated results with consideration of the spin-aligned two neutron holes in the $h_{11/2}$ orbit are in good agreement with experimental data for $I = 8, 10$ states.

On the other hand, Lei et al. [162] used the same set of interaction parameters as optimized in the SD-pair subspace for the subspace of SD plus collective pairs (5^- and 6^-). The calculated results of Ref. [162] demonstrated that SD pairs, the lowest 5^- and 6^- nucleon pairs describe very well the yrast states (including the backbending) in ^{132}Ba and the transition rates between these states. Further investigation shows that the wave functions of those backbending states calculated in these two NPA calculations are very different. Thus one has a dilemma: Two different wave functions present nice agreement with experimental data. Evaluation of overlaps between the wave functions with and those without considering non-collective pair of two valence neutron holes in the $h_{11/2}$ orbit for the ground, 2_1^+ and 4_1^+ states, shows that these low-lying yrast states are largely affected by the non-collective pair with spin ten and the new set of interaction parameters given in Refs. [158,159]. This is different from the general conclusion that these states are essentially represented by SD nucleon pairs. Another disadvantage by using the new set of interaction parameters of Refs. [158,159] for the configuration of SD plus non-collective pair of two valence neutron holes in the $h_{11/2}$ orbit is that the seniority-zero state will be more or less degenerate to the 2^+ state, for six valence neutron holes in the 50–82 shell. This is brought about by the large quadrupole–quadrupole interaction for valence neutron holes adopted in Refs. [158,159]. In calculated results of Ref. [162], the wave functions of these states are not much affected by the inclusion of the lowest 5^- and 6^- nucleon pairs and no adjustments of interaction parameters are necessary.

The NPA calculations in Refs. [158,159] predicted a much larger value of $B(E2, 12_1^+ \rightarrow 10_1^+)$ than in Ref. [162]. Therefore experimental measurements of this E2 transition rates will be very interesting, and further studies of pair truncated shell model calculations are warranted, for example, one might consider the NPA calculations with the lowest 5⁻ and 6⁻ nucleon pairs, the non-collective pair of two valence neutron holes in the $h_{11/2}$ orbit, and some other possible nucleon pairs, in addition to the conventional SD nucleon pairs.

4.2.5. Negative parity levels of even-even nuclei

In Ref. [163] Lei et al. studied the low-lying negative-parity states of a few $N = 74$ isotones (^{128}Xe , ^{130}Ba and ^{132}Ce). The dominant configurations of the 8₁⁻ isomers are investigated in terms of correlated nucleon pairs. They included the octupole-octupole interaction in the separable form of the shell model Hamiltonian, in addition to the pairing plus quadrupole type interactions (i.e., the same form assumed in Refs. [143,151,157–160]). The collective negative-parity pairs for neutrons with spin $J = 3$ and 8 were coupled to the conventional SD-pair subspace. The calculated energy levels, E1, M1, E2, E3 transition rates and magnetic moments of low-lying states are reasonably consistent with experimental data. Lei et al. suggested that the 3₁⁻, 5₁⁻, and 7₁⁻ states of ^{130}Ba and ^{132}Ca are dominantly given by D pairs coupled to one negative-parity pair with spin $J = 3$, and thus these states correspond to an octupole vibration or quadrupole-octupole coupling. The wave functions of the NPA calculations are consistent with the previous conjecture [182] that these 8₁⁻ isomers are approximated by $\left(\frac{7}{2}^+[404]\otimes\frac{9}{2}^-[514]\right)^{8^-}$ two quasi-particle excitation. Similar 8⁻ isomers were predicted in the $N = 72$ even-even isotones in the NPA calculation.

4.2.6. Chiral bands in odd-odd nuclei

In Refs [164,171] Higashiyama et al. applied the SD-pair approximation to study the doublet band structure in odd-odd $^{130,132}\text{Cs}$ and $^{132,134}\text{La}$ isotopes. The occurrence of doublet band structure in these odd-odd nuclei was suggested by Frauendorf and Meng [183,184] as a manifestation of the chiral symmetry in low-lying states of atomic nuclei, by using the particle-rotor model and tilted axis cranking approach for the triaxially deformed nuclei. Higashiyama et al. adjusted the interaction parameters of Eq. (18) in order to fit experimental low-lying states of the even-even nuclei, $^{130,132}\text{Xe}$ and $^{132,134}\text{Ba}$, in the SD-pair subspace. They applied the same set of interactions to calculate low-lying states of their neighboring doubly odd nuclei, $^{130,132}\text{Cs}$ and $^{132,134}\text{La}$. They paid their attention to the configurations constructed by even-even core coupled to an unpaired $h_{11/2}$ proton and an unpaired $h_{11/2}$ neutron, and investigated whether or not one obtains the doublet band structure in such configurations. The results of Ref. [164] seem to indicate another picture instead of the chirality, i.e., a chopstick motion of the two unpaired particles (i.e., the last valence proton and the last neutron-hole) with different spins weakly coupled to the even-even core, for the doublet bands of $^{132,134}\text{La}$ nuclei. It seems that neither of these two different explanations [164,183] is able to refute the other. Here we would like to point out that the calculated results of Ref. [164] are sensitive to the “optimal-pair” subspaces. If one included a few other “favored” nucleon pairs, the calculated results by using the same set of parameters would be different from Ref. [164]. Therefore more studies are warranted for these doublet bands, from the NPA perspective.

4.2.7. $B(E2)$ and g factors of even-even Tin isotopes

In Ref. [165] the NPA was applied to study the shallow minimum of the $B(E2)$ values at the middle of the 50–82 shell for even-even Tin isotopes [71]. This minimal $B(E2)$ is interesting, because in the seniority scheme the $B(E2)$ value reaches the peak at the middle of the shell (i.e., $N = 66$). There have been discussions on this shallow minimum in a few models such as the generalized seniority scheme [70], large-scale shell model calculations [185], relativistic quasi-particle random phase approximation [186], and quasiparticle phonon model calculations [187]. In Ref. [165] Jiang et al. applied two sets of interaction parameters, one for cases with neutron number below 66, the other with neutron number equal to or above 66. Both the interactions and SD pairs are very similar to Refs. [143,151,157]. The NPA describes the experimental data of $B(E2)$ as well as the first 2⁺ state energies very well. According to Ref. [165], the minimum of $B(E2)$ values is very robust. The key reason for the presence of the minimal $B(E2)$ value in the midshell is the subshell effect at neutron number 64. In other words, the interesting behavior of $B(E2)$ values in even-even Sn isotopes was interpreted to be a reflection of the interplay between the generalized seniority and the subshell effect.

New measurements of $g(2_1^+)$ factor for even-even Tin isotopes have been performed in recent years [188–190]. Theoretical calculations have been also made in a few models such as the quasi-particle random phase approximation in Refs. [191,192] and the shell model in Refs. [188,193]. The NPA study of the 2₁⁺ states in even-even $^{102–130}\text{Sn}$ were performed in Ref. [173]. It was shown that for $A \sim 100$ the $g(2_1^+)$ values are practically determined by the shells $g_{7/2}$ and $d_{5/2}$, and for A larger than 108 but less than 116 the contribution from the shell $d_{3/2}$ becomes important. In the case of $A > 116$, the contribution from the shell $h_{11/2}$ is important, and the shell $d_{3/2}$ starts to be relevant as A is less than 122. In all cases one sees strong cancellations among the contributions of different shells, which makes the magnetic moment a powerful tool to probe the corresponding wave function. Analysis of the spin and orbital angular momentum contributions to the $g(2_1^+)$ value demonstrated that the overall trend of $g(2_1^+)$ with A is essentially determined by the spin contribution. The orbital part is practically constant for $A < 116$, and almost zero for $A > 116$.

4.3. Other regions

4.3.1. $A \sim 80\text{--}100$

The NPA was applied to Ga-Zn nuclei with $A \sim 80$. Low-lying states of even-even Zn and odd-mass Ga nuclei with neutron numbers between 42 and 50 were studied in Ref. [166] by using the SDG-pair approximation to the nuclear shell model and assuming the schematic interactions given in Eq. (18). For single-particle energies, constant values for $\epsilon_{p_{1/2}\pi}$ and $\epsilon_{g_{9/2}\pi}$ were assumed, while ϵ_{j_π} for $f_{5/2\pi}$ and $p_{3/2\pi}$ was adjusted. This assumption of adjustable ϵ_{j_π} was enlightened by Ref. [141], in which effective single-particle energy of the proton $f_{5/2}$ orbit comes down rapidly relative to the $p_{3/2}$ orbit as the neutron $g_{9/2}$ orbit is occupied for $N > 40$, and becomes lower than the $p_{3/2}$ for $N \geq 48$. Reasonable agreement of the calculated low-lying level schemes, electric quadrupole and magnetic dipole moments, E2 and M1 transition rates was achieved in comparison with experimental data. Dominant configurations in the ground states of odd-mass Ga nuclei were discussed in terms of pair correlations. The weak-coupling picture for some states of odd-mass Ga nuclei was studied. In Ref. [167], Zhang et al. studied the low-lying states of $^{94\text{--}100}\text{Mo}$ by using the NPA. They diagonalized the shell model Hamiltonian, which consists of the surface-delta interaction between like valence nucleons and quadrupole-quadrupole interactions between valence protons and neutrons, in the SD pair space. The energy level, E2 and M1 transition rates were calculated. The O(6)-symmetric behavior and mixed-symmetry states were discussed. In Ref. [168] Yoshinaga et al. performed both the SM and NPA calculations for even-even $^{76\text{--}80}\text{Ge}$ and $^{78\text{--}82}\text{Se}$. They analyzed the expectation numbers of SDG pairs and non-collective $(g_{9/2}g_{9/2})^{(J)}$ pairs in the yrast states versus spin I of the states. It was conjectured that the spin-aligned pair of $(g_{9/2}g_{9/2})^{(J)}$ is responsible for the sudden change of the first $I = 8$ states in ^{80}Ge and ^{82}Se .

In Ref. [172] low-lying structure of ^{109}Te and ^{109}I were studied in terms of SD nucleon pair subspace. Although measurement of electromagnetic transition strengths in this nuclear region is a challenging task due to the very small reaction cross sections, some experimental transition rates have been recently available. In the NPA calculation [172], some of the single-particle energies are taken from experimental excitation energies of the ^{101}Sn nucleus and the other unknown are taken from previous NSM calculations. The two-body interactions are assumed to be a separable pairing plus quadrupole interaction. The weak-coupling description of low-lying positive parity bands of these two nuclei in terms of an even-even ^{108}Te core and one unpaired proton or neutron is studied by calculating the overlaps of the NPA wave functions with the weak-coupling wave functions. The $7/2_1^+$ and $11/2_1^+$ states of ^{109}I and the $5/2_1^+$ and $9/2_2^+$ states of ^{109}Te are well described by such weak-coupling model. The calculated electromagnetic transitions to the ground states are very sensitive to the quadrupole-quadrupole proton-neutron interaction strength. In order to obtain an overall good agreement with experimental data, a relatively weak proton-neutron interaction is adopted, and experimental E2 and M1 transition rates are better represented by the NPA calculation than previous calculations.

4.3.2. $A \sim 200\text{--}210$

In Refs. [150,169] isotopes with proton number $Z \sim 77\text{--}88$ and $A \sim 200\text{--}210$ were studied by using the NPA, with the separable form of the shell model Hamiltonian given in Eq. (18). Nucleon-pair structure coefficients were fixed by diagonalizing the Hamiltonian H in the $|S^n\rangle$ and $|S^{n-1}X\rangle$ (X denote the spin of favored nucleon pair to be considered) subspaces, respectively, namely, by the same procedure as explained in Section 3.2.1 for semi-magic nuclei $^{43,45}\text{Ca}$. One G pair for valence neutrons and one G , I , and K pair for the valence protons are considered, in addition to the conventional SD-pair subspace. In Ref. [150] empirical formulas with very few parameters are assumed, and in Ref. [169] the two-body interaction parameters were adjusted in a small range to get the best fit to experimental data. With few exceptions, the calculated results including energy levels, magnetic dipole and quadrupole moments, E2 transition rates, were found to be consistent with the available experimental data.

The results of Ref. [150] are presented as an example of the NPA calculations in Section 4.5. Among many results of Ref. [169], we mention here the discussion of the anomalous behavior of the yrast energy for ^{200}Hg . The values of $E_{2_1^+}$, $E_{4_1^+}$ and $E_{8_1^+}$ are smaller than those for ^{198}Hg and ^{202}Hg . In Ref. [169] these minima were connected to very low D -pair and G -pair energies of neutron holes in the ^{200}Hg nucleus. As the number of valence protons and neutron holes is not large, many of the low-lying states were suggested to be dominated by very simple configurations of collective nucleon pairs. The calculated energy levels, transition rates and simple configurations of Ref. [169] have been found to be “very useful to guide the experimental studies” of β -delayed γ -ray spectroscopy of $^{203,204}\text{Au}$ and $^{200\text{--}202}\text{Pt}$ nuclei, presented in Ref. [194].

4.4. Isoscalar nucleon-pair approximations

In the above we concentrate on the NPA for the case in which the isovector $T = 1$ pairing interaction plays a dominant role and valence neutrons and protons are in different shells. The nucleon pairs in such case consist of either two valence protons or two valence neutrons. If valence neutrons and valence protons are in the same shell, the neutron-proton $T = 0$ pair correlation might be important in low-lying states [195]; in particular, when protons and neutrons are confined in a high- j orbit, $T = 0$ spin-aligned nucleon pairs (coupled to maximal spin $2j$) might play a dominant role in the configurations

for low-lying states [196–199]. The $T = 1$ and $T = 0$ pair correlation has been investigated in low-lying states of the ^{74}Ru nucleus [200]. Configurations of $T = 1$ and $T = 0$ pairs are studied analytically for some special cases [201].

Ref. [202] interpreted some of the low-lying states of the ^{92}Pd nucleus in terms of the $T = 0$ spin-aligned nucleon pairs. The ^{92}Pd nucleus has four proton holes and four neutron holes with respect to the doubly-closed shell nucleus ^{100}Sn , and the dominant orbit of these valence holes is mainly the $0g_{9/2}$ shell [203]. Dominant nucleon pairs in low-lying states of ^{92}Pd were suggested to be the $T = 0, J = 9$ neutron–proton pairs [202]. In Ref. [170] the shell model wave functions by using realistic interactions were analyzed by Zerguine and Isacker in terms of nucleon pairs with different J and T . For ^{96}Cd the nucleon-pair approximation was applied by using $T = 0, J = 9$ neutron–proton pairs, and for ^{94}Ag and ^{92}Pd calculations were carried out by a mapping to an appropriate version of the interacting boson model. According to Ref. [170] some of the low-lying states are indeed well represented by the $T = 0$ spin-aligned pairs. They further showed that the inclusion of S pairs with $T = 1$ improves the description. In Refs. [116,117] shell model calculations using realistic interactions were performed for four-, six-, and eight-hole $N = Z$ nuclei below ^{100}Sn , within the restricted $0g_{9/2}$ shell. Their analysis suggested that the low-lying yrast states of these $N = Z$ nuclei are mainly given by isoscalar neutron–proton pairs, each of which carries the maximum angular momentum of one proton–neutron pair in the $0g_{9/2}$ shell.

Very recently, the NPA with isospin symmetry was formulated [45]. Shell model calculations were performed in terms of nucleon pair with all possible spins and isospins [115], up to eight nucleons in the $p_{1/2}p_{3/2}f_{5/2}g_{9/2}$ shell, by using the JUN45 interactions [204]. The NPA analysis showed that isoscalar neutron–proton pairs with spin $J = 9$ are dominant configurations for some of the low-lying states [115]. This is consistent with the picture that $T = 0$ spin-aligned pairs play a dominant role in the low-lying states of these nuclei. Closer scrutiny of the calculated results show that the lowest $T = 0, J = 8$ state of ^{96}Cd is well represented by a S pair and a spin-eight pair with $T = 1$ (in the $0g_{9/2}$ orbit) other than two spin-aligned isoscalar pairs with spin $J = 9$. It is worthy to note that the configuration of two SD nucleon pairs with $T = 1$ also presents a good description of the lowest $J = 0$ and 2 states with $T = 0$ (see Fig. 1(e) of Ref. [115]) in ^{96}Cd . This dual description is a consequence of non-orthogonality feature of nucleon-pair basis. Similarly, further consideration of $T = 1$ pairs with spin zero, two, and eight are found to improve substantially the overlap between the wave functions by using the isoscalar neutron–proton pairs with spin $J = 9$ and those calculated by exact shell model calculations for ^{94}Ag .

4.5. Exemplification: a few nuclei around ^{208}Pb

In this subsection we exemplify numerical calculations of the NPA by using a few nuclei with proton number $Z \sim 82\text{--}88$ and neutron number $N \sim 120\text{--}126$, based on calculations by Xu et al. [150], where single-particle energies of nuclei with proton number $Z \sim 82\text{--}88$ and neutron number $N \sim 120\text{--}126$ were taken to be the energies of the lowest $p_{1/2}, p_{3/2}, f_{5/2}, f_{7/2}, h_{9/2}$ and $i_{13/2}$ states of ^{209}Bi for valence protons (ϵ_{j_π}), and those of ^{207}Pb for valence neutrons holes (ϵ_{j_ν}), respectively. The Hamiltonian parameters took the following form (see the appendix of Ref. [157]):

$$\begin{aligned} G_{0\sigma} &= -\alpha_\sigma \frac{27}{A}, & G_{2\sigma} &= \beta_\sigma \frac{G_\sigma^0}{r_0^4}, & \kappa_\sigma &= -\frac{1}{2}\chi\eta_\sigma^2, & \kappa_{\nu\pi} &= -\chi\eta_\nu\eta_\pi, \\ \eta_\nu &= -\gamma_\nu \left[\frac{2(A-Z)}{A} \right]^{\frac{2}{3}}, & \eta_\pi &= \gamma_\pi \left(\frac{2Z}{A} \right)^{\frac{2}{3}}, \\ \chi A^{\frac{5}{3}} &= - \left\{ 242 \left[1 + \left(\frac{2}{3A} \right)^{\frac{1}{3}} \right] - \frac{10.9}{A^{\frac{1}{3}}} \left[\left[1 + 2 \left(\frac{2}{3A} \right)^{\frac{1}{3}} \right] \left(19 - 0.36 \frac{Z^2}{A} \right) \right] \right\}. \end{aligned} \quad (25)$$

Here the parameters $\alpha_\sigma, \beta_\sigma, \gamma_\sigma$, and η_σ , are dimensionless. $G_{0\sigma}$ is in the unit of MeV, and $G_{2\sigma}$ and χ are in unit of MeV/r_0^4 . In Ref. [150] Xu et al. used a negative η_ν value, because the valence space of these nuclei is hole-like for neutrons. It was assumed that interactions between valence protons (and those between valence neutron holes) are constants with respect to the number of different valence neutrons (and protons), in order to reduce the number of adjustable parameters. Namely, the same values of α_π, β_π and γ_π were taken for an isotope chain, and likewise the same values of α_ν, β_ν and γ_ν for an isotope chain. The values of these parameters change smoothly in a small range. The values of $\alpha_\sigma, \beta_\sigma$ and γ_σ were optimized by using experimental data on single-closed even–even nuclei. The same parameters were taken for odd- A nuclei as for the corresponding even–even core. The parameters such obtained are given in Table 8, and pair structure coefficients were obtained by the same procedure as explained in Section 3.2.1 for semi-magic nuclei $^{43,45}\text{Ca}$.

For neutrons, the configuration space was expanded to $(SD)^{N_\nu} + (SD)^{N_\nu-1}G$. For protons, the configuration space becomes $(SD)^{N_\pi} + (SD)^{N_\pi-1}G + (SD)^{N_\pi-1}I + (SD)^{N_\pi-1}K$, where G, I and K represent collective pairs with spin $J = 4, 6$ and 8, respectively. For odd- A nuclei, the building blocks include an unpaired valence nucleon, as well as $SD + GIK$ pairs with the same pair structure coefficients as for their even–even “cores”.

In Fig. 7 the calculated binding energies (BE) are compared with experimental data. BE is defined as

$$\text{BE} = \text{BE}^{(208)\text{Pb}} - \langle H \rangle,$$

Table 8

Parameters α_π , β_π , γ_π , α_ν , β_ν , and γ_ν (see Eq. (25) for explanations of these quantities) for nuclei with both protons and neutrons in the 82–126 shell, and mass number $A \sim 202. The parameters in this table is dimensionless.$

Source: Taken from Ref. [150].

	α_π	β_π	γ_π		α_ν	β_ν	γ_ν
^{210}Po	1.1	3	0.6	^{206}Pb	0.9	2.7	0.6
^{212}Rn	1.1	2.5	0.8	^{204}Pb	0.85	2	0.6
^{214}Ra	1.1	2.5	0.8	^{202}Pb	0.9	2.7	0.7

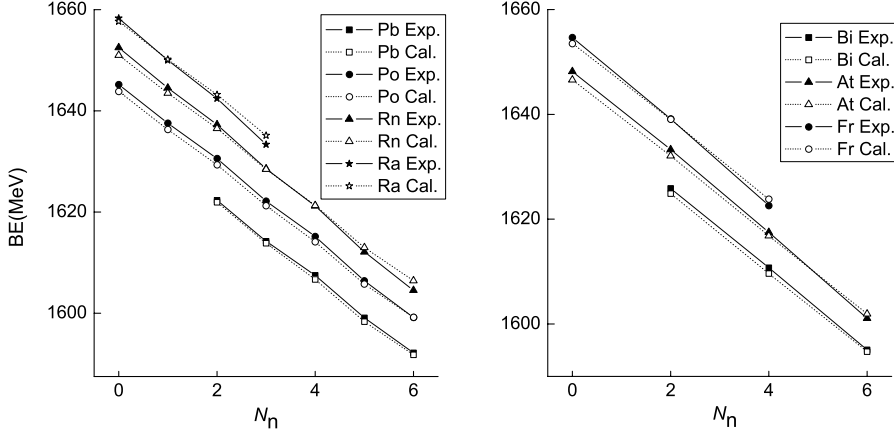


Fig. 7. Calculated binding energies and corresponding experimental data. N_n corresponds to the number of valence neutron holes. The left panel corresponds to both even–even and odd- A nuclei with even numbers of protons, and the right panel to odd- A nuclei with odd numbers of protons.

Source: Experimental data are taken from Ref. [205].

where $\text{BE}(^{208}\text{Pb})$ is the experimental binding energy of ^{208}Pb . $\text{BE}(^{208}\text{Pb}) = 1636\,446$ keV, according to Ref. [205]. Two additional parameters were used to fix the single-particle energies relative to the Fermi energies. These two parameters were adjusted via χ^2 -fitting to achieve the best agreement with experimental data and lead to $\epsilon_{9/2\pi} = -2918$ keV and $\epsilon_{1/2\nu} = 7648$ keV. The RMS deviation of predicted binding energies from experimental results is 0.98 MeV. Based on the direct use of experimental binding energies we would have obtained $\epsilon_{9/2\pi} = -3798$ keV and $\epsilon_{1/2\nu} = 7368$ keV [205], which are reasonably consistent with the parameters obtained above from the χ^2 fit.

For short we show here only the energy levels of $^{203,205}\text{Pb}$, $^{205,207,209}\text{Po}$, $^{207,209,211}\text{Rn}$ and $^{211,213}\text{Ra}$ in Fig. 8. Readers should go to Ref. [150] for other cases. One sees that the calculations nicely reproduce the experimental structure of the odd-mass levels and their relative energies. Most low-lying states of the odd- A nuclei in Fig. 8 have negative parity, with the lowest positive parity state having spin 13/2. The calculated results reproduce this behavior.

One of the interesting issues for these nuclei is the so-called multiplet states, which is nothing but a weak-coupling between the even–even core and unpaired nucleon for a number of states in odd- A nuclei. Ref. [206] suggested that the $(\frac{1}{2})^-$, $(\frac{3}{2})^-$, $(\frac{5}{2})^-$, $(\frac{7}{2})^-$ and $(\frac{9}{2})^-$ states around 600 keV in ^{209}Rn are given by the 2_1^+ state of the neighboring even–even core (^{210}Rn) coupled to a single valence neutron-hole in the $j = 5/2^-$ orbit. A similar phenomenon in ^{205}Pb and ^{207}Po was discussed in Refs. [218,219]. It is therefore interesting to investigate whether or not the calculated results in the NPA are consistent with such a picture. This can be done by looking at the overlap between the wave functions of these states and the configuration $|(\nu f_{5/2})^{-1} \times (2_1^+, \text{even–even core})\rangle$. The calculated results for these overlaps are listed in Table 9. From Table 9, one sees that most of the results are very close to 1 except for the $1/2_1^-$ state. Furthermore, the calculations suggest that a similar picture holds for ^{211}Ra : calculated $(\frac{1}{2})_1^-$, $(\frac{3}{2})_2^-$, $(\frac{5}{2})_2^-$, $(\frac{7}{2})_1^-$ and $(\frac{9}{2})_1^-$ states are generated by coupling a single valence neutron-hole in the $j = 5/2^-$ orbit to the 2_1^+ state of the neighboring even–even ^{212}Ra core.

Ref. [150] also calculated electromagnetic moments and $B(E2)$ values. The spin g -factors were taken to be $g_{s\pi} = 5.586 \times 0.7\mu_N$ and $g_{sv} = -3.826 \times 0.7\mu_N$ (0.7 is the usual quenching factor). The orbital g -factors, $g_{l\pi}$ and g_{lv} , were obtained by a χ^2 fit to the experimental magnetic moments for odd- A nuclei of this region, leading to values of $g_{l\pi} = 1.15\mu_N$, $g_{lv} = -0.03\mu_N$. Effective charges of valence neutrons and valence protons, e_v and e_π , were obtained by a χ^2 fit to experimental $B(E2)$ values, resulting in $e_\pi = 1.82e$ and $e_v = -0.88e$. In Table 10 we present the calculated results of magnetic moments (μ) and electric quadrupole moments (\mathcal{Q}) of odd- A nuclei (with even numbers of proton number Z), as typical examples. One sees an overall agreement of the calculated results for μ and \mathcal{Q} with the available experimental data. The $B(E2)$ values of other even–even and odd- A nuclei in this region can also be well represented by the NPA. For details, one refers to Tables V–IX of Ref. [150].

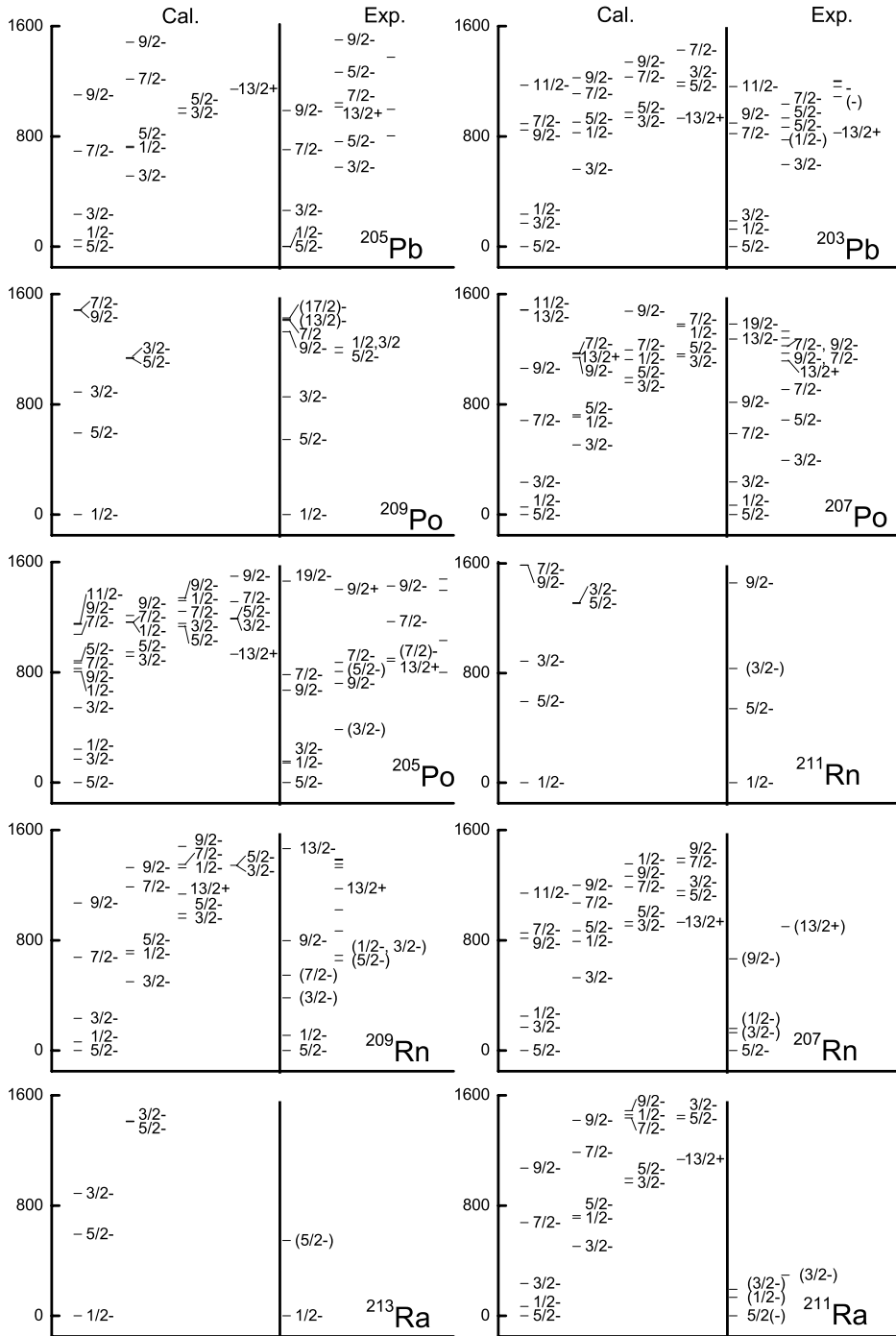


Fig. 8. Energy spectra (in unit of keV) of odd- A nuclei (neutron numbers N is odd). For each nucleus, the energy levels plotted on the left side are obtained by the NPA calculations, and those on the right side are based on experimental results. Experimental data of ^{209}Rn are taken from Ref. [206], and experimental data of ^{211}Ra are taken from Ref. [207]. Other experimental data are taken from Ref. [144]. The spin-parity J^π of the levels in parenthesis "()", more than one assignments, or no appointment, is not well determined experimentally.

4.6. Other applications

In addition to numerical calculations, there have been applications of the NPA to studies of the vibration–rotation phase transition, and regularities of nuclear structure under random interactions.

Table 9

Overlaps between wave functions of a few low-lying states around 500–1000 keV for a few odd- A nuclei and the simple configuration $|(\nu f_{5/2})^{-1} \times (2^+_1, \text{even-even core})\rangle$. The column “exp” are experimental energies of corresponding states (in unit of keV) while the column “cal” are calculated results. The column “overlap” are calculated overlaps between corresponding state and $|(\nu f_{5/2})^{-1} \times (2^+_1, \text{even-even core})\rangle$. The spin and parity corresponding to states with $E = 382.3, 652.6, 547.1$ (keV) of ^{209}Rn and $E = 134, 295$ (keV) of ^{211}Ra are not yet fully assigned experimentally. Experimental data of ^{209}Rn is taken from Ref. [206], other experimental data are taken from Ref. [144].

J^π	exp ^{205}Pb	cal	overlap	exp ^{207}Po	cal	overlap
$1/2^-$	2.33	47.4	0.728	68.57	54.9	0.718
$3/2^-$	576.19	512.2	0.970	392.99	505.2	0.966
$5/2^-$	751.43	728.2	0.935	685.79	723.8	0.927
$7/2^-$	703.43	693.1	0.991	588.31	682.5	0.988
$9/2^-$	987.63	1100.5	0.921	814.42	1060.7	0.873
	^{209}Rn			^{211}Ra		
$1/2^-$	110.3	63.09	0.730	134	68.58	0.736
$3/2^-$	382.3	499.31	0.962	295	503.03	0.962
$5/2^-$	652.6	724.47	0.926	–	726.99	0.929
$7/2^-$	547.1	676.1	0.985	–	676.22	0.985
$9/2^-$	797.8	1070.89	0.934	–	1071.76	0.930

Table 10

Magnetic moments μ (in unit of μ_N) and electric quadrupole moments \mathcal{Q} (in unit of eb) of the odd- A nuclei (neutron numbers N are odd). The columns “cal” are calculated results. The columns “exp” are experimental data which are taken from : ^a Ref. [208], ^b Ref. [209], ^c Ref. [210], ^d Ref. [211], ^e Ref. [212], ^f Ref. [213], ^g Ref. [214], ^h Ref. [215], ⁱ Ref. [216], ^s Ref. [217]. If the sign of an experimental value is not well determined, only the magnitude is listed.

μ moment		\mathcal{Q} moment		μ moment		\mathcal{Q} moment	
cal	exp	cal	exp	cal	exp	cal	exp
^{205}Pb		^{203}Pb		^{207}Po		^{209}Rn	
$3/2_1^-$	-1.039		+0.147	$3/2_1^-$	-1.208		+0.143
$5/2_1^-$	+0.771	+0.7117(4) ^a	+0.229	$5/2_1^-$	+0.803	+0.6864(5) ^d	+0.064
$7/2_1^-$	+0.656		+0.148	$7/2_1^-$	+0.015		-0.064
$13/2_1^-$	+0.546		+0.505	$13/2_1^-$	+0.668		+0.229
$17/2_1^-$	+2.314		+0.431	$17/2_1^-$	-0.131		+0.322
$13/2_1^+$	-1.518	-0.975(40) ^b	+0.384	$13/2_1^+$	-1.517		+0.398
^{209}Po		^{207}Po		^{209}Rn		^{211}Rn	
$1/2_1^-$	+0.426	0.68(8) ^s	–	$1/2_1^-$	+0.427		–
$3/2_1^-$	-1.286		+0.165	$3/2_1^-$	-1.035		+0.169
$5/2_1^-$	+0.882		+0.231	$5/2_1^-$	+0.776	+0.79(6) ^d	+0.268
$13/2_1^-$	+5.803	6.13(9) ^d	-0.148	$13/2_1^-$	+4.629		+0.320
$17/2_1^-$	+7.655	7.75(5) ^d	-0.706	$17/2_1^-$	+6.258		+0.002
$13/2_1^+$	-1.518		+0.369	$13/2_1^+$	-1.516	-0.910(14) ^d	+0.453
^{205}Po		^{211}Rn		^{207}Rn		^{213}Ra	
$3/2_1^-$	-1.202		+0.169	$1/2_1^-$	+0.426	+0.601(7) ^g	–
$5/2_1^-$	+0.805	+0.76(6) ^f	+0.076	$3/2_1^-$	-1.303		+0.179
$7/2_1^-$	+0.125		-0.069	$5/2_1^-$	+0.888		+0.255
$13/2_1^-$	+4.431		+0.297	$13/2_1^-$	+5.810		-0.079
$17/2_1^-$	+6.195		-0.102	$17/2_1^-$	+7.690	+7.75(8) ^d	-0.282
$13/2_1^+$	-1.516	-0.95(5) ^d	+0.471	$13/2_1^+$	-1.517		0.18(2) ^d
^{209}Rn		^{207}Rn		^{211}Ra		^{213}Ra	
$3/2_1^-$	-1.034		+0.186	$3/2_1^-$	-1.196		+0.191
$5/2_1^-$	+0.781	(+0.8388(4) ^d	+0.298	$5/2_1^-$	+0.806	+0.816(9) ^d	+0.085
$7/2_1^-$	+0.716		+0.128	$7/2_1^-$	+0.125		-0.082
$13/2_1^-$	+4.473		+0.352	$13/2_1^-$	+4.408		+0.173
$17/2_1^-$	+6.227		+0.214	$17/2_1^-$	+6.198		<0.001
$13/2_1^+$	-1.515		+0.510	$13/2_1^+$	-1.514	-0.903(3) ^d	+0.532
^{213}Ra		^{211}Ra		^{213}Ra		^{211}Rn	
$1/2_1^-$	+0.426	+0.613(2) ^h	–	$3/2_1^-$	-1.038		+0.195
$3/2_1^-$	-1.322		+0.183	$5/2_1^-$	+0.713	+0.8780(38) ^d	+0.311
$5/2_1^-$	+0.886		+0.264	$7/2_1^-$	+0.783		+0.201
$13/2_1^-$	+5.821		-0.020	$13/2_1^-$	+4.383		+0.261
$17/2_1^-$	+7.736	7.4(4) ^j	+0.131	$17/2_1^-$	+6.182		+0.301
$13/2_1^+$	-1.517		+0.427	$13/2_1^+$	-1.515		+0.533

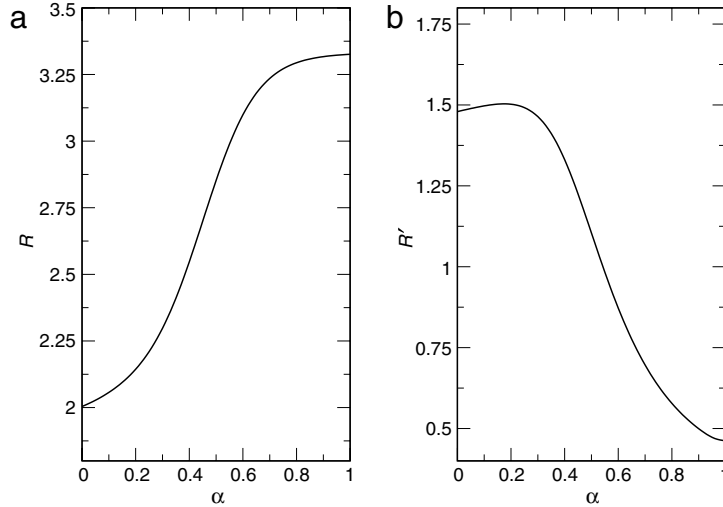


Fig. 9. Evolution of ratio between $E_{4_1^+}$ and $E_{2_1^+}$ (denoted by R) and ratio between $E_{6_1^+}$ and $E_{0_2^+}$ (denoted by R') in terms of an adjustable parameter α , introduced in $H = (1-\alpha)H_{U(5)} + \alpha H_{SU(3)}$. Here $H_{U(5)}$ ($H_{SU(3)}$) is a quasi- $U(5)$ ($SU(3)$) symmetric, monopole pairing plus quadrupole–quadrupole Hamiltonian in the SD -pair space.

Source: Taken from Ref. [224].

4.6.1. Shape phase transitions in the nucleon-pair approximations

The quantum phase transition in mesoscopic systems (here nuclei) has been first studied in the IBM, by Dieperink, Scholten, and Iachello, and independently by Feng, Gilmore and Deans [220]. In the IBM, the vertices of the Casten triangle (or the three limits with strict dynamical symmetries) represent three extreme modes of collective motion in low-lying states of atomic nuclei: vibrational, rotational and γ unstable. Adjusting parameters of the boson Hamiltonian, one obtains various motions with these competing modes, and in particular, transitions linking these modes. Iachello and Zamfir [220] studied the transitions between the $U(5)$ to $SU(3)$ limit, and those between the $U(5)$ and $O(6)$ limit, and showed that the main features of phase transitions, defined for infinite number of particles, persist even for moderate number of particles (say, ten).

Because the SD nucleon-pair approximation is very similar to the IBM in spirit, it is interesting to investigate whether or not these phase transitions arise in the nucleon-pair subspaces and how these transitions behave. In Refs. [221–223] Luo and collaborators obtained these phase transitions in a SD nucleon-pair subspace, with a schematic shell model Hamiltonian (monopole pairing interaction between like particles and quadrupole–quadrupole interactions between all valence nucleons). The S pairs are taken to be the BCS pairs and D pairs are given by the commutator $D^\dagger = [S^\dagger, Q^{(2)}]$, where $Q^{(2)}$ is the quadrupole operator defined in Section 2. They adjusted their parameters in order to approximately reproduce the results of the $U(5)$, $O(6)$, $SU(3)$, and $SU^*(3)$ symmetry limits, and the critical-point symmetry, the $X(5)$, in the SD -pair subspace. They showed, for example, that $G_{0\pi} = G_{0\nu} = -0.5$ MeV, $\kappa = -0.1$ (MeV/ r_0^4) gives typical vibrational spectra in low-lying states in the SD -pair subspace [222–224]. They studied transitions between these limiting cases, by investigating the evolution of a few typical excitation energies and $B(E2)$ values. Here we exemplify their results of the $U(5)$ – $SU(3)$ transition by Fig. 9 (taken from Ref. [224]). A Hamiltonian $H = (1-\alpha)H_{U(5)} + \alpha H_{SU(3)}$ is assumed, where $H_{U(5)}$ and $H_{SU(3)}$ are those which reproduce the similar energy spectrum and relative $E2$ transition rates for low-lying states as the corresponding limits in the IBM—these “limiting” Hamiltonians do not precisely give the dynamical symmetry states but give states which are close to them. α is an adjustable parameter, which varies between 0 and 1. In Fig. 9 one sees a sharp change of the energy ratios $R = E_{4_1^+}/E_{2_1^+}$ (also denoted by R_4 below) and $R' = E_{6_1^+}/E_{0_2^+}$ when $\alpha \sim 0.3$ – 0.6 , similar to the phase transition in the IBM. One disadvantage of these calculations is that the SD pairs taken in Refs. [222–224] are likely appropriate in vibrational regions, and that for deformed nuclei such pairs do not incorporate any effects of the neutron–proton interaction.

In Ref. [225] Lei et al. demonstrated that the nucleon-pair approximation to the shell model is indeed able to more meaningfully describe the shape transition from vibrational to rotational behavior versus the number of valence neutrons. The key step of Ref. [225] is that the Hartree–Fock–Bogoliubov (HFB) approximation is applied to variationally generate an optimum intrinsic pair, from which pairs of definite angular momentum can then be projected (see Ref. [95] for details). Lei et al. exemplified the phase transition by using even–even 144 – ^{148}Ce isotopes, and assuming a $Z = 50$, $N = 82$ doubly-magic core, with the pairing plus quadrupole–quadrupole interaction of Eq. (18). The single-particle energies are extracted from the spectra of ^{133}Sb and ^{133}Sn , and $G_{0\pi} = -0.18$ MeV, $G_{2\pi} = 0$, $G_{0\nu} = -0.13$ MeV, $G_{2\nu} = -0.012$ MeV/ r_0^4 , and $\kappa = -0.20$ MeV/ r_0^4 . These one-body and two-body interactions were fixed for all these Ce isotopes. It was also shown that pairs taken in Ref. [224] are not able to describe the shape transition versus valence neutron pairs, because those pairs leave out important effects of the neutron–proton interaction and thus are not suitable in a truncated description of collective

nuclei with valence neutrons and protons. In contrast, a description which uses collective pairs from the HFB approximation do contain the requisite correlation effects and are able to produce the observed shape transition. The shortcoming of this calculation is that the shape transition of the calculations in Ref. [225] is too sharp, and the moments of inertia are not very well reproduced.

4.6.2. Nucleon-pair approximation with random interactions

The *SD* nucleon-pair approximation has been also applied to investigate regularities of nuclear structure under random interactions. The work along this line was stimulated by an interesting discovery of the spin-zero ground state dominance in the presence of random interactions in 1997, by Johnson, Bertsch, and Dean [226]. This discovery has sparked off an intensive interest in its origin [227]. In Ref. [228], it was reported that the spin-zero ground states obtained by random interactions are reminiscent of the pairing features described by the generalized seniority scheme [4]. Strong correlations in low-lying states of many-body systems under random interactions were noted in both fermion and boson systems [229].

In Ref. [230], it was found that in a truncated *SD*-pair subspace collective vibrations arise naturally for a general two-body random Hamiltonian whereas collective rotations do not. The calculations are done in the following procedure. First, one selects only the sets of random interactions/parameters for which the Hamiltonian produces an $I^\pi = 0^+$ ground state and an $I^\pi = 2^+$ first excited state for two identical nucleons. These two states are assumed to represent collective *S* and *D* pairs, respectively. For each case, the same two-body interactions are used to calculate the low-lying states of six identical nucleons. This procedure is iterated until there are stable statistics. In the analysis one investigates R_4 values of these cases for which the ground states have spin zero. For a two-body random ensemble the distribution of R_4 obtained in the *SD*-pair subspace is very similar to the exact shell model results. It is found that a Hamiltonian restricted to include only a few randomly generated separable terms is able to produce collective rotational behavior, as long as it includes a reasonably strong quadrupole-quadrupole component. Similar results arise in the full shell model space. Therefore, the structure of the Hamiltonian seems to be the key to produce generic collective rotation under random interactions. This also suggests an explanation of the puzzle that the interacting boson model with fully random boson parameters is able to give rise to rotations, while the shell model truncated to *SD* pairs cannot. Namely, the interacting boson model should not be thought of as simply a pair truncation of the model space, but rather as a truncation of the model space that arises from the dominance of quadrupole correlations.

In Ref. [231], numerical calculations were performed by using *SD* pairs with two dynamical symmetries, *SP*(6) and *SO*(8) groups in the Fermion Dynamical Symmetry Model [43], and assuming random interaction parameters. It was shown that a Hamiltonian and the basis with the *SO*(8) symmetry does not give the vibrational and rotational peaks while the Hamiltonian of the pairing plus quadrupole-quadrupole interaction and the basis with the *SP*(6) symmetry does, although for both cases there is the quadrupole-quadrupole interaction. The results are shown for $N = 5, 6$ and 7 in Fig. 10(a), (b) and (c). These results suggest that collective motions such as vibration and rotation are related not only to the quadrupole-quadrupole correlation but also to the dynamical symmetries of the Hamiltonian—the *SP*(6) group has the *SU*(3) subgroup while the *SO*(8) group does not.

As in the IBM calculations [232], the random samples which yield R_4 other than 2.0 or 3.33 in Fig. 10 (a) and (b) were taken to be random noises to the regular structures such as vibration and rotation arising from random interactions [231]. Scrutinizing the correlations of higher yrast states under random interactions, however, remarkably regular patterns were recently observed in both the *SP*(6) and *SO*(8) symmetry-dictated *SD* pairs [233]. We exemplify the results in Fig. 10 by the *SP*(6) symmetry. One sees a sharp correlations between R_4 and R_6 (R_8). This correlation is a reflection of the anharmonic vibrations. For $N = 6$ with the *SP*(6) symmetry, there arises another pattern originated from the missing 2^+ state of the vibrational limit. These are very similar to the results of random *sd* bosons studied in Ref. [234].

In Ref. [235], the *S*-pair correlation was studied for the two semi-magic pseudo nuclei ^{22}O and ^{46}Ca in the presence of random one- and two-body interactions. It was shown that the pure two-body random ensemble does not favor the generalized seniority picture for ^{46}Ca . However, when one includes single-particle splittings through a sufficiently strong random one-body term in the Hamiltonian, an *S*-pair correlation structure becomes dominant in the spin-zero ground states. When the magnitude of the average random single-particle splittings matches the widths of the KB3 [236] and the GXPF1A [141] interactions, an *S* pair correlation structure in the ground states becomes dominant.

Here we exemplify these studies by the role played by the single-particle splittings in the generalized seniority picture for the spin-zero ground states and the first 2^+ states under random interactions, studied in Ref. [235]. The random one-body and two-body interactions are taken to be independent of each other, and both are assumed to follow Gaussian distributions with a zero average. The single-particle energies, denoted by ε_j , follow $\langle \varepsilon_j \rangle = 0$, $\langle \varepsilon_j \varepsilon_{j'} \rangle = \sigma^2 \delta_{jj'}$, here σ is an adjustable parameter. The pair structure coefficients were obtained in the same way as for realistic nuclei, i.e., *S* pair was obtained by maximizing the overlap between the shell-model ground state $|0_1(\text{SM})\rangle$ and the correlated $|S^3\rangle$ state, for each spin-zero ground state, and *D* pair was obtained by maximizing the overlap between the shell-model wave function of the lowest spin-two state (denoted by $|2_1(\text{SM})\rangle$) and $|DS^2\rangle$. Let us denote $\theta_0 = \langle 0_1(\text{SM}) | S^3 \rangle$, $\theta_2 = \langle 2_1(\text{SM}) | DS^2 \rangle$. The θ_0 and θ_2 are overlaps between the exact shell-model states and the states represented by three *S* pairs for ground states and one-*D*-two-*S* pairs for the $|2_1(\text{SM})\rangle$ states under random interactions.

The calculations with 5000 samplings of the two-body random ensemble (i.e., $\sigma = 0$) were performed for two pseudo nuclei ^{22}O and ^{46}Ca and given in Fig. 11 (a-a'). One sees a peak of both θ_0 and $\theta_2 \sim 1$ for ^{22}O , but not for ^{46}Ca . Now let us add one-body random terms, with $\sigma = 1.25$ and 2.5 for ^{22}O , and 2 and 4 for ^{46}Ca ; the values of σ are so chosen because

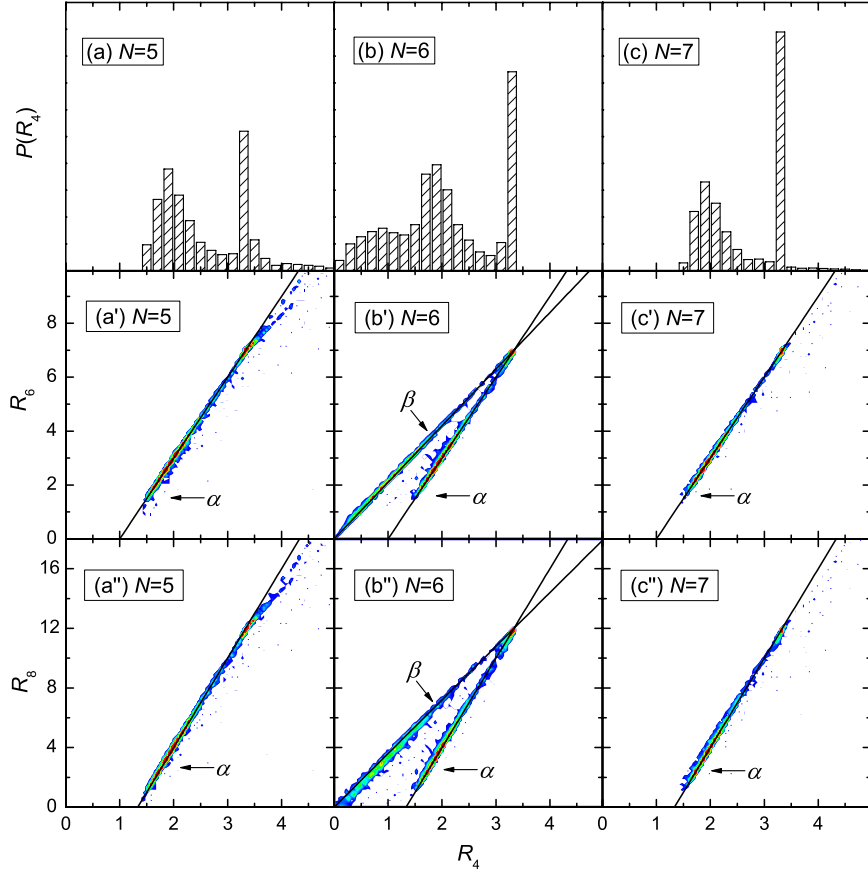


Fig. 10. (Color online) Relative distribution of R_4 , and correlation between R_4 and R_6 (R_8), for five to seven SD pairs with random interactions in the SP(6) case of the Fermion Dynamical Symmetry Model. $R_4 = E_{4+}^+ / E_{2+}^+$, $R_6 = E_{6+}^+ / E_{2+}^+$, $R_8 = E_{8+}^+ / E_{2+}^+$. The distribution of R_4 and R_6 (R_8) follows linear correlations which are denoted by α and β .

single-particle energies $\bar{\epsilon}_j = 3.84$ for ^{22}O and 4.43 for ^{46}Ca best match the widths of realistic effective two-body matrix elements being 1, such as the Wildenthal interaction for the sd shell and the GXPF1A interaction for the pf shell. The results are given in Fig. 11(b–c) and (b'–c'). For both nuclei, as σ increases the likelihood of finding θ_0 and θ_2 larger than 0.9 goes up dramatically. The results also suggest a very strong correlation between θ_0 and θ_2 . This means that when the ground state is well represented by correlated S pairs, the first 2^+ state is well represented by the same S pairs and a single correlated D pair.

The regularity of nuclear structure (spin-zero ground state dominance and the seniority pattern with reasonable single-particle splittings, strong correlations between low-lying states) under random interactions are all interesting. However, their origins remain to be open problems.

4.7. Current status of applications

The last twenty years witnessed a number of major developments of the NPA. The techniques developed by Chen in Ref. [49] have been applied to the evaluation of commutators between coupled operators. By these techniques one is able to recursively calculate the matrix elements of the shell model Hamiltonian, both the general form in Eqs. (8)–(9) and the separable form in Eq. (18), in the coupled nucleon-pair basis. In principle there is no limitation on the structure coefficients of the nucleon pairs, nor on the form of the Hamiltonian. Therefore the NPA to the shell model is a very flexible theory.

The central task of the NPA is to describe low-lying states of medium and heavy nuclei in the collective nucleon-pair truncated subspace of the full shell model configuration space. Its advantage lies in the fact that, although the nucleon-pair subspace is so small in comparison with the gigantic SM space, the model space of the NPA contains, to a large extent, essential configurations of low-lying states. Therefore the NPA provides us with not only a practical approach to study the low-lying states in the SM configuration but also an efficient approach to select the correlated configurations from the prohibitively large space, and is very useful to see the physics from the complexity. In terms of S and D nucleon pairs (and G nucleon pairs for deformed cases) constructed by valence nucleons in one major shell, low-lying states of many medium and heavy nuclei are reasonably described and interpreted. The calculated results in the NPA have been very useful as a guide of experimental studies.

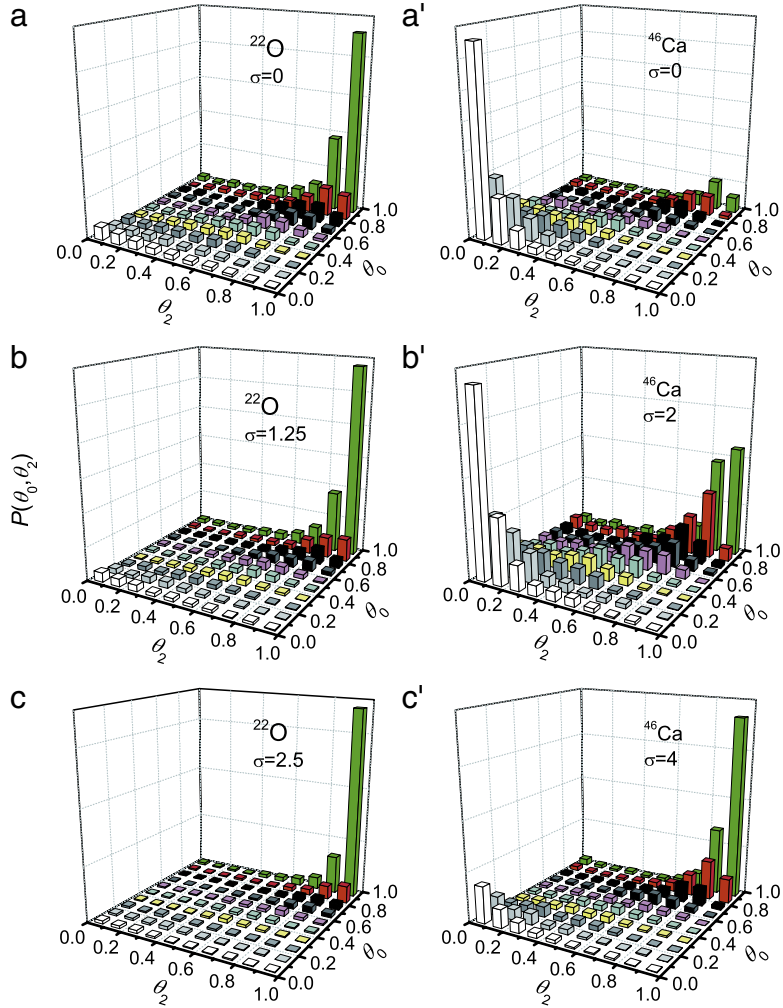


Fig. 11. (Color online) Distribution of θ_0 and θ_2 for random one-body and two-body ensemble, with $\sigma = 0, 1.25, 2.5$ for ^{22}O and $\sigma = 0, 2, 4$ for ^{46}Ca . The results demonstrate that most spin-zero ground states and yrast spin-two (2_1^+) states among the random samples are well represented by the generalized seniority scheme when σ is 2.5 (or larger) for ^{22}O and 4 (or larger) for ^{46}Ca . When θ_0 is large, so is θ_2 .

The second important advantage is that the NPA calculations are much less time-consuming than the SM calculations when the dimension of the SM configuration space is larger than 10^4 . In SD nucleon-pair truncated subspace, one is able to diagonalize the shell model Hamiltonian for nuclei with the numbers for both valence protons and valence neutrons below eight or ten (i.e., four or five pairs for each species of nucleons), for a separable phenomenological shell model Hamiltonian, by using desktop computers. If one restricts the number of non-S pairs to be less than three (e.g., for low-lying states of Tin isotopes), one easily goes to six and seven pairs. If one restricts oneself to one non-S pair excitation only, a configuration of eight nucleon pairs can be handled by a personal computer. As the number of both valence protons and neutrons are larger than ten (i.e., five proton pairs and five neutron pairs), nuclei become well deformed; and in such cases other schemes such as geometric approximations become more economic. In calculations of the isospin-dictated NPA, one can go to a system with six valence nucleons in many- j shells by a desktop computer. For systems with more particles, one has to use super computers. A comparison between the CPU time of the NPA calculations and that of the SM calculations is given in Table 11. One sees that although for very small configurations the SM calculations are less time-consuming, the NPA calculations are much more realizable for large configurations. One characteristic is that the computing time for the NPA calculations does not increase as explosively as for the SM calculations with the number of single-particle levels. This provides us with an opportunity to apply the NPA to the studies of low-lying states in exotic nuclei (see the next subsection).

In recent years some other nucleon pairs, such as spin-four (G), spin-six (I), spin-eight (K) pairs have been also considered (e.g., see Ref. [150]). A non-collective pair with spin ten constructed by two valence neutrons in the $h_{11/2}$ orbit was suggested to play a decisive role in the back-bending phenomenon in yrast states of Ba^{132} [159]. In Ref. [163] a few nucleon pairs with negative parity have been also considered in a study of the 8^- isomers of the neutron number $N = 74$ isotones with the

Table 11

Dimension and computing time (denoted by “time”, in seconds) for 0^+ states of the pf -shell nuclei, for both the NPA and the SM calculations with monopole plus quadrupole interaction, and for a single CPU with main frequency 2.66 giga-Hertz and memory four giga-bytes. Here the computing time is based on the Nusheal code for the SM calculations, and the Fortran version of the NPA codes. The last two cases, i.e., four or six protons and six neutrons in the pf shell, are not accessible by using the Nusheal code [237] with a computer of four giga-bytes memory, while it is very easy to deal with in terms of the NPA (only fourteen or twenty-four states, six or eleven seconds of computing time).

(N_p, N_n)	(2, 2)	(2, 4)	(2, 6)	(4, 4)	(4, 6)	(6, 6)
SM: dimension/time	158/0.5	2343/3	14177/33	41355/256	267054/–	1777116/–
NPA: dimension/time	2/2	4/2	6/6	9/2	14/6	24/11

NPA. These studies show that, on the one hand S and D nucleon pairs are dominant configurations in low-lying states, and on the other hand some other nucleon pairs are also necessary to describe certain low-lying states.

A practical way to find which nucleon pairs, in addition to S and D pairs, are useful for a given state, is by performing numerical experiment. If the calculated results with the inclusion of certain nucleon pair are very different from those without this nucleon pair, one should take this pair in the NPA calculation. Another simple way to find an intuition of relevant nucleon pairs is based on the single-particle energy levels. For example, single-hole energies of valence neutrons in the 82–126 major shell in Ref. [150] were based on the experimental data on the lowest $p_{1/2}$, $p_{3/2}$, $f_{5/2}$, $f_{7/2}$, $h_{9/2}$, and $i_{13/2}$ states in ^{207}Pb , for which one sees that the $p_{1/2}$, $p_{3/2}$, $f_{5/2}$ orbits are much lower than the others. For low-lying states of nuclei with proton number Z from 76 to 81 and neutron number N from 120 to 125, the configurations for valence neutron holes are reasonably well described by SDG pairs.

The recent development of the NPA with isospin symmetry has paved a straightforward way to study the proton–neutron pair correlations in nuclei with $N \sim Z$ below the double magic nucleus ^{100}Sn [12,116,202]. One can investigate explicitly the relevance of certain proton–neutron pairs and/or like-nucleon pairs in the SM wave functions. Recent studies can be found in Refs. [115–117,170], where it was emphasized that isoscalar spin-aligned proton–neutron pairs play a dominant role in yrast states of $N = Z$ nuclei with mass number $A \sim 92$ –100 (except the 8_1^+ state which is given essentially by the seniority two configuration [115]).

4.8. Future theoretical applications

There are many works that could be done in terms of the NPA. Here we list a few subjects which should be studied in foreseeable future. As mentioned above, direct applications of the SM to the low-lying states of heavy nuclei are not yet practical due to their huge configuration spaces. One cannot describe the transition from vibrational to rotational motion of heavy nuclei in terms of the SM. The NPA can be used to study systems up to ten valence protons and ten valence neutrons, for which deformations have set in. Recent efforts have been made in the description of low-lying states for a few even–even isotopes ($^{144,152}\text{Nd}$), by using the same set of shell model parameters in the framework of the NPA [238]. In doing so, the nucleon pairs are constructed by angular momentum projection of the optimum intrinsic nucleon pairs in the ground states given by the Hartree–Fock–Bogoliubov approximation. Another application of the NPA is to study the low-lying negative-parity states of even–even nuclei. This has been done in the IBM by introducing the f bosons. In the NPA, the nucleon pairs are flexible, and one easily incorporates relevant nucleon pairs with negative parity as building blocks of the configuration space. Ref. [163] is an attempt along this line. As the configuration space of the NPA is small, applications to studies of low-lying states in heavy nuclei remain to be the central task of the NPA in future.

Besides the general interests in nuclear structure of heavy nuclei, there are a number of specific topics in the horizons for future applications of the NPA. The first interesting subject is the interplay between the isovector ($T = 1$) and isoscalar ($T = 0$) pairing interactions, because one obtains explicitly the wave functions in the nucleon-pair basis. If the SM wave function is also available, one is able to investigate how well the physics is described in terms of only a few important isoscalar and/or isovector nucleon pairs, based on the overlap between the wave functions in the nucleon-pair truncated subspace and those in the SM space. For nuclei that the SM wave functions are not accessible, one may construct the NPA space by using nucleon pairs with the lowest energies, and perform the NPA calculations to study low-lying states of such systems. The physics is much more transparent in the NPA results, as the dimension of the NPA wave functions is small and dominant configurations are easy to discern in the nucleon pair basis.

The second application is to study quartet (or alternatively α) correlations in self-conjugate nuclei. Pioneering works of quartet structures in nuclei can be found in Refs. [239–241]. A general quartet model is formulated straightforwardly in terms of the NPA with isospin symmetry (see Sec. V of Ref. [45]). It is possible to combine the calculation of Hamiltonian matrix elements with a variational determination of the structure coefficients that define the pairs of the model and in doing so to study an optimal quartet condensation description of these nuclei.

The third application is to study the shape coexistence in nuclei [242]. This phenomenon was thought to be exotic, but it is now realized that it occurs in all nuclei except the lightest ones. Multiple particle–hole excitations across closed shells lead to low-lying collective states that appear side by side with states originated from one major shell. In such cases one has to deal with configurations of two major shells simultaneously. The shell model space is too gigantic, and the application of the NPA is of great interest owing to its simplicity and good practicability in many- j shells.

The fourth application is to study the effect of unbound states which are crucial in studying the low-energy structure of exotic nuclei, in particular, of nuclei near the drip lines. Some unbound states are very important building blocks of halos and resonant states of weakly bound nuclei [243,244]. An ideal approach would be to treat bound and unbound states (including Gamow states and the continuum states) on the same footing, i.e., as single particle states in the configuration space. However, this is an impossible task—the model space is too gigantic due to many single-particle levels. A reasonable truncation is necessary, and the NPA is a practical approach along this line.

4.9. Summary of this section

In this section we reviewed applications of the NPA in studies of low-lying states of atomic nuclei. We tabulated the results of the NPA calculations for nuclei with mass number $A \sim 80, 100, 130\text{--}150$, and $200\text{--}220$, with short discussions of these works. Even-even, odd- A and doubly odd nuclei are treated on the same footing. The low-lying states of nuclei in transitional region are found to be well represented by simple configurations in the collective nucleon-pair basis. A lot of states of odd- A nuclei are interpreted in terms of weak couplings between the unpaired nucleon and the even-even core. The NPA with isospin symmetry has been recently developed and applied to study the isoscalar spin-aligned pair correlation for $N = Z$ nuclei with mass number A approaching to 100. The NPA calculated results have been found to be very useful in subsequent experimental measurements. In addition, the NPA has been used in studies of phase transitions of low-lying states in nuclei and collective motion with random interactions.

Future perspective of the NPA is discussed. The central task of the NPA is to study the low-lying states which are not accessible for the shell model calculations. One of the goals is to describe the transition from vibrational to rotational motion in heavy nuclei. A number of interesting topics (such as the resonant states of exotic nuclei, shape coexistence due to particle-hole excitations across closed shells, competition between isovector and isoscalar pairing correlations, beta decay) are in consideration of future research plans.

5. Summary

The nucleon-pair approximation (NPA) to the shell model is an old, efficient and convenient idea in nuclear structure physics. Although there have been impressive developments in numerical computations by using the nuclear shell model, yet the full shell model diagonalizations for heavy nuclei are not accessible in foreseeable future. The NPA is therefore one of the practical tools in studies of low-lying states of heavy nuclei, and furthermore a much smaller nucleon-pair configuration (rather than a prohibitively gigantic shell model configuration) that allows a direct interpretation of physics.

In Section 1 we presented a brief historical survey of the nuclear shell model, the seniority scheme and its generalizations, the Bardeen-Cooper-Schrieffer theory for the superconductivity of metals at very low temperatures, the interacting boson model, and their links to the NPA. The original idea of the NPA comes from the short-range nature of nucleon-nucleon interaction. For two identical nucleons in the same orbit, a zero-range attractive potential leads to the spin-zero ground state. For semi-magic even-even nuclei, the ground states are well approximated by S pair condensates. Above the spin-zero ground states of even-even nuclei come the first excited states, dominantly with spin two. This suggests that the monopole and quadrupole pairing, and the quadrupole-quadrupole correlation are the dominant terms in the effective interactions of the shell model Hamiltonian, and thus the S and D nucleon pairs must be the most important building blocks of low-lying states for even-even nuclei. For rotational motion, some other pairs (but still very few) such as G pair have been realized to be important. Therefore constant efforts have been made to study the low-lying states of atomic nuclei based on various pair approximations.

In Section 2 we established the notations and conventions in the NPA. We gave a self-contained presentation, including the nucleon-pair basis, the nuclear shell model Hamiltonian, and other operators. We explained how to compute the matrix elements of various operators in the basis constructed by step-wise couplings of nucleon pairs. Even-even nuclei, odd-mass nuclei and odd-odd nuclei are treated on the same footing. All essential formulas have been presented. Instead of discussing the differences between the original NPSM [36] and the refined version [37] in details, we presented in this paper (see Appendix B) the latest version of the NPA. Previous models such as the generalized seniority scheme, the broken pair approximation, the Ginocchio model and the Fermion dynamical symmetry model, are special versions of the NPA. We also discussed nucleon-pair approximation by m -scheme code, and multi-step shell model, as well as the recent efforts of the NPA with isospin symmetry (Appendix C).

In Section 3, we discussed the validity of the NPA for both single- j and many- j shells, for both semi-magic and open-shell nuclei. For a single- j shell, we discussed the schematic J -pairing interaction and quadrupole-quadrupole interaction. For semi-magic many- j shell nuclei we discussed the low-lying states of $^{43,45}\text{Ca}$ with the GXPF1A interaction; and for open shells we exemplified the study by using ^{130}Te with a phenomenological pairing plus quadrupole interaction. From these examples, one sees that although the configuration constructed by a few collective nucleon pairs are drastically smaller than the shell model space, the NPA results are in very good agreement with those of the SM calculations for low-lying states. We should emphasize once more that the applicability of the NPA originates from the fundamental features of the nuclear shell model Hamiltonian which consists of one-body mean field plus residual two-body interactions dominated by monopole and quadrupole correlations. Necessity of other “favored” pairs in description of some low-lying states reflects

the complexity of the two-body interactions. In recent years the validity of the NPA has been studied mainly for cases in which the deformation is not large; in such cases one can optimize the pair structure coefficients via a few well-known procedures. In the future the validity of the NPA should be extended to deformed nuclei by using effective interactions.

In Section 4, we discussed applications of the NPA. We presented compiled references of numerical calculations obtained by using the nucleon-pair approximation in recent years. There are dozens of papers which concentrate on low-lying states with positive parity of even-even nuclei in the ^{132}Ba region. The nucleon-pair approximation has been also applied to describe the low-lying states of nuclei with $A \sim 80, 100, 140\text{--}150$, and 210. The NPA calculations are also performed to study low-lying states of odd-mass and odd-odd nuclei. The NPA calculated results have been used as one of the useful guides in a number of experimental analyses. Some of the predicted results of the NPA calculations have been confirmed in subsequent experimental measurements. Recent development of the NPA with isospin symmetry provides us with an ideal tool to study the isoscalar pairing correlation in low-lying states of $N = Z$ nuclei with A towards 100. The NPA has been also applied to study regular structure arising in the low-lying states of atomic nuclei with random interactions and the phase transitions of low-lying states in nuclei. We exemplified these applications by a few typical results.

In conclusion, the nucleon-pair approximation to the nuclear shell model is both interpretive and predictive in studies of low-lying states of atomic nuclei. Various efforts have been made in the mathematical formulations as well as the applications. In foreseeable future we expect many more applications of this approach to studies of low-lying states of heavy nuclei for which the traditional shell model calculations are not yet accessible, and to studies of the competition between isovector and isoscalar neutron-proton pairing correlations, many particle-hole excitations across closed shells, and continuum states of exotic nuclei.

Acknowledgments

We are grateful to Drs. B.R. Barrett, W. Bentz, R.F. Casten, J.N. Ginocchio, P.V. Isacker, C.W. Johnson, R.J. Liotta, S. Pittel, and I. Talmi for their reading of this manuscript. We also gratefully acknowledge collaborations with Drs. M. Bao, J. Q. Chen, Y.Y. Cheng, G.J. Fu, J.N. Ginocchio, M. Ichimura, F. Iachello, P.V. Isacker, L.Y. Jia, H. Jiang, Y. Lei, Y. Lu, T. Otsuka, O. Scholten, J.J. Shen, I. Talmi, Sugawara K. Tanabe, Z.Y. Xu, S. Yamaji, E. Ydrefors, N. Yoshinaga, and L.H. Zhang at various stages, and discussions with a much longer list of colleagues. We thank Drs. Y. Lei and Y.A. Luo for plotting some of the figures in this paper. We thank the National Natural Science Foundation of China (Grant No. 11225524), the 973 Program of China (Grant No. 2013CB834401) and Shanghai key laboratory (Grant No. 11DZ2260700) for financial support.

Appendix A. Mathematical notations

$A(Z, N)$	mass number (proton number, neutron number) of an atomic nucleus
$N_p(N_n)$	valence proton (neutron) number outside closed shells
N	number of pairs for valence nucleons
$N_\pi(N_\nu)$	number of pairs for valence protons (neutrons)
n	number of radial nodes of the three dimensional oscillator wave function
j	angular momentum of a single particle state, usually the harmonic oscillator wave function
a, b, c, d	angular momentum of a single particle state, or represent (nlj)
l	orbital angular momentum of the j orbit
$Y_{lm_l}(\theta, \phi)$	the spherical harmonic function
r	radius coordinate or total angular momentum of two valence nucleons
r_i, s_i	angular momentum of two valence nucleons ($i = 0, 1, 2, \dots, N$)
m_x	z -component of x
t	isospin for a nucleon
T	total isospin of two or more nucleons
ϵ_j	single particle energy of valence protons or neutrons
$G_{JT}(j_1 j_2, j_3 j_4)$	two-body matrix elements of nucleons with total spin J and isospin T
G_j	abbreviation of $G_{JT}(j_1 j_2, j_3 j_4)$ for single j fermions
I	total angular momentum for a given state of nuclei
v	seniority number
$R_4(R_6, R_8)$	ratio between $E_{4_1^+}(E_{6_1^+}, E_{8_1^+})$ and $E_{2_1^+}$
H	the shell model Hamiltonian
$C_{a\alpha}^\dagger$	creation operator of a nucleon in the $j = a$ single particle orbit with z projection α
$\tilde{C}_{a\alpha}$	$(-)^{a-\alpha} C_{a-\alpha}$, time-reversal operator of the annihilation operator $C_{a\alpha}$
$A^{r\dagger}$	creation operator of a collective nucleon pair with spin r in pair basis
\mathcal{A}^s	pair creation operator in the shell model Hamiltonian
$y(abr)$	pair structure coefficient of $A^{r\dagger}$
$y_0(abr)$	pair structure coefficient of $\mathcal{A}^{r\dagger}$

$A^{J_N\dagger}(\tau)$	$A_{M_N}^{J_N\dagger}(r_0 r_1 r_2 \cdots r_N, J_1 J_2 \cdots J_N) = \left(\cdots \left((A^{r_0\dagger} \times A^{r_1\dagger})^{(J_1)} \times A^{r_2\dagger} \right)^{(J_2)} \times \cdots \times A^{r_N\dagger} \right)^{(J_N)}$
$ \tau J_N M_N\rangle$	$A_{M_N}^{J_N\dagger}(\tau) 0\rangle = A_{M_N}^{J_N\dagger}(r_0 r_1 r_2 \cdots r_N, J_1 J_2 \cdots J_N) 0\rangle$
Q_m	$r^2 Y_{2m}$, quadrupole operator
Q^t	$\sum_{ab} q(abt) (C_a^\dagger \times \tilde{C}_b)^{(t)}$, an arbitrary particle-hole operator
$Q_i(t), H_k(s_i)$	six $-j$ coefficient arising from the angular momentum recouplings
$\bar{G}_k(s_i t), \bar{M}_k(tr'_i)$	six $-j$ coefficient arising from the angular momentum recouplings
S, D, G, I pairs	nucleon pairs with spin zero, two, four, six
I_{\max}	maximum of I
$[I]$	the largest integer not exceeding I_{51}
\hat{I}	$\sqrt{2I+1}$

Appendix B. Fundamental formulas of the NPA

We first discuss commutators of coupled operators, including commutators between the operator of an unpaired nucleon and that of a collective pair, those between a cluster of nucleon operators and a collective pair, etc. These commutators are fundamental practice in the NPA of the shell model.

Let F^a, F^b be two operators of arbitrarily coupled fermion clusters with total angular momentum a and b , respectively. A commutator of F^a and F^b with definite angular momentum e is defined by

$$[F^a, F^b]_\epsilon^{(e)} = -(-1)^{e-a-b} \theta_{ab} [F^b, F^a]_\epsilon^{(e)} \equiv \sum_{\alpha\beta} C_{a\alpha, b\beta}^{ee} [F_\alpha^a, F_\beta^b] \\ = (F^a \times F^b)_\epsilon^{(e)} - (-1)^{e-a-b} \theta_{ab} (F^b \times F^a)_\epsilon^{(e)},$$

where $C_{a\alpha, b\beta}^{e\gamma}$ is a Clebsch–Gordan coefficient, and

$$\theta_{ab} = \begin{cases} -1, & \text{if both } a \text{ and } b \text{ are half integers,} \\ +1, & \text{for otherwise.} \end{cases}$$

We have

$$[(F^a \times F^b)^e, F^c]^{(d)} = \sum_f U(abdc; ef) (F^a \times [F^b, F^c]^{(f)})^{(d)} \\ + \sum_f U(abcd; ef) (-1)^{a+d-e-f} \theta_{bc} ([F^a, F^c]^{(f)} \times F^b)^{(d)}, \quad (\text{B.1})$$

where $U(abdc; ef)$ is a unitary Racah coefficient. When $a = b$ and $e = 0$, Eq. (B.1) is reduced to

$$[F^b, (\mathcal{F}^a \times F^a)^{(0)}]^{(b)} = \sum_c U(aabb; 0c) \left\{ [[F^b, \mathcal{F}^a]^{(c)}, F^a]^{(b)} \right. \\ \left. + (-1)^{c-a-b} \left[\theta_{ab} (\mathcal{F}^a \times [F^b, F^a]^{(c)})^{(b)} + (-1)^{2a} \theta_{ac} (F^a \times [F^b, \mathcal{F}^a]^{(c)})^{(b)} \right] \right\}.$$

Let F^t be an arbitrary fermion cluster of angular momentum t . A recursion of Eq. (B.1) gives

$$[A^{J_N\dagger}, F^t]^{(L_N)} = \sum_{k=N}^0 \sum_{r'_k L_k \cdots L_{N-1}} Q_N(t) \cdots Q_{k+1}(t) \bar{M}_k(tr'_k) \\ \times \left(\cdots \left((A^{k-1\dagger} \times [A^{k\dagger}, F^t]^{(r'_k)})^{(L_k)} \times A^{r_{k+1}\dagger} \right)^{(L_{k+1})} \times \cdots \times A^{r_N\dagger} \right)^{(L_N)}, \quad (\text{B.2})$$

where $Q_i(t)$ is the propagator of the cluster P^t for crossing over the pair i ,

$$Q_i(t) = (-)^{J_{i-1}+L_i-J_i-L_{i-1}} U(r_i L_i j_{i-1} t; L_{i-1} J_i), \quad \bar{M}_k(tr'_k) = U(r_k t j_{k-1} L_k; r'_k J_k),$$

with the convention that

$$Q_N(t) \cdots Q_{k+1}(t) = \begin{cases} 1, & \text{for } k = N, \\ Q_N(t), & \text{for } k = N-1. \end{cases}$$

Eq. (B.2) is called the Wick Theorem for coupled clusters [49].

A simple physical interpretation of (B.2) is as follows: The cluster F^t moves leftward across the pairs $N, N-1, \dots, k+1$, changes the angular momenta J_n to L_n , $n = N, N-1, \dots, k+1$, and arrives at the right of the pair r_k . The propagation contributes the factor $Q_N(t) \cdots Q_{k+1}(t)$. Then the cluster F^t transforms the pair r_k to a new pair (r'_k) associated with the recoupling coefficient $\tilde{M}_k(tr'_k)$ and the change of $J_k \rightarrow L_k$.

If F^t is a scalar with $t = 0$, it can propagate freely with all the coefficients $Q_k(t)$ and $\tilde{M}_k(tr'_k)$ being equal to 1, the summation indices $r'_k L_k \cdots L_{N-1}$ disappear (because $t = 0$), and Eq. (B.2) is reduced to

$$[A^{l_N\dagger}, F^0] = \sum_{k=N}^0 \left(\cdots \left(\left(A^{l_{k-1}\dagger} \times [A^{r_k\dagger}, F^0]^{(r_k)} \right)^{(J_k)} \times A^{r_{k+1}\dagger} \right)^{(J_{k+1})} \times \cdots \times A^{r_N\dagger} \right)^{(J_N)}. \quad (B.2)$$

This formula is very useful in calculating matrix elements of the shell model Hamiltonian in the nucleon pair subspace.

The key commutators used in evaluating the overlaps and matrix elements of the shell model Hamiltonian are as follows: $[A^{l_N\dagger}(\tau), \tilde{A}^s]^{(L_N)}$, $[\tilde{A}^{l_N\dagger}(\tau), A^{s\dagger}]^{(L_N)}$, $[A^{l_N\dagger}(\tau), Q^t]^{(L_N)}$, and $[\tilde{A}^{l_N}(\tau), Q^t]^{(L_N)}$, where $A^{s\dagger}$, \tilde{A}^s , $A^{l_N\dagger}(\tau)$, $\tilde{A}^{l_N}(\tau)$, and Q^t are defined in Eqs. (1)–(4) and (15), respectively. These commutators are studied in detail in Ref. [49]. Below we list two fundamental commutators.

$$\begin{aligned} [\tilde{A}^{r_k}, A^{s\dagger}]^{(t)} &= 2\hat{r}_k \delta_{t0} \delta_{s,r_k} \sum_{ab} y(ab r_k) y(b s) - \sum_{ad} \left(4\hat{r}_k \hat{s} \sum_b y(ab r_k) y(b d s) \begin{Bmatrix} r_k & s & t \\ d & a & b \end{Bmatrix} \right) (\tilde{C}_d^\dagger \times \tilde{c}_a)^{(t)}, \\ A^{r'_k\dagger} &= [Q^t, A^{r_k\dagger}]^{(r'_k)} = (-)^{r_k+r'_k} \begin{cases} \sum_{da} y'(d a r'_k) A^{r'_k\dagger}(d a), & 1 \leq k \leq N, \\ (-)^{t-j-j'} q(j j' t) \hat{t} / \hat{j}' C_{j'}^\dagger, & k = 0 (r_k = j, r'_k = j'), \end{cases} \\ y'(d a r'_k) &= z(d a r'_k) - \theta(d a r'_k) z(a d r'_k), \quad z(d a r'_k) = \hat{r}_k \hat{t} \sum_{b_k} y(a b_k r_k) q(b_k d t) \begin{Bmatrix} r_k & t & r'_k \\ d & a & b_k \end{Bmatrix}. \end{aligned} \quad (B.3)$$

By an recursive application of Eq. (B.2), one obtains the overlaps of pair basis as follows.

$$\begin{aligned} \langle j_0 s_1 \cdots s_N J'_1 \cdots J'_N | j r_1 \cdots r_N, J_1 \cdots J_N \rangle &= \frac{\hat{J}'_{N-1}}{\hat{J}_N} (-1)^{J_N - J'_{N-1} + s_N} \sum_{k=N}^1 \sum_{L_{k-1} \cdots L_{N-2}} H_N(s_N) \cdots H_{k+1}(s_N) \\ &\times \left[\psi_k \delta_{s_N r_k} \delta_{L_{k-1} J_{k-1}} \langle j_0 s_1 \cdots s_{N-1} J'_1 \cdots J'_{N-1} | j r_1 \cdots r_{k-1} r_{k+1} \cdots r_N, J_1 \cdots J_{k-1} L_k \cdots J_{N-1} \rangle \right. \\ &+ \sum_{i=k-1}^0 \sum_{tr'_i L_i \cdots L_{k-2}} \tilde{G}_k(s_N t) \tilde{M}_i(tr'_i) Q_{k-1}(t) \cdots Q_{i+1}(t) \\ &\times \left. \langle j_0 s_1 \cdots s_{N-1} J'_1 \cdots J'_{N-1} | j r_1 \cdots (r'_i)_B \cdots r_{k-1} r_{k+1} \cdots r_N, J_1 \cdots J_{i-1} L_i \cdots J_{N-1} \rangle \right], \end{aligned} \quad (B.4)$$

where

$$\psi_k = 2(-)^{J_k - J_{k-1} - r_k} \hat{r}_k / \hat{J}_{k-1} \sum_{ab} y(ab r_k) y(b s_N),$$

$$H_k(s_N) = (-)^{J_{k-1} + L_{k-1} - J_k - L_{k-2}} U(r_k L_{k-1} J_{k-1} s_N; L_{k-2} J_k),$$

$$\tilde{G}_k(s_N t) = -U(r_k s_N J_{k-1} L_{k-1}; t J_k),$$

with the convention

$$H_N(s_N) \cdots H_{k+1}(s_N) = \begin{cases} 1, & \text{for } k = N, \\ H_N(s_N), & \text{for } k = N-1. \end{cases}$$

$$r_0 = J_0 = j, \quad r'_0 = L_0 = j', \quad J_{-1} \equiv 0,$$

$$\tilde{G}_0(st) = -U(r_0 s J_{-1} L_{-1}; t J_0) = -1, \quad \tilde{M}_0(tr'_0) = U(r_0 t J_{-1} L_0; r'_0 J_0) = 1.$$

In Eq. (B.4), $(r'_i)_B \equiv \mathcal{B}^{r'_i}$ represents a new collective pair ($i \neq 0$) or a nucleon ($i = 0$), suggesting that the nucleon-pair basis does not form a closed subspace in the recursions, in principle.

$$\tilde{\mathcal{B}}^{r'_i} = -[\tilde{A}^{r_i}, [\tilde{A}^{r_k}, A^{s_N\dagger}]^t]^{r'_i} = \begin{cases} \sum_{aa'} [z(aa' r'_i) - (-)^{a+a'+r'_i} z(a' a r'_i)] \tilde{A}^{r'_i}(aa'), & 1 \leq i \leq N, \\ (-1)^{t-j-j'} 4\hat{r}_k \hat{s}_N \hat{t} \sum_b y(j' b r_k) y(b j s_N) \begin{Bmatrix} r_k & s_N & t \\ j & j' & b \end{Bmatrix} \tilde{C}_{j'}^\dagger / \hat{j}', & i = 0 (r'_0 = j'), \end{cases} \quad (B.5)$$

where

$$z(aa'r'_i) = 4\hat{r}_i\hat{r}_k\hat{s}_N\hat{t} \sum_{bb'} y(bb's_N)y(abr_k)y(a'b'r_i) \begin{Bmatrix} r_k & s_N & t \\ b' & a & b \end{Bmatrix} \begin{Bmatrix} r_i & t & r'_i \\ a & a' & b' \end{Bmatrix}.$$

Matrix elements for multipole operator in Eq. (16) are given by

$$\langle j_0s_1 \cdots s_N, J'_1 \cdots J'_N \| Q^t \| jr_1 \cdots r_N, J_1 \cdots J_N \rangle = \sum_{k=N}^0 \sum_{r'_k L_k \cdots L_{N-1}} (-)^{t+r_k+r'_k} Q_N(t) \cdots Q_{k+1}(t) \bar{M}_k(tr'_k) \times \langle j_0s_1 \cdots s_N, J'_1 \cdots J'_N | jr_1 \cdots (\mathbf{r}'_k) \cdots r_N, J_1 \cdots J_{k-1} L_k \cdots L_N \rangle, \quad (\text{B.6})$$

where (\mathbf{r}'_k) represents $\mathbf{A}^{r'_k\dagger}$ given in Eq. (B.3). Here we take the Rose convention for the reduced matrix elements, i.e., $\langle \tau' J' M' | Q_{m_t}^t | \tau J M \rangle = C_{J M m_t}^{J' M'} \langle \tau' J' \| Q^t \| \tau J \rangle$.

The matrix elements of $V_p^{(s)} = G_s \sum_M \mathcal{A}_M^{s\dagger} \mathcal{A}_M^s$ in Eq. (18) is given by

$$\begin{aligned} & \langle jr_1 \cdots r_N, J_1 \cdots J_N | V_p^{(s)} | j_0s_1 \cdots s_N, J'_1 \cdots J'_N \rangle \\ &= G_s \delta_{J_N J'_N} \sum_{k=N}^1 \left[\hat{s} \varphi_0 \delta_{r_k, s} \langle jr_1 \cdots r_{k-1} s r_{k+1} \cdots r_N, J_1 \cdots J_N | j_0s_1 \cdots s_N, J'_1 \cdots J'_N \rangle \right. \\ & \quad - G_s \sum_{i=k-1}^0 \sum_{tr'_i L_i \cdots L_{k-1}} (-1)^{t-s-r_k} \frac{\hat{t}}{\hat{r}_k} U(J_{k-1} t J_k s; L_{k-1} r_k) Q_{k-1}(t) \cdots Q_{i+1}(t) \bar{M}_i(tr'_i) \\ & \quad \times \left. \langle jr_1 \cdots (r'_i)_B \cdots r_{k-1} s r_{k+1} \cdots r_N, J_1 \cdots J_{i-1} L_i \cdots L_{k-1} J_k \cdots J_N | j_0s_1 \cdots s_N, J'_1 \cdots J'_N \rangle \right]. \end{aligned} \quad (\text{B.7})$$

Here $\varphi_0 = \frac{2}{s} \sum_{ab} y(abr_k) y_0(abs)$, and $(r'_i)_B$ represents the pair $\tilde{\mathcal{B}}^{r'_i} = -[\tilde{A}^{r_i}, [\tilde{A}^{r_k}, \mathcal{A}^{s_N\dagger}]^t]$ which is given by Eq. (B.5) except that s_N , $y(bjs_N)$, and $y(bb's_N)$ are replaced by s , $y_0(bjs)$ and $y_0(bb's)$, respectively.

The matrix elements of $V_{ph}^{(t)} = \kappa_t Q^t \cdot Q^t$ of Eq. (18) is given by

$$\begin{aligned} & \langle jr_1 \cdots r_N, J_1 \cdots J_N | \kappa_t Q^t \cdot Q^t | j_0s_1 \cdots s_N, J'_1 \cdots J'_N \rangle \\ &= \kappa_t \sum_{k=N}^0 \sum_{r'_k} (-1)^{r'_k-r_k} \frac{\hat{r}'_k}{\hat{r}_k} \langle jr_1 \cdots (r_k)_B r_{k+1} \cdots r_N, J_1 \cdots J_N | j_0s_1 \cdots s_N, J'_1 \cdots J'_N \rangle \\ & \quad + \kappa_t (-)^t \sum_{k=N}^0 \sum_{i=k-1}^0 \sum_{r'_i r'_k L_i \cdots L_{k-1}} 2 \frac{\hat{r}'_k}{\hat{r}_k} U(J_{k-1} t J_k r'_k; L_{k-1} r_k) Q_{k-1}(t) \cdots Q_{i+1}(t) \bar{M}_i(tr'_i) \\ & \quad \times \langle jr_1 \cdots (r'_i) r_{i+1} \cdots (r'_k) r_{k+1} \cdots r_N, J_1 \cdots J_{i-1} L_i \cdots L_{k-1} J_k \cdots J_N | j_0s_1 \cdots s_N, J'_1 \cdots J'_N \rangle. \end{aligned} \quad (\text{B.8})$$

Here (\mathbf{r}'_k) represents the time-reversal form of pair operator given by

$$\tilde{\mathbf{A}}^{r'_k} = [\tilde{A}^{r_k}, Q^t]^{r'_k} = \begin{cases} \sum_{ab} y'(abr'_k) \tilde{A}^{r'_k}(ab), & 1 \leq k \leq N, \\ (-)^{t-j-j'} q(jj't) \hat{t}/\hat{j'} C_j^\dagger, & k = 0 (r_0 = j, r'_0 = j'), \end{cases}$$

where $y'(abr)$ is given in Eq. (B.3). One should be aware that the structure coefficients of $\tilde{\mathbf{A}}^{r'_k} = [\tilde{A}^{r_k}, Q^t]^{r'_k}$ and those of $\mathbf{A}^{r'_k\dagger} = [Q^t, A^{r_k\dagger}]^{r'_k}$ are different by a phase factor $(-)^{r_k+r'_k}$. In Eq. (B.8) $(r_k)_B$ represents $\tilde{\mathbf{B}}^{r_k}(r'_k)$ which comes from a double commutator,

$$\tilde{\mathbf{B}}^{r_k}(r'_k) = [[\tilde{A}^{r_k}, Q^t]^{r'_k}, Q^t]^{(r_k)} = [\tilde{A}^{r'_k}, Q^t]^{(r_k)}.$$

For $k \geq 1$,

$$\begin{aligned} \tilde{\mathbf{B}}^{r_k}(r'_k) &= \sum_{ab} [\bar{z}(abr_k) - (-)^{a+b+r_k} \bar{z}(bar_k)] \tilde{A}^{r_k}(ab), \quad \bar{z}(abr_k) = \hat{r}'_k \hat{t} \sum_d \bar{y}(bdr'_k) q(dat) \begin{Bmatrix} r'_k & t & r_k \\ a & b & d \end{Bmatrix}, \\ \bar{y}(bdr'_k) &= [z(bdr'_k) - (-)^{b+d+r'_k} z(dbr'_k)], \quad z(bdr'_k) = \hat{r}'_k \hat{t} \sum_{d_0} y(dd_0 r_k) q(d_0 bt) \begin{Bmatrix} r_k & t & r'_k \\ b & d & d_0 \end{Bmatrix}, \end{aligned}$$

and for $k = 0$,

$$\tilde{\mathbf{B}}^j(j') = \left[\left[\tilde{\zeta}_j, Q^t \right]^{j'}, Q^t \right]^j = \frac{2t+1}{\hat{j}'} q(j'jt) q(jj't) \tilde{\zeta}_j.$$

Appendix C. The NPA with isospin symmetry

Neutrons and protons are the two components of an isospin doublet of nucleons, and the nuclear force is an isospin scalar. When active neutrons and protons are in the same shell, isospin symmetry should be explicitly taken into account in the NPA, with the basis in the form of Eq. (5).

The time-reversal form of nucleon-pair annihilation operator is given by

$$\tilde{A}_{M_{r_i} M_{t_i}}^{(r_i t_i)} = (-)^{r_i - M_{r_i}} (-)^{t_i - M_{t_i}} A_{-M_{r_i} - M_{t_i}}^{(r_i t_i)} = - \sum_{ab} y(ab r_i t_i) \left(\tilde{a} \times \tilde{b} \right)_{M_{r_i} M_{t_i}}^{(r_i t_i)}.$$

The time-reversal form of Eq. (5) is

$$\begin{aligned} \tilde{A}_{M_N M_T}^{J_N T_N}(\tau) &\equiv \tilde{A}_{M_N M_T}^{J_N T_N}(r_0 t_0, r_1 t_1, r_2 t_2, \dots, r_N t_N; J_1 T_1, J_2 T_2, \dots, J_N T_N) \\ &= \left(\dots \left(\left(\tilde{A}^{(r_0 t_0)} \times \tilde{A}^{(r_1 t_1)} \right)^{(J_1 T_1)} \times \tilde{A}^{(r_2 t_2)} \right)^{(J_2 T_2)} \times \dots \times \tilde{A}^{(r_N t_N)} \right)^{(J_N T_N)}_{M_N M_T}. \end{aligned} \quad (\text{C.1})$$

The basic commutator between a single-nucleon creation and an annihilation operator is given by

$$(\tilde{C}_a, C_b^\dagger)^{(et)} = \delta_{e0} \delta_{t0} \delta_{ab} \sqrt{2} \hat{a}.$$

Eq. (B.1) is generalized as below.

$$\begin{aligned} &\left((A^{(at_a)} \times B^{(bt_b)})^{(et_e)}, C^{(ct_c)} \right)^{(dt_d)} \\ &= \sum_{f_f} U(abdc, ef) U(t_a t_b t_d t_c, t_e t_f) \left(A^{(at_a)} \times (B^{(bt_b)}, C^{(c, t_c)})^{(ft_f)} \right)^{(dt_d)} \\ &+ \theta_{bc} \sum_{f_f} (-)^{a+d-e-f} (-)^{t_a+t_d-t_e-t_f} U(abcd, ef) U(t_a t_b t_c t_d, t_e t_f) \left((A^{(at_a)}, C^{(c, t_c)})^{(f, t_f)} \times B^{(bt_b)} \right)^{(dt_d)}. \end{aligned} \quad (\text{C.2})$$

This is the key to factorize commutators of the NPA with isospin. The coupled commutator between two nucleon pairs, $(\tilde{A}^{(r_1 t_1)}, A^{(r_2 t_2)^\dagger})^{(JT)}$ is given by

$$(\tilde{A}^{(r_1 t_1)}, A^{(r_2 t_2)^\dagger})^{(JT)} = 2\hat{r}_1 \hat{t}_1 \delta_{r_1 r_2} \delta_{j_0} \delta_{t_1 t_2} \delta_{T_0} \sum_{ab} y(ab r_1 t_1) y(ab r_2 t_2) + 4 \sum_{ca} q'(ca JT) (C_c^\dagger \times \tilde{C}_a)^{(JT)}, \quad (\text{C.3})$$

where

$$q'(cat) = \hat{r}_1 \hat{t}_1 \hat{r}_2 \hat{t}_2 \left\{ \begin{array}{ccc} \frac{1}{2} & \frac{1}{2} & t_1 \\ t_2 & T & \frac{1}{2} \end{array} \right\} \sum_b y(ab r_1 t_1) y(bc r_2 t_2) \left\{ \begin{array}{ccc} a & b & r_1 \\ r_2 & J & c \end{array} \right\}. \quad (\text{C.4})$$

Suppose that $P^{(rt)}$ is a tensor operator with spin r and isospin t . By recursive applications of Eq. (C.2), we obtain the commutator between an N -pair operator and this tensor operator, viz.,

$$\begin{aligned} &\left(\tilde{A}^{(J_N T_N)}(r_0 t_0 r_1 t_1 \dots r_N t_N, J_0 T_0 J_1 T_1 \dots J_N T_N), P^{(rt)} \right)^{(L_N T'_N)} \\ &= \sum_{i=N}^0 \sum_{r'_i t'_i L_i T'_i L_{i+1} T'_{i+1} \dots L_{N-1} T'_{N-1}} \overline{Q}(rt, L_N T'_N) \dots \overline{Q}(rt, L_{i+1} T'_{i+1}) \overline{M}(rt, r'_i t'_i) \\ &\times \left(\dots \left(\left(\tilde{A}^{(J_{i-1} T_{i-1})} \times (\tilde{A}^{(r_i t_i)}, P^{(rt)})^{(r'_i t'_i)} \right)^{(L_i T'_i)} \times \tilde{A}^{(r_{i+1} t_{i+1})} \right)^{(L_{i+1} T'_{i+1})} \times \dots \times \tilde{A}^{(r_N t_N)} \right)^{(L_N T'_N)}, \end{aligned} \quad (\text{C.5})$$

where

$$\begin{aligned}\overline{M}(rt, r'_N T'_N) &= U(J_{N-1} r_N L_N r, L_N r'_N) U(T_{N-1} t_N T'_N t, T'_N t'_N), \\ \overline{Q}(rt, L_N T'_N) &= (-)^{J_N + L_{N-1} - J_{N-1} - L_N} (-)^{T_N + T'_{N-1} - T_{N-1} - T'_N} U(J_{N-1} r_N L_N, J_N L_{N-1}) U(T_{N-1} t_N t T'_N, T_N T'_{N-1}), \\ \overline{M}(rt, r'_0 T'_0) &= 1, \\ \overline{Q}(rt, L_N r'_N) \cdots \overline{Q}(rt, L_{i+1} T'_{i+1}) &= \begin{cases} 1, & \text{if } i = N; \\ \overline{Q}(rt, L_N r'_N), & \text{if } i = N - 1. \end{cases}\end{aligned}$$

$r_0 = J_0 = j$, $t_0 = T_0 = \frac{1}{2}$ for odd- A systems and $r_0 = J_0 = 0$, $t_0 = T_0 = 0$ for even- A systems. By using this formula, one readily obtains commutators such as

$$\begin{aligned}&\left(\tilde{A}^{(J_N T_N)} (r_0 t_0 \cdots r_N t_N, J_0 T_0, J_1 T_1 \cdots J_N T_N), A^{(s_{\text{ft}})^\dagger} \right)^{(L_{N-1} T'_{i-1})}, \\ &\left(\tilde{A}^{(J_N T_N)} (r_0 t_0 \cdots r_N t_N, J_0 T_0, J_1 T_1 \cdots J_N T_N), \left(A_1^{(st)^\dagger} \times \tilde{A}_2^{(st)} \right)^{(00)} \right)^{(J_N T_N)}.\end{aligned}$$

These formulas have been presented in Eqs. (20) and (36) in Ref. [45]. By using these formulas one readily calculates the matrix elements of the one- and two-body tensor operators with given spin and isospin in the nucleon pair basis, see Ref. [45] for details.

References

- [1] M.G. Mayer, Phys. Rev. 75 (1949) 1969.
- [2] J.H.D. Jensen, J. Suess, O. Haxel, Naturwissenschaften 36 (1949) 155.
- [3] O. Haxel, J.H.D. Jensen, H.E. Suess, Phys. Rev. 75 (1949) 1766.
- [4] A. de-Shalit, I. Talmi, Nuclear Shell Theory, Academic Press, New York, 1963;
I. Talmi, Simple Models of Complex Nuclei, Harwood, New York, 1993.
- [5] R.D. Lawson, Theory of the Nuclear Shell Model, Clarendon, Oxford, 1980.
- [6] T. Otsuka, M. Honma, T. Mizusaki, N. Shimizu, Y. Utsuno, Prog. Part. Nucl. Phys. 47 (2001) 319.
- [7] E. Caurier, G. Martinez-Pinedo, F. Nowacki, A. Poves, A.P. Zuker, Rev. Modern Phys. 77 (2005) 427.
- [8] S.E. Koonin, D.J. Dean, K. Langanke, Phys. Rep. 278 (1997) 1.
- [9] DOE/NSF Nuclear Science Advisory Committee, the Frontiers of Nuclear Science, a Long Range plan, arXiv:0809.3137.
- [10] M.G. Mayer, Phys. Rev. 78 (1950) 22.
- [11] G.F. Bertsch, Nuclear pairing basic phenomena revisited, arXiv:1203.5529.
- [12] D.J. Dean, M. Hjorth-Jensen, Rev. Modern Phys. 75 (2003) 607.
- [13] G. Racah, Phys. Rev. 62 (1942) 438; Phys. Rev. 63 (1943) 367.
- [14] G. Racah, L. Farkas Memorial Volume, Research council of Israel, Jerusalem, 1952, p. 294.
- [15] B.H. Flowers, Proc. Roy. Soc. (London) 212 (1952) 248.
- [16] J. Bardeen, L.N. Cooper, J.R. Schrieffer, Phys. Rev. 106 (1957) 162; Phys. Rev. 108 (1957) 1175.
- [17] A. Bohr, B.R. Mottelson, D. Pines, Phys. Rev. 110 (1958) 936.
- [18] S.T. Belyaev, Mat. Fys. Medd. Vid. Selsk. 31 (1959) 11.
- [19] A. Midgal, Nuclear Phys. 13 (1959) 655.
- [20] A.K. Kerman, Ann. Phys. (N.Y.) 12 (1961) 300.
- [21] K. Helmers, Nuclear Phys. 23 (1961) 594.
- [22] M. Ichimura, Progr. Theoret. Phys. 32 (1964) 757;
M. Ichimura, Progr. Theoret. Phys. 33 (1965) 215;
A. Arima, M. Ichimura, Progr. Theoret. Phys. 36 (1966) 296;
M. Ichimura, Prog. Nucl. Phys. 10 (1968) 309.
- [23] J.N. Ginocchio, Nuclear Phys. A 74 (1965) 321.
- [24] I. Talmi, Nuclear Phys. 172 (1971) 1;
S. Shlomo, I. Talmi, Nuclear Phys. A198 (1972) 81.
- [25] Y.K. Gambir, S. Haq, J.K. Suri, Ann. Phys.(N.Y.) 133 (1981) 154.
- [26] K. Allart, E. Boeker, G. Bonsignori, M. Saroia, Y.K. Gambhir, Phys. Rep. 169 (1988) 209.
- [27] A. Arima, F. Iachello, Phys. Rev. Lett. 35 (1975) 1069.
- [28] A. Arima, F. Iachello, Ann. Phys. 99 (1976) 253.
- [29] A. Arima, F. Iachello, Ann. Phys. 111 (1978) 201.
- [30] A. Arima, F. Iachello, Ann. Phys. 123 (1979) 468.
- [31] A. Arima, F. Iachello, Adv. Nucl. Phys. 13 (1984) 139;
F. Iachello, A. Arima, The Interacting Boson Model, Cambridge University Press, 1987.
- [32] R.F. Casten, D.D. Warner, Rev. Modern Phys. 60 (1988) 389.
- [33] T. Otsuka, A. Arima, F. Iachello, Nuclear Phys. A 309 (1978) 1.
- [34] S. Pittel, P.D. Duval, B.R. Barrett, Ann. Phys. (N.Y.) 144 (1982) 168.
- [35] F. Iachello, I. Talmi, Rev. Modern Phys. 59 (1987) 339;
I. Talmi, Prog. Part. Nucl. Phys. 9 (1983) 27.
- [36] J.Q. Chen, Nuclear Phys. A 626 (1997) 686.
- [37] Y.M. Zhao, N. Yoshinaga, S. Yamaji, J.Q. Chen, A. Arima, Phys. Rev. C 62 (2000) 014304.
- [38] J.N. Ginocchio, Phys. Lett. B 79 (1978) 173.
- [39] J.N. Ginocchio, Phys. Lett. B 85 (1979) 9.
- [40] J.N. Ginocchio, Ann. Phys. 126 (1980) 234.
- [41] C.L. Wu, D.H. Feng, X.G. Chen, J.Q. Chen, M.W. Guidry, Phys. Lett. B 168 (1986) 313;
C.L. Wu, D.H. Feng, X.G. Chen, J.Q. Chen, M.W. Guidry, Phys. Rev. C 36 (1987) 1157.
- [42] W.M. Zhang, D.H. Feng, J.N. Ginocchio, Phys. Rev. C 37 (1988) 1281;
W.M. Zhang, C.L. Wu, D.H. Feng, J.N. Ginocchio, Phys. Rev. C 38 (1988) 1475.

- [43] C.L. Wu, D.H. Feng, M. Guidry, *Adv. Nucl. Phys.* 21 (1994) 227.
- [44] J.N. Ginocchio, *Phys. Rev. C* 71 (2005) 064325.
- [45] G.J. Fu, Y. Lei, Y.M. Zhao, S. Pittel, A. Arima, *Phys. Rev. C* 87 (2013) 044310.
- [46] M. Baranger, K. Kumar, *Nuclear Phys.* 62 (1968) 113;
M. Baranger, K. Kumar, *Nuclear Phys.* 110 (1968) 490; *A* 122 (1968) 241;
K. Kumar, M. Baranger, *Nuclear Phys.* 110 (1968) 529;
K. Kumar, M. Baranger, *Nuclear Phys.* 122 (1968) 273;
K. Kumar, M. Baranger, *Nuclear Phys.* 122 (1968) 529.
- [47] K. Kumar, *Prog. Part. Nucl. Phys.* 9 (1983) 223.
- [48] J.Q. Chen, B.Q. Chen, A. Klein, *Nuclear Phys. A* 554 (1993) 61.
- [49] J.Q. Chen, *Nuclear Phys. A* 563 (1993) 218.
- [50] K.V. Protasov, B. Silvestre-Brac, R. Piepenbring, M. Grinberg, *Phys. Rev. C* 53 (1996) 1646.
- [51] R. Piepenbring, K.V. Protasov, B. Silvestre-Brac, *Nuclear Phys. A* 586 (1995) 396; *Nuclear Phys. A* 586 (1995) 413;
K.V. Protasov, R. Piepenbring, *Nuclear Phys. A* 632 (1998) 39.
- [52] M. Grinberg, R. Piepenbring, K.V. Protasov, B. Silvestre-Brac, *Nuclear Phys. A* 597 (1996) 355.
- [53] F.Q. Luo, M.A. Caprio, *Nuclear Phys. A* 849 (2011) 35.
- [54] M.A. Caprio, F.Q. Luo, K. Cai, V. Hellermans, Ch. Constantinou, *Phys. Rev. C* 85 (2012) 034324.
- [55] M.A. Caprio, F.Q. Luo, K. Cai, Ch. Constantinou, V. Hellermans, *J. Phys. G: Nucl. Part. Phys.* 39 (2012) 105108.
- [56] D.J. Rowe, G. Rosensteel, *Phys. Rev. Lett.* 87 (2001) 172501;
A. Leviatan, *Prog. Part. Nucl. Phys.* 66 (2011) 93.
- [57] A. Escuderos, L. Zamick, *Phys. Rev. C* 73 (2006) 044302.
- [58] L. Zamick, P.V. Isacker, *Phys. Rev. C* 78 (2008) 044327.
- [59] P.V. Isacker, S. Heinze, *Phys. Rev. Lett.* 100 (2008) 052501;
P. Van Isacker, *J. Phys.: Conf. Ser.* 322 (2011) 012003.
- [60] C. Qi, X.B. Wang, Z.X. Xu, R.J. Liotta, R. Wyss, F.R. Xu, *Phys. Rev. C* 82 (2010) 014304.
- [61] I. Talmi, *Nuclear Phys. A* 846 (2010) 31.
- [62] G. Bonsignori, K. Allaart, A. Wan Egmond, *Prog. Part. Nucl. Phys.* 9 (1983) 431.
- [63] O. Scholten, H. Kruse, *Phys. Lett. B* 125 (1983) 113.
- [64] J.N. Ginocchio, *Phys. Rev. C* 48 (1993) 1460.
- [65] O. Monnoye, S. Pittel, J. Engel, J.R. Bennett, P.V. Isacker, *Phys. Rev. C* 65 (2002) 044322.
- [66] J. Engel, P. Vogel, X. Ji, S. Pittel, *Phys. Lett. B* 225 (1989) 5.
- [67] N. Auerbach, W.R. Gibbs, J.N. Ginocchio, W.B. Kaufmann, *Phys. Rev. C* 38 (1988) 1277.
- [68] J.N. Ginocchio, *Nuclear Phys. A* 560 (1993) 321;
H.C. Wu, J.N. Ginocchio, A.E.L. Dieperink, O. Scholten, *Phys. Rev. C* 54 (1996) 1208.
- [69] N. Sandulescu, J. Blomqvist, T. Engeland, M. Hjorth-Jensen, A. Holt, R.J. Liotta, E. Osnes, *Phys. Rev. C* 55 (1997) 2708.
- [70] I.O. Morales, P.V. Isacker, I. Talmi, *Phys. Lett. B* 703 (2011) 606.
- [71] A. Jungclaus, J. Walker, J. Leske, K.H. Speidel, A.E. Stuchbery, M. East, P. Boutachkov, J. Cederkall, P. Doornenbal, J.L. Egido, A. Ekstrom, J. Gerl, R. Gernhauser, N. Goel, M. Gorska, I. Kojocharov, P. Maier-Komor, V. Modamio, F. Naqvi, N. Pietralla, S. Pietri, W. Prokopowicz, H. Schaffner, R. Schwengner, H.J. Wollersheim, *Phys. Lett. B* 695 (2011) 110.
- [72] M. Gai, A. Arima, D. Strottman, *Phys. Lett. B* 106 (1981) 6.
- [73] J. Dukelsky, S. Pittel, S. Sierra, *Rev. Modern Phys.* 76 (2004) 643.
- [74] O. Schwentker, J. Dawson, S. McCaffrey, J. Robb, J. Heisenberg, J. Lichtenstadt, C.N. Papanicolas, J. Wise, J.S. McCarthy, N. Hintz, H.P. Blok, *Phys. Lett. B* 112 (1982) 40;
O. Schwentker, J. Dawson, J. Robb, J. Heisenberg, J. Lichtenstadt, C.N. Papanicolas, J. Wise, J.S. McCarthy, L.T. van der Bijl, H.P. Blok, *Phys. Rev. Lett.* 50 (1983) 15;
J. Heisenberg, J. Heisenberg, J. Dawson, T. Milliman, O. Schwentker, J. Lichtenstadt, C.N. Papanicolas, J. Wise, J.S. McCarthy, N. Hintz, H.P. Blok, *Phys. Rev. C* 29 (1984) 97.
- [75] L.T. Van Der Bijl, H. Blok, H.P. Blok, R. Ent, J. Heisenberg, O. Schwentker, A. Richter, P.K.A. De Witt Huberts, *Nuclear Phys. A* 423 (1984) 365.
- [76] P.J. Blankert, H.P. Blok, J. Blok, *Nuclear Phys. A* 333 (1980) 116.
- [77] C.D. Siegal, Y. Gambhir, *Phys. Lett. B* 39 (1972) 151;
Y.K. Gambhir, A. Rimini, T. Weber, *Phys. Rev. C* 7 (1973) 1454;
P.J. Blankert, *Nuclear Phys. A* 356 (1981) 74.
- [78] P. Hofstra, K. Allaart, Z. *Phys. A* 292 (1979) 159.
- [79] W.F.v. Gunsteren, K. Allaart, P. Hofstra, Z. *Phys. A* 288 (1978) 49.
- [80] W.F.v. Gunsteren, K. Allaart, E. Boeker, *Nuclear Phys. A* 266 (1976) 365.
- [81] W.F.v. Gunsteren, *Nuclear Phys. A* 265 (1976) 263.
- [82] B.O. ten Brink, J. Akkermans, P. van Nes, H. Berheul, *Nuclear Phys. A* 330 (1979) 409.
- [83] A. Arima, M. Harvey, K. Shimizu, *Phys. Lett. B* 30 (1969) 517;
K.T. Hecht, A. Adler, *Nuclear Phys. A* 137 (1969) 129;
J.N. Ginocchio, *Phys. Rev. Lett.* 78 (1997) 436;
J.N. Ginocchio, *Phys. Rep.* 414 (2005) 165.
- [84] A. Arima, N. Yoshida, J.N. Ginocchio, *Phys. Lett. B* 101 (1981) 209.
- [85] A. Arima, J.N. Ginocchio, N. Yoshida, *Nuclear Phys. A* 384 (1982) 112.
- [86] D.H. Feng, C.L. Wu, M.W. Guidry, Z.P. Li, *Phys. Lett. B* 205 (1988) 157.
- [87] M.W. Guidry, C.L. Wu, D.H. Feng, J.N. Ginocchio, X.G. Chen, J.Q. Chen, *Phys. Lett. B* 176 (1986) 1.
- [88] M.W. Guidry, C.L. Wu, Z.P. Li, D.H. Feng, J.N. Ginocchio, *Phys. Lett. B* 187 (1987) 210.
- [89] J.L. Ping, J.Q. Chen, C.L. Wu, D.H. Feng, *Phys. Rev. C* 43 (1991) 2224.
- [90] C.L. Wu, D.H. Feng, Guidry M W, *Phys. Rev. C* 46 (1992) 1339.
- [91] Y.M. Zhao, N. Yoshinaga, S. Yamaji, A. Arima, *Phys. Rev. C* 62 (2000) 024322.
- [92] P. Hulse, *Phys. Rev. C* 39 (1989) 1104.
- [93] J.Q. Chen, D.H. Feng, M.W. Guidry, C.L. Wu, *Phys. Rev. C* 44 (1991) 559.
- [94] For a review, see R.F. Casten, N.V. Zamfir, *J. Phys. G* 22 (1996) 1521.
- [95] S. Pittel, J. Dukelsky, *Phys. Lett. B* 128 (1983) 9.
- [96] F. Catara, A. Insolia, E. Maglione, A. Vitturi, *Phys. Rev. C* 29 (1984) 1916.
- [97] D.R. Bes, R.A. Broglia, E. Maglione, A. Vitturi, *Phys. Rev. Lett.* 48 (1982) 1001.
- [98] E. Maglione, A. Vitturi, R.A. Broglia, C.H. Dasso, *Nuclear Phys. A* 404 (1983) 333.
- [99] T. Otsuka, A. Arima, N. Yoshinaga, *Phys. Rev. Lett.* 48 (1982) 387.
- [100] Sugawara K. Tanabe, A. Arima, *Phys. Lett. B* 110 (1982) 87.
- [101] A. Bohr, B.R. Mottelson, *Phys. Scr.* 22 (1980) 468.
- [102] F. Catara, A. Insolia, E. Maglione, A. Vitturi, *Phys. Lett. B* 123 (1983) 375.

- [103] M. Sambataro, A. Isolia, Phys. Lett. B 166 (1986) 259.
- [104] G.G. Dussel, H.M. Sofia, Phys. Rev. C 72 (2005) 024302; G.G. Dussel, H.M. Sofia, Phys. Rev. C 78 (2008) 014316.
- [105] L.C. De Winter, N.R. Walet, P.J. Brussaard, Nuclear Phys. A 486 (1988) 235.
- [106] C.W. Johnson, J.N. Ginocchio, Phys. Rev. C 50 (1994) 571; J.N. Ginocchio, C.W. Johnson, Phys. Rev. C 51 (1995) 1861.
- [107] E. Maglione, A. Vitturi, Prog. Part. Nuclear Phys. 9 (1983) 87.
- [108] Y.D. Devi, V.K.B. Kota, Pramana J. Phys. 39 (1992) 413.
- [109] L.J. Liotta, C. Pomar, Nuclear Phys. A 362 (1981) 137.
- [110] L.J. Liotta, C. Pomar, Phys. Lett. B 105 (1981) 92; Phys. Rev. Lett. 49 (1982) 1142; C. Pomar, L.J. Liotta, Phys. Rev. C 25 (1982) 1656.
- [111] J. Blomqvist, L. Rydstrom, L.J. Liotta, C. Pomar, Nuclear Phys. A 423 (1984) 253.
- [112] N. Sandulescu, J. Blomqvist, R.J. Liotta, Nuclear Phys. A 582 (1995) 257.
- [113] N. Sandulescu, A. Insolia, J. Blomqvist, R.J. Liotta, Phys. Rev. C 47 (1993) 554.
- [114] N. Sandulescu, A. Insolia, B. Fant, J. Blomqvist, R.J. Liotta, Phys. Lett. B 288 (1992) 235.
- [115] G.J. Fu, J.J. Shen, Y.M. Zhao, A. Arima, Phys. Rev. C 87 (2013) 044312.
- [116] C. Qi, J. Blomqvist, T. Back, B. Cederwall, A. Johnson, L.J. Liotta, R. Wyss, Phys. Rev. C 84 (2011) 021301.
- [117] Z.X. Xu, C. Qi, J. Blomqvist, R.J. Liotta, R. Wyss, Nuclear Phys. A 877 (2012) 51.
- [118] E. Maglione, F. Catra, A. Insolia, A. Vitturi, Nuclear Phys. A 397 (1982) 102.
- [119] F. Catara, M. Sambataro, A. Insolia, A. Vitturi, Phys. Lett. B 180 (1986) 1.
- [120] Y.Y. Gao, F. Catara, M. Sambataro, A. Vitturi, Europhys. Lett. 16 (1991) 711.
- [121] E. Kwasniewicz, J. Brzostowski, E. Hetmaniok, J. Phys. G: Nucl. Part. Phys. 29 (2003) 1383.
- [122] B.R. Barrett, P.D. Duval, S. Pittel, Prog. Part. Nuclear Phys. 9 (1983) 535.
- [123] S. Pittel, O. Scholten, T. Otsuka, Phys. Lett. B 157 (1985) 239.
- [124] C.H. Druce, S. Pittel, B.R. Barrett, P.D. Duval, Ann. Phys. (N.Y.) 176 (1987) 114.
- [125] N. Yoshinaga, Nuclear Phys. A 570 (1994) 421.
- [126] N. Yoshinaga, D.M. Brink, Nuclear Phys. A 515 (1990) 1.
- [127] M.R. Zirnbauer, D.M. Brink, Nuclear Phys. A 384 (1982) 1.
- [128] P. Halse, Nuclear Phys. A 451 (1986) 91.
- [129] P. Halse, L. Jaqua, B.R. Barrett, Phys. Rev. C 40 (1989) 968.
- [130] N. Yoshinga, Nuclear Phys. A 493 (1989) 323; N. Yoshinga, Nuclear Phys. A 503 (1989) 65.
- [131] H. Nakada, T. Otuska, Phys. Rev. C 55 (1997) 748; H. Nakada, Prog. Theor. Phys. suppl. 125 (1996) 151.
- [132] N. Yoshinaga, T. Mizusaki, A. Arima, Y.D. Devi, Prog. Theor. Phys. suppl. 125 (1996) 65.
- [133] H.T. Chen, D.H. Feng, C.L. Wu, Phys. Rev. Lett. 69 (1992) 418; H.T. Chen, D.H. Feng, Phys. Rep. 264 (1996) 91; C.L. Wu, H.T. Chen, D.H. Feng, Phys. Rep. 242 (1994) 433.
- [134] Y.M. Zhao, N. Yoshinaga, S. Yamaji, A. Arima, Phys. Rev. C 62 (2000) 014316.
- [135] Y.M. Zhao, A. Arima, Phys. Rev. C 70 (2004) 034306.
- [136] Y.M. Zhao, A. Arima, J.N. Ginocchio, N. Yoshinaga, Phys. Rev. C 68 (2003) 044320.
- [137] G.J. Fu, Y.M. Zhao, A. Arima, Phys. Rev. C 88 (2013) 054303.
- [138] Y. Lei, Z.Y. Xu, Y.M. Zhao, A. Arima, Phys. Rev. C 80 (2009) 064316.
- [139] Y. Lei, Z.Y. Xu, Y.M. Zhao, A. Arima, Phys. Rev. C 82 (2010) 034303.
- [140] Y. Lei, Y.M. Zhao, A. Arima, Phys. Rev. C 84 (2011) 044301.
- [141] M. Honma, T. Otsuka, B.A. Brown, T. Mizusaki, Phys. Rev. C 69 (2004) 034335.
- [142] P. Halse, Phys. Rev. C 41 (1990) 2340.
- [143] L.Y. Jia, H. Zhang, Y.M. Zhao, Phys. Rev. C 75 (2007) 034307.
- [144] Isotops explorer 3.0, <http://ie.lbl.gov/ensdf/>.
- [145] L.H. Zhang, H. Jiang, Y.M. Zhao, Sci. China G 54 (S1) (2011) 103.
- [146] Y. Lei, Z.Y. Xu, Y.M. Zhao, D.H. Lu, Sci. China G 53 (2010) 1460.
- [147] L.M. Yang, Prog. Part. Nuclear Phys. 9 (1983) 147.
- [148] D.H. Lu, Phys. Rev. C 47 (1993) 1886; D.H. Lu, Phys. Rev. C 58 (1998) 2588.
- [149] M.P. Kartamyshev, T. Engeland, M. Hjorth-Jensen, E. Osnes, Phys. Rev. C 76 (2007) 024313.
- [150] Z.Y. Xu, Y. Lei, Y.M. Zhao, S.W. Xu, Y.X. Xie, A. Arima, Phys. Rev. C 79 (2009) 054315.
- [151] L.Y. Jia, H. Zhang, Y.M. Zhao, Phys. Rev. C 76 (2007) 054305.
- [152] X.W. Pan, J.L. Ping, D.H. Feng, J.Q. Chen, C.L. Wu, M.W. Guidry, Phys. Rev. C 53 (1996) 715.
- [153] J.Q. Chen, Y.A. Luo, Nuclear Phys. A 639 (1998) 615.
- [154] Y.A. Luo, J.Q. Chen, Phys. Rev. C 58 (1998) 589; Y.A. Luo, J.W. Chen, J.P. Draayer, Nuclear Phys. A 669 (2000) 101.
- [155] Y.A. Luo, X.B. Zhang, F. Pan, P.Z. Ning, J.P. Draayer, Phys. Rev. C 64 (2001) 047302.
- [156] X.F. Meng, F.R. Wang, Y.A. Luo, F. Pan, J.P. Draayer, Phys. Rev. C 77 (2008) 047304.
- [157] Y.M. Zhao, S. Yamaji, N. Yoshinaga, A. Arima, Phys. Rev. C 62 (2000) 014315.
- [158] N. Yoshinaga, K. Higashiyama, Phys. Rev. C 69 (2004) 054309.
- [159] K. Higashiyama, N. Yoshinaga, K. Tanabe, Phys. Rev. C 67 (2003) 044305.
- [160] T. Takahashi, N. Yoshinaga, K. Higashiyama, Phys. Rev. C 71 (2005) 014305.
- [161] K. Higashiyama, N. Yoshinaga, Phys. Rev. C 83 (2011) 034321.
- [162] Y. Lei, Z.Y. Xu, Y.M. Zhao, Preprint (to be published).
- [163] Y. Lei, G.J. Fu, Y.M. Zhao, Phys. Rev. C 87 (2013) 044331.
- [164] K. Higashiyama, N. Yoshinaga, K. Tanabe, Phys. Rev. C 72 (2005) 024315.
- [165] H. Jiang, Y. Lei, G.J. Fu, Y.M. Zhao, A. Arima, Phys. Rev. C 86 (2012) 054304.
- [166] H. Jiang, G.J. Fu, Y.M. Zhao, A. Arima, Phys. Rev. C 84 (2011) 034302.
- [167] R.P. Zhang, Y.A. Luo, P.Z. Ning, Euro. Phys. Lett. 73 (2006) 520.
- [168] N. Yoshinaga, K. Higashiyama, P.H. Regan, Phys. Rev. C 78 (2008) 044320.
- [169] H. Jiang, J.J. Shen, Y.M. Zhao, A. Arima, J. Phys. G 38 (2011) 045103.
- [170] S. Zerguine, P.V. Isacker, Phys. Rev. C 83 (2011) 064314.
- [171] K. Higashiyama, N. Yoshinaga, Phys. Rev. C 88 (2013) 034315.
- [172] H. Jiang, C. Qi, Y. Lei, R. Liotta, R. Wyss, Y.M. Zhao, Phys. Rev. C 88 (2013) 044332.
- [173] H. Jiang, Y. Lei, C. Qi, R. Liotta, R. Wyss, Y.M. Zhao, Phys. Rev. C 89 (2014) 014320.
- [174] R.F. Casten, P. von Brentano, Phys. Lett. B 152 (1985) 22.

- [175] C.J. Barton, M.A. Caprio, D. Shapira, N.V. Zamfir, D.S. Brenner, R.L. Gill, T.A. Lewis, J.R. Cooper, R.F. Casten, C.W. Beausang, R. Krucken, J.R. Novak, Phys. Lett. B 551 (2003) 269.
- [176] N. Benczer-Koller, G.J. Kumbartzki, G. Guerdel, C.J. Gross, A.E. Stuchbery, B. Krieger, R. Hatarik, P. O’Malley, S. Pain, L. Segen, C. Baktash, J. Beene, D.C. Radford, C.H. Yu, N.J. Stone, J.R. Stone, C.R. Bingham, M. Danchev, R. Grzywacz, C. Mazzocchi, Phys. Lett. B 664 (2008) 241.
- [177] X. Chen, D.G. Sarantites, W. Reviol, J. Snyder, Phys. Rev. C 87 (2013) 044305.
- [178] J.M. Allmond, A.E. Stuchbery, D.C. Radford, A. Galindo-Uribarri, N.J. Stone, C. Baktash, J.C. Batchelder, C.R. Bingham, M. Danchev, C.J. Gross, P.A. Hausladen, K. Lagergren, Y. Larochelle, E. Padilla-Rodal, C.H. Yu, Phys. Rev. C 87 (2013) 054325.
- [179] D. Deleanu, D.L. Balabanski, Ts. Venkova, D. Bucurescu, N. Marginean, E. Ganioglu, Gh. Cata-Danil, L. Atanasova, I. Cata-Danil, P. Detistov, D. Filipescu, D. Ghita, T. Glodariu, M. Ivascu, R. Marginean, C. Mihai, A. Negret, S. Pascau, T. Sava, L. Stroe, G. Suliman, N.V. Zamfir, Phys. Rev. C 87 (2013) 014329.
- [180] S. Harissopoulos, A. Gelberg, A. Dewald, M. Hass, L. Weissman, C. Broude, Phys. Rev. C 52 (1995) 1796.
- [181] P. Das, R.G. Pillay, V.V. Krishnamurthy, S.N. Mishra, S.H. Devare, Phys. Rev. C 53 (1996) 1009.
- [182] T. Morek, J. Srebrny, Ch. Droste, M. Kowalczyk, T. Rzaca-Urban, K. Starosta, W. Urban, R. Kaczarowski, E. Ruchowska, M. Kisielinski, A. Kordyasz, J. Kownacki, M. Palacz, E. Wesolowski, W. Gast, R.M. Lieder, P. Bednarczyk, W. Meczynski, J. Styczen, Phys. Rev. C 63 (2001) 034302 and references therein.
- [183] S. Frauendorf, J. Meng, Nuclear Phys. A 617 (1997) 131; S. Frauendorf, Rev. Modern Phys. 73 (2001) 463.
- [184] J. Meng, S.Q. Zhang, J. Phys. G: Nucl. Part. Phys. 37 (2010) 064025.
- [185] A. Banu, J. Gerl, C. Fahlander, M. Gorska, H. Grawe, T.R. Saito, H.-J. Wollersheim, E. Caurier, T. Engeland, A. Gniady, M. Hjorth-Jensen, F. Nowacki, T. Beck, F. Becker, P. Bednarczyk, M.A. Bentley, A. Burger, F. Cristancho, G. de Angelis, Zs. Dombradi, P. Doornenbal, H. Geissel, J. Grebosz, G. Hammond, M. Hellstrom, J. Jolie, I. Kojouharov, N. Kurz, R. Lozeva, S. Mandal, N. Marginean, S. Muralithar, J. Nyberg, J. Pochodzalla, W. Prokopowicz, P. Reiter, D. Rudolph, C. Rusu, N. Saito, H. Schaffner, D. Sohler, H. Weick, C. Wheldon, M. Winkler, Phys. Rev. C 72 (2005) 061305.
- [186] A. Ansari, Phys. Lett. B 623 (2005) 37; A. Ansari, P. Ring, Phys. Rev. C 74 (2006) 054313.
- [187] N. Lo Iudice, Ch. Stoyanov, D. Tarpanov, Phys. Rev. C 84 (2011) 044314.
- [188] M.C. East, A.E. Stuchbery, A.N. Wilson, P.M. Davidson, T. Kibedi, A.I. Levon, Phys. Lett. B 665 (2008) 147.
- [189] J. Walker, A. Jungclaus, J. Leske, K.-H. Speidel, A. Ekström, P. Boutachkov, J. Cederkall, P. Doornenbal, J. Gerl, R. Gernhauser, N. Goel, M. Gorska, I. Kojouharov, P. Maier-Komor, V. Modamio, F. Naqvi, N. Pietralla, S. Pietri, W. Prokopowicz, H. Schaffner, R. Schwengner, H.-J. Wollersheim, Phys. Rev. C 84 (2011) 014319.
- [190] G.J. Kumbartzki, N. Benczer-Koller, D.A. Torres, B. Manning, P.D. O’Malley, Y.Y. Sharon, L. Zamick, C.J. Gross, D.C. Radford, S.J.Q. Robinson, J.M. Allmond, A.E. Stuchbery, K.H. Speidel, N.J. Stone, C.R. Bingham, Phys. Rev. C 86 (2012) 034319.
- [191] J. Terasaki, J. Engel, W. Nazarewicz, M. Stoitsov, Phys. Rev. C 66 (2002) 054313.
- [192] A. Ansari, P. Ring, Phys. Lett. B 649 (2007) 128.
- [193] B.A. Brown, N.J. Stone, J.R. Stone, I.S. Towner, M. Hjorth-Jensen, Phys. Rev. C 71 (2005) 044317.
- [194] A.I. Morales, J. Benlliure, M. Gorska, H. Grawe, S. Verma, P.H. Regan, Zs. Podolyak, S. Pietri, R. Kumar, E. Casarejos, A. Algora, N. Alkhomashi, H. Alvarez-Pol, G. Benzoni, A. Blazhev, P. Boutachkov, A.M. Bruce, L.S. Caceres, I.J. Cullen, A.M. Denis Bacelar, P. Doornenbal, M.E. Estevez-Aguado, G. Farrelly, Y. Fujita, A.B. Garnczarsky, W. Gelletly, J. Gerl, J. Grebosz, R. Hoischen, I. Kojouharov, N. Kurz, S. Lalkovski, Z. Liu, C. Mihai, F. Molina, D. Muecher, W. Prokopowicz, B. Rubio, H. Schaffner, S.J. Steer, A. Tamii, S. Tashenov, J.J. Valiente-Dobon, P.M. Walker, H.J. Wollersheim, P.J. Woods, Phys. Rev. C 88 (2013) 014319.
- [195] D.D. Warner, M. Bentley, P.V. Isacker, Nat. Phys. 2 (2006) 311.
- [196] A.L. Goodman, Adv. Nuclear Phys. 11 (1979) 260.
- [197] J. Engel, S. Pittel, M. Stoitsov, P. Vogel, J. Duliksky, Phys. Rev. C 55 (1997) 1781.
- [198] W. Satula, R. Wyss, Phys. Lett. B 393 (1997) 1.
- [199] O. Civitarese, M. Reboiro, P. Vogel, Phys. Rev. C 56 (1997) 1840.
- [200] D. Rudolph, C.J. Gross, J.A. Sheikh, D.D. Warner, I.G. Bearden, R.A. Cunningham, D. Foltescu, W. Gelletly, F. Hannachi, A. Harder, T.D. Johnson, A. Jungclaus, M.K. Kabadiyski, D. Kast, K.P. Lieb, H.A. Roth, T. Shizuma, J. Simpson, O. Skeppstedt, B.J. Varley, M. Weiszlog, Phys. Rev. Lett. 76 (1996) 376.
- [201] V.K.B. Kota, J.A. Castilho Alcaras, Nuclear Phys. A. 764 (2006) 181.
- [202] B. Cederwall, F. Ghazi Moradi, T. Back, A. Johnson, J. Blomqvist, E. Clement, G. France, R. Wadsworth, K. Andgren, K. Lagergren, A. Dijon, G. Jaworski, R. Liotta, C. Qi, B.M. Nyako, J. Nyberg, M. Palacz, H. Al-Azri, A. Algora, G. de Angelis, A. Atac, S. Bhattacharyya, T. Brock, J.R. Brown, P. Davies, A. Di Nitto, Zs. Dombradi, A. Gadea, J. Gal, B. Hadinia, F. Johnston-Theasby, P. Joshi, K. Juhasz, R. Julin, A. Jungclaus, G. Kalinka, S.O. Kara, A. Khaplanov, J. Kownacki, G. La Rana, S.M. Lenzi, J. Molnar, R. Moro, D.R. Napoli, B.S. Nara Singh, A. Persson, F. Recchia, M. Sandzelius, J.-N. Scheurer, G. Sletten, D. Sohler, P.-A. Soderstrom, M.J. Taylor, J. Timar, J.J. Valiente-Dobon, E. Vardaci, S. Williams, Nature 469 (2011) 68.
- [203] B.S. Nara Singh, Z. Liu, R. Wadsworth, H. Grawe, T.S. Brock, P. Boutachkov, N. Braun, A. Blazhev, M. Gorska, S. Pietri, D. Rudolph, C. Domingo-Pardo, S.J. Steer, A. Atac, L. Bettermann, L. Caceres, K. Eppingen, T. Engert, T. Faestermann, F. Farinon, F. Finke, K. Geibel, J. Gerl, R. Gernhauser, N. Goel, A. Gottardo, J. Grebosz, C. Hinke, R. Hoischen, G. Ilie, H. Iwasaki, J. Jolie, A. Kaskas, I. Kojouharov, R. Krucken, N. Kurz, E. Merchan, C. Nociforo, J. Nyberg, M. Pfutzner, A. Prochazka, Zs. Podolyak, P.H. Regan, P. Reiter, S. Rinta-Antila, C. Scholl, H. Schaffner, P.-A. Soderstrom, N. Warr, H. Weick, H.J. Wollersheim, P.J. Woods, F. Nowacki, K. Sieja, Phys. Rev. Lett. 107 (2011) 172502.
- [204] M. Honma, T. Otsuka, T. Mizusaki, M. Hjorth-Jensen, Phys. Rev. C 80 (2009) 064323.
- [205] A.H. Wapstra, G. Audi, C. Thibault, Nuclear Phys. A 729 (2003) 129; G. Audi, A.H. Wapstra, C. Thibault, Nuclear Phys. A 729 (2003) 337 also see <http://www.nndc.bnl.gov/masses/mass.mas03>.
- [206] S.W. Xu, Y.X. Xie, Y.X. Guo, R.C. Ma, Y.X. Ge, Z.K. Li, C.F. Wang, B. Guo, J.P. Xing, T.M. Zhang, S.F. Zhu, W. Xu, Z. Physica A 354 (1996) 343.
- [207] P. Kuusiniemi, F.P. Heßberger, D. Ackermann, S. Hofmann, B. Sulignano, I. Kojouharov, R. Mann, Eur. Phys. J. A 25 (2005) 397.
- [208] M. Anselment, W. Faubel, S. Goring, A. Hanser, G. Meisel, H. Rebel, G. Schatz, Nuclear Phys. A 451 (1986) 471.
- [209] K.H. Maier, J.R. Leigh, R.M. Diamond, Nuclear Phys. A 176 (1971) 497.
- [210] D. Riegel, Phys. Scr. 11 (1975) 228.
- [211] P. Raghavan, At. Data Nucl. Data Tables 42 (1989) 189.
- [212] C.M. Olsmats, S. Axensten, G. Liljegren, Arkiv. Fysik. 19 (1961) 469.
- [213] P. Herzog, H. Walitzki, K. Freitag, H. Hildebrand, K. Schlosser, Z. Physica A 311 (1983) 351.
- [214] W. Borchers, R. Neugart, E.W. Otten, H.T. Duong, G. Ulm, K. Wendt, and the ISOLDE Collaboration, Hyp. Interact. 34 (1987) 25.
- [215] E. Arnold, W. Borchers, M. Carre, H.T. Duong, P. Juncar, J. Lerme, S. Liberman, W. Neu, R. Neugart, E.W. Otten, M. Pellarin, J. Pinard, G. Ulm, J.L. Vialle, K. Wendt, Phys. Rev. Lett. 59 (1987) 771.
- [216] G. Neyens, R. Nouwen, G. S’heeren, M. Van Den Bergh, R. Coussement, Phys. Rev. C 49 (1994) 645.
- [217] N.J. Stone, At. Data Nucl. Data Tables 90 (2005) 75.
- [218] V.G. Chumin, et al., Izv. Akad. Nauk SSSR Ser. Fiz. 45 (1981) 2102.
- [219] M.R. Schmorak, Nucl. Data Sheets 45 (1985) 145.
- [220] A.E.L. Dieperink, O. Scholten, F. Iachello, Phys. Rev. Lett. 44 (1980) 1747; D.H. Feng, R. Gilmore, S.R. Deans, Phys. Rev. C 23 (1981) 1254; F. Iachello, N.V. Zamfir, Phys. Rev. Lett. 92 (2004) 212501.
- [221] Y.A. Luo, F. Pan, C. Bahri, J.P. Draayer, Phys. Rev. C 71 (2005) 044304.
- [222] Y.A. Luo, F. Pan, T. Wang, P.Z. Ning, J.P. Draayer, Phys. Rev. C 73 (2006) 044323.

- [223] L. Li, Y.A. Luo, T. Wang, F. Pan, J.P. Draayer, *J. Phys. G* 36 (2009) 125107.
- [224] Y.A. Luo, Y. Zhang, X. Meng, F. Pan, J.P. Draayer, *Phys. Rev. C* 80 (2009) 014311.
- [225] Y. Lei, G.J. Fu, S. Pittel, Y.M. Zhao, Preprint (to be published).
- [226] C.W. Johnson, D. Dean, G. Bertsch, *Phys. Rev. Lett.* 80 (1998) 2749.
- [227] H.A. Weidenmueller, G.E. Mitchell, *Rev. Modern Phys.* 81 (2009) 539; Y.M. Zhao, A. Arima, N. Yoshinaga, *Phys. Rep.* 400 (2004) 1; V. Zelevinsky, A. Volya, *Phys. Rep.* 391 (2004) 311.
- [228] C.W. Johnson, G.F. Bertsch, D.J. Dean, I. Talmi, *Phys. Rev. C* 61 (1999) 014311.
- [229] C.W. Johnson, H.A. Nam, *Phys. Rev. C* 75 (2007) 047305.
- [230] Y.M. Zhao, S. Pittel, R. Bijker, A. Frank, A. Arima, *Phys. Rev. C* 66 (2002) 041301.
- [231] Y.M. Zhao, J.L. Ping, A. Arima, *Phys. Rev. C* 76 (2007) 054318.
- [232] R. Bijker, A. Frank, *Phys. Rev. Lett.* 84 (2000) 420; *Phys. Rev. C* 62 (2000) 14303.
- [233] G.J. Fu, Y.M. Zhao, J.L. Ping, A. Arima, *Phys. Rev. C* 88 (2013) 037302.
- [234] Y. Lei, Y.M. Zhao, N. Yoshida, A. Arima, *Phys. Rev. C* 83 (2011) 044302.
- [235] Y. Lei, Z.Y. Xu, Y.M. Zhao, S. Pittel, A. Arima, *Phys. Rev. C* 83 (2011) 024302.
- [236] T.T.S. Kuo, G.E. Brown, *Nuclear Phys. A* 114 (1968) 235; B.H. Wildenthal, *Prog. Part. Nuclear Phys.* 11 (1984) 5.
- [237] W.D.M. Rae, <http://ns.ph.liv.ac.uk/~dsj/NuShell/>.
- [238] M. Bao, Y. Lei, Y.M. Zhao, S. Pittel, A. Arima, in preparation.
- [239] B.H. Flowers, M. Vujičić, *Nuclear Phys.* 49 (1963) 586.
- [240] A. Arima, V. Gillet, J. Ginocchio, *Phys. Rev. Lett.* 25 (1970) 1043.
- [241] A. Arima, V. Gillet, *Ann. Phys. (NY)* 66 (1971) 117.
- [242] K. Heyde, J.L. Wood, *Rev. Modern Phys.* 83 (2011) 1467.
- [243] J. Okolowicz, M. Płoszajczak, I. Rotter, *Phys. Rep.* 374 (2003) 271 and references therein.
- [244] N. Michel, W. Nazarewicz, M. Płoszajczak, T. Vertse, *J. Phys. G: Nucl. Part. Phys.* 36 (2009) 013101.